Investigations of the Potential Schizophrenia Susceptibility Gene Kinase Interacting with Stathmin (KIS)

Greg Colin Bristow

Wolfson College, University of Oxford

Submitted for degree of D.Phil.

Hilary Term 2011

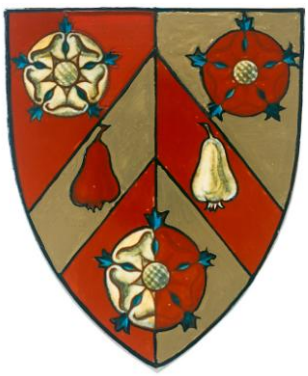

Abstract

Single nucleotide polymorphisms (SNPs) within the gene encoding the serine threonine kinase KIS (Kinase Interacting with Stathmin, also known as UHMK1) have recently been associated with schizophrenia. However, little is known about the neurobiology of KIS or the mechanisms through which disease-associated SNPs may increase susceptibility to schizophrenia. The studies presented in this thesis focus on the distribution of KIS and its mRNA, address the mechanisms through which KIS may confer susceptibility to schizophrenia, and investigate the physiological role(s) of KIS in the brain using two lines of knockout mice.

The regional and cellular distribution of KIS was characterised in the brains of adult humans and mice, and through mouse neurodevelopment. The results of these experiments demonstrated that KIS is widely expressed in neurons in the brain regions examined in both species, its encoded protein is localised to the nucleus and cytoplasm, and KIS expression in mouse brain peaked around seven days after birth.

KIS protein and mRNA was quantified in two large human post-mortem brain series to determine if KIS expression is altered in schizophrenia or bipolar disorder, or in relation to the leading schizophrenia-associated SNP (rs7513662). Using tissue from the superior temporal gyrus, dorsolateral prefrontal cortex, anterior cingulate cortex, and cerebellum, no difference in KIS expression (either mRNA or protein) was found between diagnostic or genotype groups in any brain region examined. Furthermore, KIS expression in lymphoblast cell lines also did not differ between diagnostic or genotype groups.

Lastly, KIS expression (mRNA and protein) was characterised in two separate lines of KIS knockout mice. The results were complex, and left uncertainty as to whether either line was a true knockout or, conversely, whether any of the available KIS antibodies were specific. Nevertheless, the absence of KIS mRNA was robustly confirmed in one knockout mouse line, and brains from this line were subsequently used in three experiments. First, investigation of the quantity and phosphorylation state of the KIS targets stathmin and $p27^{kip1}$; no differences were found compared to wildtype mice. Second, quantification of mRNA expression of several other genes of interest with regard to schizophrenia; altered expression of GAP43, VGlut1, MAP2, spinophilin, and stathmin was found. Finally, stereological measurements were performed, and while no differences in whole or regional brain volumes in KIS knockout mice were found, there was a relative reduction in hippocampal volume.

The results of these studies do not support the hypothesis that altered expression is the mechanism by which genetic variation of KIS may increase susceptibility to schizophrenia, nor that KIS expression is altered in the disease. However, the knockout mice data suggest that KIS may play a role in synaptic plasticity and function, providing novel information on the potential neurobiological roles of KIS.

Acknowledgements

A big thank you must go to my supervisors Paul Harrison and Sharon Eastwood for their help, guidance, and support throughout this thesis. An extra thank you goes to Paul for taking the time to give me SPSS tutorials and going through my results, and to Sharon for always being on hand with help and advice.

There are several people who helped to make the work in this thesis possible. Mary Walker was generally helpful with everything, and particularly with the stereology work, and thanks go to Tracy Lane for her help with the lymphoblast cell lines, Inga Deakin for providing the developmental mouse tissue, Phil Burnet for providing the antipsychotic treated rat tissue, and Li Chen for providing technical assistance. Further thanks go to the people at NIH and Wyeth for providing the tissue from the KIS knockout mouse series.

I'd also like to thank everyone in the Harrison group who I've worked with over the past few years for making the Neurosciences Building an enjoyable place to work, particularly those who I've shared the scientists' office with. A particular mention goes to Sarah Farrell for the amusement provided by her constant search for men.

Last but not least I'd like to thank my family, mum, dad, and my sister Sarah, whose support was always a great help, and I'd also like to thank Louisa.

Table of Contents

This thesis contains approximately 40,000 words.

Index of Tables

Index of Figures

Abbreviations

ACC	Anterior Cingulate Cortex
ANOVA	Analysis of Variance
B2M	β-2-Microglobulin
BSA	Bovine Serum Albumin
CA1-4	Cornu Ammonis (areas 1-4)
CAPON	Carboxy-Terminal PDZ Ligand of Neuronal Nitric Oxide Synthase
cDNA	Complementary DNA
CNV	Copy Number Variant
CPM	Counts Per Minute
COMT	Catechol-O-Methyltransferase
C_t	Threshold Cycle
DAAO	D-Amino Acid Oxidase
DAOA	D-Amino Acid Oxidase Activator
ddH_2O	Double-Distilled Water
dH_2O	Distilled Water
DEPC	Diethyl Pyrocarbonate
DISC1	Disrupted In Schizophrenia 1
DLPFC	Dorsolateral Prefrontal Cortex
dNTP	Deoxyribonucleotide triphosphates (A, adenosine; C, cytosine; G, guanine; T, thymine)
DSM-IV	Diagnostic and Statistical Manual of Mental Disorders Fourth Revision
DTT	Dithiothreitol
eEF1A	Eukaryotic Translation Elongation Factor 1 Alpha
ECL	Electrochemiluminescence
ELISA	Enzyme Linked Immunosorbant Assay
FoxM1	Forkhead Box Protein M1
GAP-43	Growth Associated Protein 43
GAPDH	Glyceraldehyde-3-Phosphate Dehydrogenase
gDNA	Genomic DNA
GABA	Gamma-aminobutyric Acid
GABP	GA-Binding Protien
GRM3	Metabotropic Glutamate Receptor 3
GUSB	Glucuronidase, Beta
HKG	Housekeeping Gene
HPRT	Hypoxanthine Guanine Phosphoribosyl Transferase
HRP	Horseradish Peroxidase
IHC	Immunohistochemistry
IMS	Industrial Methylated Spirits
ISHH	In-Situ Hybridisation Histochemistry
kb	Kilobases
KDa	Kilodaltons
KIF3A	Kinesin Family Member 3A
KIS	Kinas Interacting with Stathmin
KO	Knockout
MAF	Minor Allele Frequency
MAP2	Microtubule Associated Protein 2
MB	Megabases
MBP	Myelin Basic Protein

mRNA	Messenger RNA
Mw	Molecular Weight
NCBI	National Center for Biotechnology Information
NIH	National Institutes of Health
NIMH	National Institutes of Mental Health
nfH_2O	Nuclease Free Water
NonO	Non-POU Domain Containing, Octamer-Binding
PAM	Peptidylglycine α–Amidating Monooxygenase
PBS	Phosphate Buffered Saline
PBS-T	PBS with 0.3% Triton X-100
PBS-Tw	PBS with 0.1% Tween20
P-CIP2	PAM COOH-Terminal Interactor Protein 2
PCP	Phencyclidine
PCR	Polymerase Chain Reaction
PMI	Post-Mortem Interval
PVDF	Polyvinylidene Fluoride
qPCR	Quantitative RT-PCR
RACE	Rapid Amplification of PCR Ends
RGS4	Regulator of G-Protein Signalling 4
RIN	RNA Integrity Number
RRM	RNA Recognition Motif
RT-PCR	Reverse Transcription PCR
SAP155	Splicing Factor 3B Subunit 1
SDS-PAGE	Sodium Dodecyl Sulphate Polyacrylamide Gel Electrophoresis
SF1	Splicing Factor 1
siRNA	Small Interfering RNA
SMRI	Stanley Medical Research Institute
SNP	Single Nucleotide Polymorphism
snRNP	Small Nuclear Ribonucleoprotein
SSC	Saline Sodium Citrate
STG	Superior Temporal Gyrus
STOP	Stable Tubule-Only Polypeptide
TAE	Tris-Acetic Acid-Ethylenediaminetetraacetic Acid
TE	Tris Ethylenediaminetetraacetic Acid
TEA	Triethanolamine
TFRC	Transferrin Receptor
U2AF	U2 snRNP Auxiliary Factor
UHM	U2AF Homology Motif
UHMK1	U2AF Homology Motif Kinase 1
UTR	Untranslated Region
VCFS	Velo-Cardio-Facial Syndrome
VGlut1	Vesicular Glutamate Transporter 1
VSMC	Vascular Smooth Muscle Cell
WT	Wildtype

Chapter 1: Introduction

1.1. Overview of Schizophrenia

1.1.1. Schizophrenia Epidemiology, Symptoms, Treatment, and Prognosis

Schizophrenia is a severe and debilitating mental illness which has a lifetime prevalence of around 0.7% in the population (Saha et al., 2005). As well as the impact of schizophrenia on the affected individuals and their families, schizophrenia is also known to carry a heavy economic burden, with both direct and indirect costs estimated at £6.7 billion each year in the England (Mangalore and Knapp, 2007).

The symptoms of schizophrenia can broadly be divided into three categories: psychotic symptoms, negative symptoms, and cognitive dysfunction. Psychotic symptoms include delusional beliefs, hallucinations (which can be visual, auditory, or can involve touch, taste, or smell), and bizarre behaviour. Negative symptoms include a lack of motivation (avolition), poverty of speech (alogia), reduced experience of pleasure (anhedonia), and a blunted affect where the individual has reduced expressiveness. The cognitive dysfunction observed can include deficits in attention, working memory, learning, verbal fluency, motor speed, and executive function. Schizophrenia symptoms usually emerge during adolescence or in early adulthood, and it has been suggested that the disorder is generally more common in men than in women, with men around 1.4 times more susceptible, although it may be that this sex difference reflects an increase in the severity of symptoms in men (Aleman et al., 2003).

The diagnostic criteria of schizophrenia as described in the Diagnostic and Statistical Manual of Mental Disorders fourth revision (DSM-IV), published by the American Psychiatric Association, are summarised in Table 1.1. An alternative diagnostic guide for schizophrenia is included in the tenth revision of the International Classification of Diseases (ICD-10) from the World Health Organisation (WHO), although both include similar criteria for diagnosis.

The general criteria for schizophrenia are:

A) The presence for a significant portion of time during a period of one month of at least two of:

1) Delusions

2) Hallucinations

3) Disorganised speech

4) Grossly disorganised or catatonic behaviour

5) Negative symptoms

Only one of these criteria is sufficient if bizarre delusions or hallucinations of voices are present.

B) Social or occupational dysfunction

C) The continuous presence of the disturbance for at least six months, including at least one month of symptoms consistent with criterion A.

D) Exclusion of schizoaffective and mood disorders

E) Exclusion of substance abuse and general medical conditions

F) Symptoms of schizophrenia are prominent over any other pervasive developmental disorders present

Table 1.1: American Psychiatric Association Diagnostic and Statistical Manual of Mental Disorders fourth revision (DSM-IV) diagnostic criteria for schizophrenia.

There are two main groups of medications used to treat schizophrenia, which are known as typical (first generation) antipsychotics, such as chlorpromazine and haloperidol, and atypical antipsychotics (second generation), such as clozapine. A problem for the treatment of patients is that while medication can be quite effective at dealing with the positive symptoms they often have little or no effect on the cognitive or negative symptoms (Andreasen, 1995).

In many schizophrenia patients there is a deteriorating course of illness, associated with periods in which the positive symptoms are more prevalent, for several years after the first episode before the level of illness becomes more stable (Lieberman, 1999; Levine et al., 2010). The level of cognitive deficit in schizophrenia appears to be relatively stable over time (Rund, 1998), although some deterioration has been reported in older patients (Kurtz, 2005). Persistent negative and cognitive symptoms often prevent patients from returning to a normal social or working life (Andreasen, 1995), and the disorder is associated with a high suicide rate, around twelve times greater than in the general population (Saha et al., 2007).

1.1.2. Neuropathology of Schizophrenia

Several neuropathological changes have been identified in schizophrenia. These changes represent differences in the mean value of measurements between schizophrenia and control groups, rather than a diagnostic pathology such as that found in Alzheimer's disease. The main findings are that there are enlarged lateral and third ventricles of the brain, decreased brain size, decreased cortical volume, and decreased hippocampal volume (Harrison, 2005). Reports have varied as to whether these pathological changes are progressive (Weinberger and McClure, 2002), but post-mortem studies of the brains

of schizophrenia patients do not typically show the signs of a neurodegenerative disorder such as neurofibrillary tangles, amyloid plaques, or Lewy bodies, and there is no evidence of gliosis, which would indicate inflammation or injury in the brain (Weinberger and McClure, 2002; Harrison, 2005).

1.1.3. Neurochemistry and Pathophysiology

Traditionally schizophrenia has been viewed as a disorder of dopaminergic hyperfunction. The hypothesis of the involvement of dopamine in schizophrenia originates from the effects of drugs. Firstly, typical antipsychotic medications cause a blockade of dopamine D2 receptors, with the binding affinity of these medications to these receptors correlating strongly with the required dose for controlling psychotic symptoms (Seeman et al., 1975). Secondly, amphetamines cause an increase in dopamine release, and amphetamine overdose can produce symptoms which are almost identical to the psychotic symptoms of schizophrenia and increase psychotic symptoms in schizophrenia patients (Lieberman et al., 1987).

More recently, glutamatergic dysfunction has been implicated as the basis of schizophrenia. Evidence supporting this theory includes the effect of phencyclidine (PCP), which acts through inhibition of NMDA receptors and mimics many of both the positive and negative symptoms of schizophrenia (Javitt and Zukin, 1991). Also a number of the genes which have been implicated to be involved in the aetiology of schizophrenia, such as DAO (D-amino acid oxidase), DAOA (D-amino acid oxidase activator), GRM3 (metabotropic glutamate receptor 3), and dysbindin, are involved in the regulation of glutamatergic synapses (Coyle, 2006).

Relevant to both the dopamine and glutamate hypotheses, findings which indicate that the expression of a number of presynaptic regulatory proteins are decreased in schizophrenia have led to the suggestion that schizophrenia is a disorder of the synapse and connectivity (Mirnics et al., 2001; Frankle et al., 2003).

1.1.4. Aetiology of Schizophrenia

The aetiology of schizophrenia has proved to be highly complex and difficult to determine. Even though it is over 100 years since Kraeplin first described the disorder (then named dementia praecox), the exact causes of the disorder have yet to be fully elucidated, though several risk factors have been implicated. It is commonly envisaged that most cases of schizophrenia are likely to be caused by a combination of several genetic and environmental factors, as is discussed in this section.

1.1.4.1. Genetic Factors

Schizophrenia is a heritable disorder, with estimates of the level of heritability reported as around 80% (Cardno et al., 1999). The heritability of the disorder can be estimated based on the level of concordance in the occurrence of schizophrenia in monozygotic twins compared to dizygotic twins, as both sets of twins will have shared the same environment and so the difference in concordance between the two types of twins should be predominantly due to genetic factors. It has been reported that the identical twin of a patient with schizophrenia has a 48% chance of also having schizophrenia, whereas the non-identical twin of a schizophrenia patient has a 17% chance of also suffering from schizophrenia (Gottesman, 1991), indicating that there is a strong genetic component to the disorder but that genes are not the only causative factor. Adoption studies have

shown that the adopted children of parents with schizophrenia are more vulnerable to develop such disorders themselves than adoptees from unaffected parents, but with the rearing environment of the adoptive family also proving to be a determining factor in the genetically susceptible adoptees (Tienari et al., 2004).

The pattern of heritability indicates the genetic risk in most cases is not inherited in a Mendelian manner, with the risk of schizophrenia in most people conferred by the combination of the effects of several genes. This, combined with environmental factors, makes it very difficult to identify the genes responsible for susceptibility to schizophrenia.

Various strategies have been adopted to try and find the genes which confer susceptibility to schizophrenia. The first strategy is to take advantage of rare examples in which there is a highly penetrant genetic form of the disease. An example of this is a Scottish family in which a translocation between chromosomes 1 and 11 was found to be the cause of psychiatric disorders. Examination of the regions of the genome affected by this translocation led to the identification of the schizophrenia susceptibility gene Disrupted In Schizophrenia 1 (DISC1) (Millar et al., 2000), which is thought to be a multifunctional protein which is particularly involved in regulation of the cytosketeton (Ross et al., 2006; Chubb et al., 2008). A further example is velo-cardio-facial syndrome (VCFS), which is a developmental disorder caused by the deletion of part of chromosome 22q11 (Driscoll et al., 1992). Individuals with VCFS are around twenty times more likely to develop schizophrenia symptoms than those in the general population (Murphy et al., 1999), and so VCFS represents a highly penetrant risk factor and implicates the 22q11 region as a likely location of one or more genes which are

involved in the aetiology of schizophrenia. Examining cases such as these examples can prove useful as the highly penetrant nature of the disease in these cases simplifies the identification of the genetic basis of the disease, although the limitation of such studies is that they do not give any indication of the extent of the involvement of these factors in schizophrenia susceptibility in the general population. In the case of DISC1, subsequent linkage and association studies have provided support for a role of the affected region of chromosome 1 and of the DISC1 gene in populations without the translocation found in the Scottish family (Chubb et al., 2008).

The standard approach to finding genes for disorders is to use linkage studies, in which DNA from members of families with a history of schizophrenia is used to determine which regions of the genome are common to affected individuals in comparison to their unaffected relatives. The literature is complex and results inconsistent (largely because the method was designed for Mendelian disorders), but the latest meta-analysis of these linkage studies indicate that regions of chromosomes 1, 2q, 3q, 4q, 5q, 8p, and 10q are likely to be linked with (and thus contain genes associated with) schizophrenia (Ng et al., 2009). A linkage finding can then be used as the start of a fine mapping and genetic association study within the region to identify the genes and variants responsible for the linkage signal. This was the strategy used, for example, for the discovery of Neuregulin 1 as a schizophrenia gene (Stefansson et al., 2002) and, directly relevant to this thesis, KIS (as described in detail in Section 1.2.1).

Genetic association studies investigate one or more polymorphisms (usually SNPs) within the gene(s) of interest, and the frequency of each allele is compared between a schizophrenia group and a control group from the same ethnic population. Until recently,

such studies were limited to, at most, a few genes at a time, and this choice was made either on the basis of linkage (as above) or because a gene was believed to be involved in the disorder, a so-called candidate gene – of which dopamine receptors were prime examples. Now, it is possible to study hundreds of thousands of SNPs, selected across the genome, at once, in a genome wide association study (GWAS). These studies use similar methods to candidate gene association studies, but have no prior hypothesis of the possible location of the susceptibility genes and examine a large number of SNPs throughout the genome. One such study identified a strong association of the putative transcription factor ZNF804A with schizophrenia (O'Donovan et al., 2008), and others have highlighted the major histocompatibility complex (MHC) locus on chromosome 6.

Another genetic factor implicated in susceptibility to schizophrenia is copy number variation (CNV). CNVs occur when a small section of the genome is deleted or duplicated, resulting in deviation from the normal two copies of each gene within the affected region. VCFS, mentioned above, could be considered an example of CNV. Several recent studies have shown that CNVs anywhere in the genome, much smaller than that of VCFS, can increase risk of schizophrenia and can be both inherited and de novo mutations. Such CNVs include duplication of regions of chromosome 16, which are rare but highly penetrant for schizophrenia, with similar findings reported regarding deletions at 1q21.1, 15q11.2, and 15q13.3 (Stefansson et al., 2008; McCarthy et al., 2009; Kirov et al., 2009). CNVs affecting genes involved in synaptic transmission have been reported to be more common in schizophrenia cases (Glessner et al., 2010). The CNV field is developing rapidly, with estimates suggesting that 2% of schizophrenia cases may be attributable to CNVs at 1q21.1, 15q13.3, and 22q11 alone, but this is a very

provisional figure and does not consider the potential effects of numerous other CNVs throughout the genome (Bassett et al., 2010).

Each of the methods and approaches mentioned here have, as noted, contributed to the discovery of many putative schizophrenia susceptibility genes, for which the evidence ranges from very weak to very strong. Genes in the latter category include neuregulin, DISC1, dysbindin, DAOA, and ZNF804A (Owen et al., 2009). Linkage to chromosome 8p and a subsequent association study implicated the neuregulin gene in schizophrenia susceptibility (Stefansson et al., 2002). More than half of the association studies investigating neuregulin have found a positive association with schizophrenia (Schwab and Wildenauer, 2009), and there has been evidence of increased neuregulin expression in schizophrenia (Hashimoto et al., 2004; Law et al., 2006; Chong et al., 2008). Neuregulin has several mechanisms which could be linked to the pathophysiology of schizophrenia, including neuronal migration, axon guidance, myelination, synaptogenesis, neurotransmission, and synaptic plasticity (Harrison and Law, 2006; Mei and Xiong, 2008).

1.1.4.2. Environmental Factors

Several environmental factors have been suggested to increase disease susceptibility in schizophrenia. Numerous prenatal factors have been implicated, including maternal malnutrition, maternal stress, and specific viral infections (Clarke et al., 2006). Obstetric complications have been reported to increase risk of schizophrenia, and these complications can be placed into three groups: complications of pregnancy (bleeding, preeclampsia, maternal diabetes, rhesus incompatibility), abnormal growth (low birth weight), and delivery complications (asphyxia, emergency Caesarean section) (Cannon et

al., 2002). These complications may confer as much as a two fold increase in schizophrenia risk (Geddes and Lawrie, 1995; Cannon et al., 2002), although they may reflect another pathological process, in that abnormal development may increase the risk of schizophrenia and also of obstetric complications, so these complications would arise as a symptom of a another pathological process rather than being a risk factor themselves. Other factors which have been implicated as factors which increase the risk of schizophrenia include winter birth (Davies et al., 2003), migration (Cantor-Graae and Selton, 2005), and urbanisation (Pedersen and Mortensen, 2001). Cannabis use has been associated with schizophrenia (Semple et al., 2005), and it is possible that cannabis use interacts with genetic predisposition to increase the risk of psychosis, which has been found to be the case with COMT (Caspi et al., 2005).

1.1.4.3. Schizophrenia as a Neurodevelopmental Disorder

Schizophrenia has been suggested to be a neurodevelopmental disorder, in which an early developmental pathology leads to the emergence of symptoms during or following the normal maturation of the affected brain areas (Weinberger, 1987).

There are several factors which have been implicated in schizophrenia aetiology which fit the neurodevelopmental hypothesis of the disorder. A number of environmental schizophrenia risk factors operate pre- or perinatally, indicating that the mechanism through which these factors increase the risk of schizophrenia is likely to have a neurodevelopmental basis. Winter birth (Davies et al., 2003), malnutrition and viral infections during pregnancy (Susser et al., 1996; St Clair et al., 2005; Brown, 2006), and obstetric complications (Geddes and Lawrie, 1995; Cannon et al., 2002) all represent risk factors which are present early in neurodevelopment. Further evidence of a

neurodevelopmental basis for schizophrenia is that some structural brain changes are present at first onset of the disorder (Vita et al., 2006), and there is typically no signs of neurodegeneration in post-mortem schizophrenia brains (Weinberger and McClure, 2002; Harrison, 2005). Cognitive impairments have been reported to be present before first onset of the disorder (Jones et al., 1994; Fuller et al., 2002; Niendam et al., 2003). Delays and abnormalities in early development in areas such as speech and motor skills have been reported to be more frequent in children who later develop schizophrenia (Jones et al., 1994). Volumetric differences in the brain of male neonates with a genetic risk of schizophrenia have also been reported (Gilmore et al., 2010). These factors all appear to support the neurodevelopmental model of schizophrenia by indicating the factors which lead to schizophrenia occur long before the onset of symptoms in adolescence.

Further genetic evidence of neurodevelopmental factors leading to schizophrenia later in life include the finding that CNVs which are more common in schizophrenia patients compared to unaffected controls appear to converge on genes which regulate neurodevelopment (Walsh et al., 2008). The neurodevelopment functions associated with a number of reported schizophrenia susceptibility genes, such as DISC1, neuregulin, dysbindin, and reelin (Rapoport et al., 2005; Owen et al., 2009) also support the neurodevelopmental model of schizophrenia.

A factor in the neurodevelopmental model of schizophrenia that needs to be considered is the delay between the pathological events in early neurodevelopment and the onset of symptoms in late adolescence or early adulthood. There are examples of a fixed brain lesions resulting in varying symptoms over time in a single patient, and of lesions of the

same brain region of different patients resulting in different symptoms depending on the age of the individual, indicating that the effect of a lesion is dependent on the maturity of the affected systems (Weinberger, 1987). This is further supported by reports that fixed lesions in the brains of rodents and non-human primates cause minimal deficits until adulthood when impairments become prominent (Lipska and Weinberger, 2000).

1.2. Kinase Interacting with Stathmin (KIS)

1.2.1. Genetic Association of KIS with Schizophrenia

As discussed earlier (Section 1.1.4.1), genetic linkage studies can be used to identify susceptibility loci for schizophrenia in the genome. One such susceptibility locus is located on chromosome 1 in the region of 1q21-q33 (Brzustowicz et al., 2000; Gurling et al., 2001; Hwu et al., 2003; Lewis et al., 2003; Ng et al., 2009). However, while linkage studies can identify regions of the genome which may be involved in determining susceptibility, they cannot identify the specific genes which confer this susceptibility.

A genetic association study attempted to identify schizophrenia susceptibility genes by mapping genetic markers within 1q23.3 in a London based case-control sample of British subjects (Puri et al., 2007). The 1q23.3 region contains the RGS4 and CAPON (NOS1AP) genes which had both previously been associated with schizophrenia (Chowdari et al., 2002; Chen et al., 2004; Morris et al., 2004; Brzustowicz et al., 2004; Zheng et al., 2005). Puri et al., 2006 and Rizig et al., 2006 found no evidence of association of markers within the RGS4 or CAPON genes with schizophrenia, but in the same samples two SNPs were found to be associated with schizophrenia within the KIS gene, which is located in the 700kb region between the RGS4 and CAPON genes (Puri et al., 2007). Further fine mapping of the KIS gene identified additional schizophrenia associated SNPs in the original London sample, as well as replicating some of these associations in an Aberdeen based Scottish population (Puri et al., 2008). In total there were three intronic SNPs within the KIS gene, and two more within the 30kb region downstream of the gene, which were associated with schizophrenia (Puri et al., 2007; 2008, see Table 1.2 for details of SNP associations and Figure 1.1 for SNP locations).

The SNP rs7513662 was the most robustly associated KIS SNP reported in the British sample, as the A-allele occurred significantly more frequently in schizophrenia cases compared to controls in both the London and Aberdeen studies, and also when the data from these two studies were combined (Puri et al., 2007; 2008, Table 1.2). An association of the rs7513662 KIS SNP with schizophrenia has also been reported in a case-control study in a Bulgarian population, although this is an equivocal finding as the association was no longer significant when additional samples were included (Betcheva et al., 2009, see Table 1.2). The reported putative risk allele for the rs7513662 SNP in the Bulgarian sample was the G-allele, rather than the A-allele reported in British samples, which brings into question whether this Bulgarian sample offers any evidence supporting KIS as a schizophrenia susceptibility gene, although it could be an example of an "allele flip" (Clarke and Cardon, 2010). It is possible that the failure to unequivocally replicate KIS association in the Bulgarian sample, and the reversed implicated risk allele, is due to population differences between the eastern and western European samples. The smaller sample size and inclusion of schizoaffective disorder cases in the Bulgarian sample (Betcheva et al., 2009) compared to the British studies (Puri et al., 2007; 2008) may also have contributed to the difference in findings. However, confirmation of the initial association of KIS with schizophrenia in a second British population combined with reports of the 1q23.3 region being within a schizophrenia susceptibility locus indicate that KIS is a plausible schizophrenia susceptibility gene candidate.

SNP	Minor Allele	London		Aberdeen		London plus Aberdeen		Bulgaria-primary screening		Bulgaria-total screening	
		Control	Schizophrenia	Control	Schizophrenia	Control	Schizophrenia	Control	Schizophrenia[£]	Control	Schizophrenia[£]
rs10494370											
MAF (N)	G	7% (434)	11% (418)	10% (570)	9% (817)	8% (1004)	9% (1235)	12%[$]	12%[$]	n/a	
P		**0.004***		0.36		0.29		1.00			
rs7513662											
MAF (N)	G	37% (427)	31% (415)	37% (573)	32% (815)	37% (1000)	32% (1230)	26% (184)	34% (176)	30% (556)	34% (246)
P		**0.043***		**0.0087***		**0.00075***		**0.027***		0.18	
rs423227											
MAF (N)	C	11% (426)	14% (426)	13% (560)	13% (815)	12% (986)	13% (1241)	n/a		n/a	
P		0.08		0.86		0.31					
rs6427680											
MAF (N)	C	50% (436)	46% (422)	48% (577)	45% (803)	49% (1013)	46% (1225)	40%[$]	45%[$]	n/a	
P		0.07		0.18		**0.025***		0.18			
rs6694863[#]											
MAF (N)	A	8% (470)	5% (457)	6% (574)	5% (837)	7% (1044)	5% (1294)	n/a		n/a	
P		**0.02***		0.26		**0.015***					
rs10753578[#]											
MAF (N)	A	18% (443)	22% (452)	23% (579)	20% (834)	21% (1022)	21% (1286)	n/a		n/a	
P		**0.017***		**0.022***		0.83					
rs6704428[#]											
MAF (N)	G	6% (452)	8% (452)	8% (572)	7% (833)	7% (1024)	7% (1285)	n/a		n/a	
P		0.089		0.11		0.89					

Table 1.2: Summary of genetic associations of KIS gene single nucleotide polymorphisms with schizophrenia. London data reported in Puri et al, 2007 except #= reported in Puri et al, 2008; Aberdeen and London plus Aberdeen data reported in Puri et al, 2008; Bulgaria primary and total screening reported in Betcheva et al, 2009. MAF = Minor Allele Frequency; N = total number of subjects in each group; * = significant association ($p<0.05$); [£] = Schizoaffective disorder patients also included; [$] = N value not published, approximately 180 subjects in each group; n/a = SNP not examined in this study.

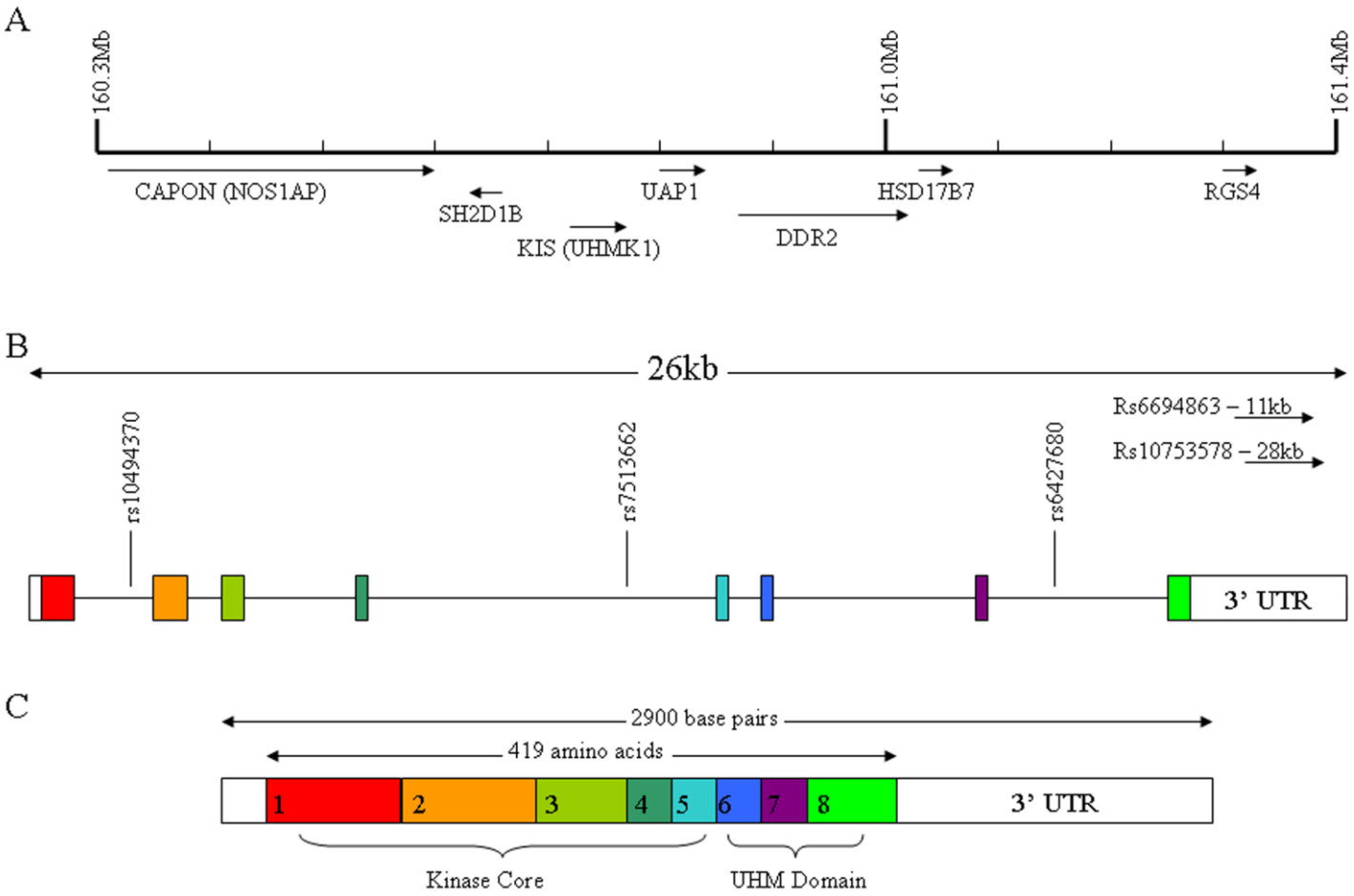

Figure 1.1: Human KIS gene, transcript and protein. (A) The position of KIS in relation to surrounding genes in the 1q23.3 region (adapted from Map Viewer, NCBI). Arrows indicate size of gene and direction of transcription. (B) The human KIS gene showing exons and introns and with schizophrenia associated SNPs marked. (C) The human KIS transcript/protein indicating the length of the KIS transcript and protein with the UHM and kinase domains of KIS as described by Maucuer et al (1997) also marked.

1.2.2. KIS Function

Other than further statistical evidence of association, the candidacy of a gene can be complemented by studies which show that the gene has functions directly relevant to the disorder concerned, and that the associated SNPs impact in some way upon these functions. Hence, in order to determine how the KIS gene could be involved in the aetiology of schizophrenia it is important to understand the function of the protein encoded by this gene. This section provides a summary of the current publications of the functional domains of KIS, the proteins with which KIS interacts, and the potential implications of these interactions.

1.2.2.1. Functional Domains of KIS

The KIS gene is approximately 26 kilobases in length and is made up of eight exons (Figure 1.1B). Reported splice variants of KIS include a transcript with an alternative first exon (variant 2, NM_001184763), a transcript without the seventh exon (variant 3, NM_144624), and a transcript with a shortened exon one, a retained intron between exons two and three, and the translation start site in exon three (AL834136) (Aceview, Genome Biology 2006, 7(Suppl 1):S12), although there is no available data on the physiological relevance or distribution of expression of these potential variants.

The KIS protein consists of a kinase domain and a U2 snRNP auxiliary factor (U2AF) homology motif (UHM) (Figure 1.1C; Maucuer et al., 1995, 1997; Kielkopf et al., 2004). The kinase domain of KIS shows sequence homology to serine/threonine kinases (Maucuer et al., 1995), and KIS has been shown to preferentially target serine residues which are immediately followed by a proline residue (Maucuer et al., 2000). To date no

other kinase containing a UHM domain has been identified (Puri et al., 2007), and this UHM domain has led to an alternative name for KIS: U2AF homology motif kinase 1 (UHMK1). UHM domains are similar to RNA recognition motifs (RRMs) but have evolved to be specialised for protein recognition (Kielkopf et al., 2001; Selenko et al., 2003). U2AF, the protein in which UHMs were first identified (Kielkopf et al., 2004), is a splicing factor consisting of two subunits, each of which contains a UHM domain. The UHM domain of the larger U2AF subunit, $U2AF^{65}$, is closely related to the UHM domain of KIS (Alam et al., 1996; Kielkopf et al., 2004).

1.2.2.2. KIS Interactions and Phosphorylation Targets

Stathmin

KIS was first identified through its interaction with the cytosolic protein stathmin in a yeast two-hybrid screen (Maucuer et al., 1995), and this interaction of KIS and stathmin was subsequently verified in a study which also showed that KIS phosphorylates stathmin on a serine residue (Maucuer et al., 1997). A mutation study in which particular serine residues were mutated to alanine showed that KIS phosphorylates stathmin on its serine 38 residue, with this phosphorylation leading to degradation of stathmin (Langenickel et al., 2008). Deletion of the UHM domain of KIS greatly reduced its ability to phosphorylate stathmin, indicating a regulatory role of the UHM for this function of KIS (Maucuer et al., 1997). Cultured vascular smooth muscle cells (VSMCs) derived from KIS knockout mice have increased levels of stathmin protein, further indicating the regulatory role of KIS on stathmin (Langenickel et al., 2008).

Stathmin is a microtubule regulatory protein which acts by increasing the rate of microtubule catastrophe, which is the process of transition from microtubule growth to disassembly (Belmont et al., 1996), and stathmin also sequesters free tubulin and thereby reduces the amount of tubulin available for microtubule formation (Jourdain et al., 1997). Phosphorylation of stathmin causes its inactivation (Larsson et al., 1997), and so it is likely that KIS acts as a negative regulator of stathmin. As previously stated, KIS phosphorylates stathmin on the serine 38 residue which leads to stathmin degradation (Langenickel et al., 2008). It has been indicated that while phosphorylation of serine 38 of stathmin may not have a direct effect on its ability to sequester tubulin or promote microtubule catastrophe, it appears phosphorylation of this residue is a prerequisite for efficient phosphorylation of other serine residues which lead to the inactivation of stathmin in vitro (Manna et al., 2009). These two studies (Langenickel et al., 2008 and Manna et al., 2009) indicate that phosphorylation of the serine 38 residue by KIS would facilitate inactivation and cause breakdown of stathmin, although KIS is not the only kinase reported to phosphorylate stathmin on serine 38 (Nakamura et al., 2006).

Regulation of the phosphorylation state of stathmin by KIS could affect cell cycle regulation and/or cell migration. Stathmin has been shown to play a key role in cell cycle regulation (Marklund et al., 1994; Rubin et al., 2004), with phosphorylation of the serine 38 residue particularly relevant to this role (Marklund et al., 1994). A role for stathmin in the regulation of cell migration has previously been speculated due to high stathmin levels reported in migrating cells (Camoletto et al., 1997, 2001; Ozon et al., 2002), and inhibition of stathmin expression in developing neurons has been shown to inhibit migration (Jin et al., 2004). Increased stathmin expression has also been shown to cause abnormal arborisation of axons (Yamada et al., 2010). Increased cell migration was

found in VSMCs lacking the KIS gene, with increased stathmin protein key to this enhanced migratory activity (Langenickel et al., 2008), indicating that KIS may regulate cell migration in vivo.

$p27^{kip1}$

KIS plays a part in control of the cell cycle through negative regulation of the cyclin-dependant kinase inhibitor $p27^{kip1}$ (Boehm et al., 2002; Lee and Kay, 2010). $p27^{kip1}$ is a nuclear protein which has an important role in cell cycle regulation (Sherr and Roberts, 1999). KIS phosphorylates the serine 10 residue of $p27^{kip1}$, which promotes the export of $p27^{kip1}$ from the nucleus to the cytoplasm (Boehm et al., 2002). This change from nuclear to cytoplasmic localization overcomes the growth arrest induced by $p27^{kip1}$, allowing cell cycle progression (Boehm et al. 2002; Petrovic et al., 2008; Nakamura et al., 2008; Lee and Kay, 2010). VSMCs which lack the KIS gene retained $p27^{kip1}$ in the nucleus when prompted to enter the cell cycle by serum stimulation, further indicating the importance of KIS in $p27^{kip1}$ regulation (Langenickel et al., 2008).

$p27^{kip1}$ has been implicated in roles beyond the cell cycle, such as the regulation of cell migration in neuronal development (Goto et al., 2004; Nguyen et al., 2006a; Nguyen et al., 2006b). $p27^{kip1}$ knockout mice showed an increase in cortical thickness and increased number of non-GABAergic neurons across the cortex, indicating an important role for $p27^{kip1}$ in cortical neurogenesis (Goto et al., 2004). Another study using $p27^{kip1}$ knockout mice showed that $p27^{kip1}$ also has a role in regulating migration of neurons during development, with reduced cortical migration of neurons in the knockout mice compared to wild type controls (Nguyen et al., 2006a). Conversely, overexpression of $p27^{kip1}$ during

embryonic development increases the proportion of cortical neurons being directed to superficial layers, indicating increased migration in these cells (Tarui et al., 2005). It is not known if phosphorylation by KIS has an effect on these roles of $p27^{kip1}$ in regulating cell migration in cortical development.

$p27^{kip1}$ has been reported to regulate cell migration through interactions with stathmin, as overexpression of $p27^{kip1}$ in fibrosarcoma cells resulted in $p27^{kip1}$ binding to stathmin and thus interfered with its tubulin-sequestering activity (Baldassarre et al., 2005). Cytoplasmic localization of $p27^{kip1}$ was required for its effect on stathmin, potentially linking this interaction to the regulation of $p27^{kip1}$ localisation by KIS. The interaction of the two KIS targets $p27^{kip1}$ and stathmin adds to the mechanisms through which KIS could potentially balance cellular functions by indicating that KIS could regulate cell migration through multiple pathways.

Potentially of interest, $p27^{kip1}$ has also been found to be phosphorylated on its serine 10 residue by Akt1 (Nacusi et al., 2006). Akt1 has been associated with schizophrenia (Emamian et al., 2004). This indicates that the phosphorylation of $p27^{kip1}$ represents a function in common for the putative schizophrenia susceptibility genes KIS and Akt1.

Splicing Factor 1 (SF1)

Due to the homology of the UHM domains of KIS and $U2AF^{65}$, the interactions of KIS with proteins known to interact with the UHM domain of $U2AF^{65}$ have been investigated (Manceau et al., 2006). U2AF is involved in the splicing of pre-mRNA (Ruskin et al., 1988). At various stages of spliceosome formation, the UHM domain of $U2AF^{65}$ interacts with splicing factor 1 (SF1; Berglund et al., 1998) and SAP155 (Gozani et al., 1998).

Based on these interactions of the UHM domain of U2AF^{65}, potential interactions of SF1 and SAP155 with KIS were investigated, and it was shown that KIS phosphorylated SF1 on two serine residues (80 and 82), with the UHM domain playing an important regulatory role, and the phosphorylation of these residues enhanced the binding of SF1 to the UHM domain of U2AF^{65} and the binding of this complex to RNA in vitro (Manceau et al., 2006), indicating a potential role for KIS in regulation of pre-mRNA splicing. KIS also interacted with SAP155, but it did not efficiently phosphorylate this protein (Manceau et al., 2008). These data indicate that the UHM domain of KIS is important in identifying and binding KIS targets, and this binding is necessary but not sufficient for phosphorylation.

RNA Granules, KIF3A, and mRNA

KIS has been found to interact with, but not phosphorylate, the microtubule-dependent motor protein kinesin family member 3A (KIF3A; Cambray et al., 2009). Interactions of KIS with KIF3A, as well as NonO and eEF1A which are both associated with RNA granules, were found in a yeast two-hybrid screen (Cambray et al., 2009). Unlike reports of the mechanism of interaction between KIS and stathmin (Maucuer et al., 1997) and SF1 (Manceau et al., 2006), the UHM domain of KIS was found to be dispensable for the interaction of KIS and these RNA granule proteins (Cambray et al., 2009). Confirmation of an interaction between KIS and KIF3A and RNA granules comes from an immunofluorescence study showing colocalisation of KIS with KIF3A and mRNA in neuritic RNA granules in cultured cortical neurons and suggest that KIS may have a role in regulating the transport of mRNAs in neurons (Cambray et al., 2009). KIS was also found to colocalise with β-actin mRNA and modulate its local translation in neurites. Investigations of KIS association with other mRNAs indicate that KIS may selectively

associate with RNA granules containing particular mRNAs (Cambray et al., 2009). The interaction of KIS with KIF3A and β-actin mRNA has been suggested as a possible mechanism through which KIS siRNA caused a reduction in neurite length and total neurite number in cultured cortical neurons (Cambray et al., 2009), as both KIF3A and β-actin have previously been shown to be necessary for normal neurite outgrowth (Aronov et al., 2002; Hüttelmaier et al., 2005).

PAM, Synapsin, and MBP

Peptidylglycine α–amidating monooxygenase (PAM) is an enzyme which modifies bioactive peptides through the addition of an amide group to their C-terminal, with this amidation modifying the activity of the peptide (Eipper et al., 1993). A yeast two-hybrid screen has found that KIS interacts with the C-terminal domain of PAM (Alam et al., 1996). This has resulted in another alternative name for KIS: PAM COOH-terminal interactor protein 2 (P-CIP2). KIS phosphorylates PAM on the serine 949 residue, which is in a region involved in regulating the trafficking of the protein (Caldwell et al., 1999; Steveson et al., 2001), and KIS activity increases the cytosolic localisation of PAM by excluding it from the nucleus (Francone et al., 2010). PAM has been found to increase the expression of specific genes, with KIS acting as a negative regulator of this function (Francone et al., 2010).

Investigations of the ability of KIS to phosphorylate various substrates have also indicated synapsin 1 and myelin basic protein (MBP) are potential KIS targets (Maucuer et al., 1997; 2000). The synapsin protein family are associated with regulation of neurotransmitter release (Hilfiker et al., 1999), neuronal development (Ferreira et al., 2002), and synaptogenesis (Chin et al., 1995). MBP is important to the myelination of

axons (Campagnoni, 1988). Maucuer et al., (2000) used a recombinant KIS protein to investigate its phosphorylation activity in vitro, identifying that the serine 164 residue of MBP and serine 438 residue of synapsin 1 are phosphorylated by KIS. To date there have been no reports of these phosphorylations of synapsin and MBP by KIS in vivo.

1.2.2.3. KIS Knockout Mice

As mentioned earlier (Section 1.2.2.2), KIS knockout mice have been produced. To date only one published study on these mice has been reported (Langenickel et al., 2008). The $KIS^{-/-}$ mice were reported to be viable and fertile with no obvious organ abnormalities. Investigation of the effects of KIS knockout in the Langenickel et al., 2008, study was limited to effects in mouse embryonic fibroblasts (MEFs) and VSMCs, specifically examining the effect the absence of KIS had on cells in culture and in vivo during vascular wound repair. The key findings were that VSMC proliferation was impaired in $KIS^{-/-}$ mice due to the impairment of nuclear export of $p27^{kip1}$, and increased stathmin protein levels caused by a reduction in stathmin degradation mediated by phosphorylation of its serine 38 residue by KIS, which resulted in increased migration of VSMCs and MEFs (Langenickel et al., 2008). The role of KIS in brain function remains to be examined in these mice.

1.2.2.4. Summary

These previously reported data summarised in this section regarding the phosphorylation targets of KIS indicate that this kinase is likely to have multiple functions in vivo, with its protein binding UHM domain playing an important regulatory role in some (Maucuer et al., 1997; Manceau et al., 2006) but not all (Cambray et al., 2009) of these functions.

The systems which KIS has, or potentially has, a regulatory role in include the cell cycle, microtubule stability, cell migration, splicing regulation, peptide amidation, synaptogenesis, neurotransmitter regulation, myelination, mRNA transport, and modulation of local mRNA translation (Figure 1.2).

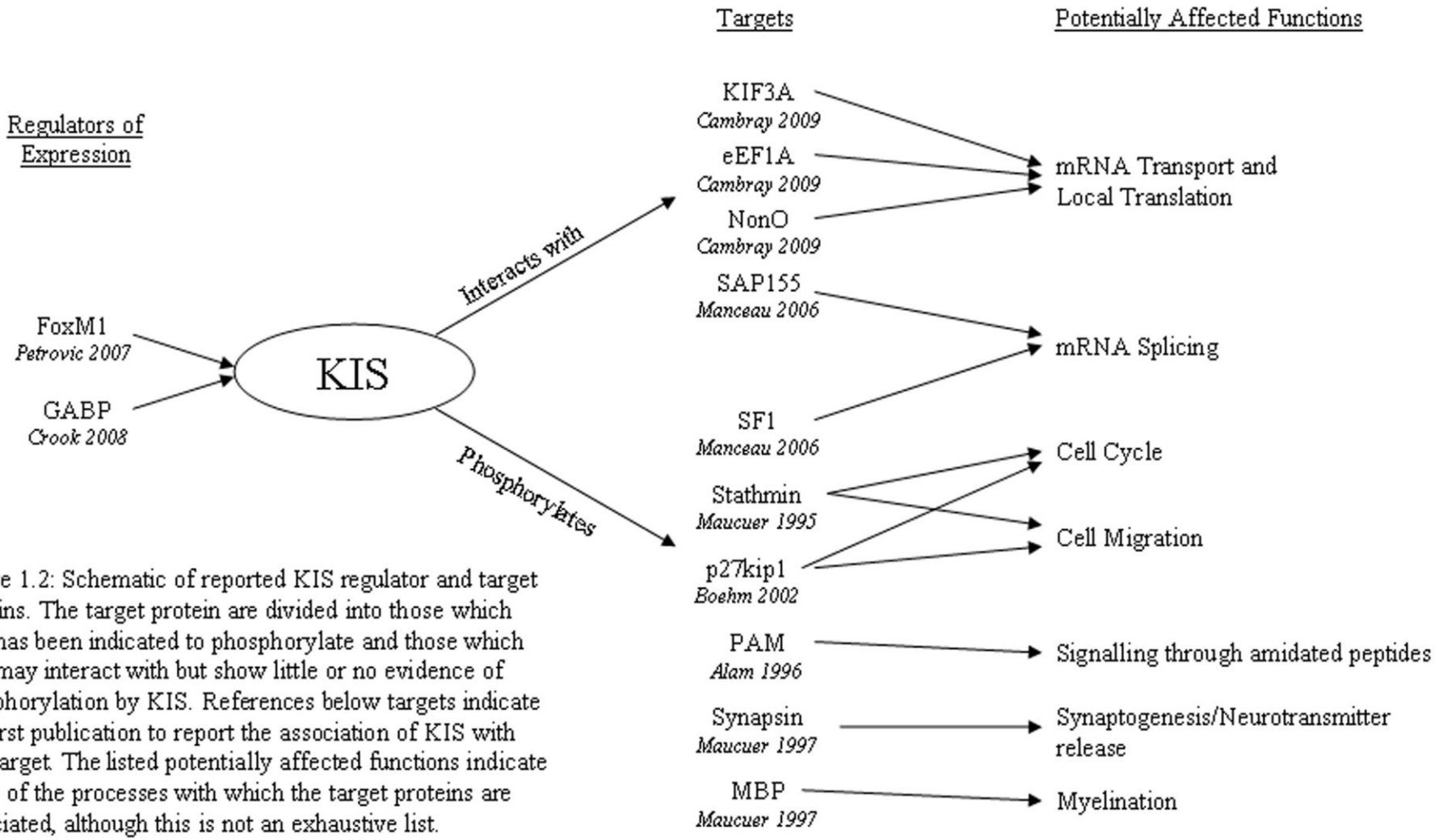

Figure 1.2: Schematic of reported KIS regulator and target proteins. The target protein are divided into those which KIS has been indicated to phosphorylate and those which KIS may interact with but show little or no evidence of phosphorylation by KIS. References below targets indicate the first publication to report the association of KIS with that target. The listed potentially affected functions indicate some of the processes with which the target proteins are associated, although this is not an exhaustive list.

1.2.3. Distribution of KIS

1.2.3.1. Regional Distribution

The studies to date which have investigated the profile of KIS expression are summarised in Table 1.3. KIS is expressed in tissues throughout the body, with the majority of studies reporting that KIS is widely expressed in various tissues but its highest levels are found in the brain in mice (Maucuer et al., 1995; Langenickel et al., 2008), rats (Maucuer et al., 1997; Caldwell et al., 1999; Bièche et al., 2003), and humans (Bièche et al., 2003). To date, only one study has reported a different profile of expression, finding in a northern blot analysis that while KIS expression is detected in the human brain, it appeared to be expressed much more in other tissues such as skeletal muscle and kidney (Boehm et al., 2002).

The distribution of KIS expression in the rat brain has been investigated in two studies, both of which found KIS widely expressed in the brain with strong expression reported in the hippocampus, amygdala, habenula, hypothalamus, substantia nigra, ventral tegmental nucleus, and in sensory and motor areas of the brain stem, and lower levels in the cerebral cortex and thalamus (Caldwell et al., 1999; Bièche et al., 2003). KIS expression and immunoreactivity has been detected in rodent neurons (Alam et al., 1996; Caldwell et al., 1999; Cambray et al., 2009). Details of the distribution of KIS within the human brain have not, to my knowledge, previously been reported. The current data available regarding human KIS distribution consist of a northern blot analysis (Boehm et al., 2002) and a quantitative reverse transcription polymerase chain reaction (qPCR) study of KIS expression in adult human tissues (Bièche et al., 2003), although both of these studies measured expression in the brain as a whole rather than examining separate brain regions.

1.2.3.2. Subcellular Localisation

At the subcellular level, KIS protein has been found both in the nucleus and in the cytoplasm, with reports varying regarding the extent of its subcellular localisation. Several studies have found KIS immunoreactivity to be mainly localised to the nucleus but with some cytoplasmic signal (Alam et al., 1996; Maucuer et al., 1997; Boehm et al., 2002; Manceau et al., 2008; Francone et al., 2010), while others have reported KIS to be a cytoplasmic protein with little or no immunoreactivity in the nucleus (Caldwell et al., 1999; Cambray et al., 2009) (Table 1.3). Possible explanations of the variation in the subcellular localisation of KIS could be differences in methods, antibody specificity, cell type, or species. These differences could also be caused by variations in the expression of KIS targets, as overexpression of the KIS target PAM in AtT-20 cells has been shown to redistribute KIS from nuclear to cytosolic localisation (Alam et al., 1996), and KIS has been found to move between the nucleus and the cytoplasm in AtT20 cell lines overexpressing KIS (Francone et al., 2010). The subcellular localisation of KIS has a considerable relevance to its function. Nuclear localisation of KIS is likely to be necessary for phosphorylation of $p27^{kip1}$ and SF1, whereas cytoplasmic localisation is likely to be necessary for KIS to regulate targets such as stathmin and PAM. Relevant to its potential role in mRNA trafficking and regulation of local translation, KIS has also been found to be localised to RNA granules in the neurites of cultured cortical neurons collected from embryonic mice, although the majority of KIS was detected in the soma (Cambray et al., 2009).

Author	Technique	Tissue/cell type	Location	Species
mRNA				
Maucuer et al.,1995	Northern Blot	Neonate various	Brain highest, follwed by kidney, faint signal in heart muscle and liver	Mouse
Alam et al.,1996	ISHH	Trigeminal nucleus	KIS expression present in neurons	Rat
Maucuer et al.,1997	ISHH	Whole embryo (E14)	mRNA mainly localised to CNS	Rat
Caldwell et al.,1999	Northern Blot	Adult various	mRNA present in every brain region examined, also in other tissues	Rat
	ISHH	Forebrain (hippocampus) to brainstem	Wide expression	Rat
Boehm et al.,2002	Northern Blot	Adult various	Skeletal muscle highest, brain low expression	Human
Bieche et al.,2003	Northern Blot	Developing rat brain/head	Increase after birth and during first month of brain development	Rat
	qPCR	Adult various	Highest in brain, expressed in all brain regions examined	Rat
		Developing rat brain/head	Dramatic increase after birth and during first month of brain development	Rat
		Human various	Expression highest in brain, plus fetal brain much lower than adult brain	Human
	ISHH	Adult brain	Broad expression, especially higher in substantia nigra and some sensory/motornuclei of brain stem	Rat
Langenickel et al.,2008	Northern Blot	Adult various	Highest in brain, present in muscle, kidney, lung, spleen, liver, and heart	Mice
Protein				
Alam et al.,1996	Immunocytochemistry	AtT20 cells	Primarily perinuclear Golgi/TGN, became diffuse cytosolic with PAM expression	Mouse
Maucuer et al.,1997	Immunoflourescence	HEK 293	Partially targetted to the nucleus, sometimes with cytoplasmic labelling as well	Human
	Fractionation/Western blot	HEK 293-overexpressing KIS	KIS protein found in both cytoplasm and associated with nuclei	Human
Caldwell et al.,1999	Immunocytochemistry	Medulla Oblongata Neurons	Staining filled the cell soma, nuclei were not stained	Rat
	Subcellular fractionation	Parietal Cortex	Negligible in nucleus, most is in cytosolic fraction	Rat
Boehm et al.,2002	Immunofluorescence	NIH 3T3	Mainly in nucleus	Mouse
Manceau et al.,2008	Immunofluorescence	CHO	Enriched in nucleus	Hamster
			UHM domain is dispensible for nuclear localisation	
Cambray et al.,2009	Immunofluorescence	Cortical neurons	KIS localises to RNA granules (lentiviral construct expressing KIS), strongest staining seen in the soma	Mouse
Francone et al., 2010	Immunocytochemistry	AtT20 cells	KIS concentrated in the nucleus with diffuse cytosolic staining	Mouse

Table 1.3: Summary of published data of KIS expression, localisation, and distribution

1.2.4. KIS Function and Schizophrenia

Though there are no data concerning KIS expression or function in schizophrenia, several aspects of the distribution and known functions of KIS make it an interesting candidate as a potential schizophrenia susceptibility gene. The abundance of KIS in the adult brain relative to other tissues (Maucuer et al., 1995, 1997; Caldwell et al., 1999; Bièche et al., 2003; Langenickel et al., 2008) suggests a particular role for KIS in the brain. The dramatic increase in KIS expression in the brain during development (Bièche et al., 2003) could, speculatively, link KIS to the hypothesis of schizophrenia as a neurodevelopmental disorder (see Section 1.1.4.3). Potential mechanisms for an effect of KIS during development on schizophrenia susceptibility could be through the KIS phosphorylation target $p27^{kip1}$ which is thought to play an important role in proliferation, differentiation, and migration of cortical neurons in mice (Goto et al., 2004; Nguyen et al., 2006a), indicating that $p27^{kip1}$ activity is important in control of cortical development. It is not known if phosphorylation by KIS has an effect on these roles of $p27^{kip1}$. Stathmin also has roles in cell migration and neuronal development (Di Paolo et al., 1997; Camoletto et al., 1997, 2001; Ozon et al., 2002; Langenickel et al., 2008) and the expression profile of stathmin also corresponds with a role in the development of the nervous system as stathmin is much more abundant in the neonate brain when compared to the adults (Koppel et al., 1990). Knockdown of KIS caused a reduction in neurite outgrowth in cortical neurons (Cambray et al., 2009), demonstrating that KIS function is involved in neuronal development in living cells.

The KIS target stathmin has been previously linked with schizophrenia, as an increase in stathmin in schizophrenia cases has been found in the grey matter of the anterior cingulate cortex (ACC) (Clark et al., 2006) and in the dorsolateral prefrontal cortex

(DLPFC) (Yamada et al., 2010), while conversely a decrease in stathmin has been reported in the cerebral cortex of an MK-801 treated rat model of schizophrenia (Paulson et al., 2003). These studies offer some indication that this KIS target protein may have some involvement in schizophrenia pathophysiology.

A role of KIS in the regulation of microtubules, via stathmin, offers a potential mechanism through which altered KIS could confer schizophrenia susceptibility via the hypothesis of altered microtubule function in the pathophysiology of schizophrenia (Kerwin et al., 1993). A potential role for microtubules in the pathophysiology of schizophrenia is supported by studies of mice which do not express the microtubule associated protein STOP (stable tubule-only polypeptide). These mice exhibited behavioural changes which were alleviated by antipsychotic medication (Andrieux et al., 2002). Also, several proteins known to play an important role in microtubule function, such as DISC1, dysbindin, and MAP2, have been identified as potential schizophrenia susceptibility genes (Millar et al., 2000; Ekelund et al., 2001; Straub et al., 2002; Rosoklija et al., 2005), further supporting the possibility of a role in microtubule function in schizophrenia pathophysiology. The role of microtubules in the regulation of synaptic function may be the mechanism through which altered microtubule function could contribute to the pathophysiology of schizophrenia (Eastwood et al., 2007).

1.3. Objectives of this Thesis

In light of the studies reviewed above, the aim of this study is to investigate aspects of the neurobiology of KIS, with particular focus on its potential role in the genetic pathophysiology of schizophrenia. The objectives are:

(1) To characterise the regional, cellular, and subcellular distribution of KIS mRNA and protein in the adult human brain.

Knowing which regions, cells, and subcellular compartments express KIS in human brain is a simple but critical precursor to studying what KIS does, and how it may be involved in schizophrenia.

(2) To characterise the expression and distribution of KIS in the developing mouse brain.

This will be done by quantifying KIS mRNA expression at several time points during maturation in the mouse brain, since the ontogenic profile of expression of a gene in the brain provides another basic facet of understanding what the role of a gene may be in neurodevelopment.

(3) To investigate quantitatively whether KIS mRNA and/or protein are altered in schizophrenia and (4) to investigate the effect of schizophrenia associated KIS SNPs on KIS expression.

Since all the KIS SNPs reported to show association with schizophrenia are in non-coding sequences (Figure 1.1), the main hypothesis is that any effect on schizophrenia susceptibility would be by altering some facet of KIS expression. KIS expression and immunoreactivity will be quantified to determine if the KIS mRNA or protein levels

differ between diagnostic groups, or with regard to KIS genotype. The existence of possible isoforms of KIS in brain will also be investigated, to examine the possibility that the SNPs affect splicing of the transcript.

(5) Studies in KIS knockout mice

KIS knockout mice will be utilised in order to elucidate the role of KIS in the brain. The importance of KIS to the phosphorylation of a selection of its reported targets will be investigated at the protein level. The expression of several molecular markers will be measured in order to characterise the more indirect effects of KIS on the brain, and a selection of measures of brain morphology will also be made.

Chapter 2: Methods

In this chapter I will provide details of the general methodologies used throughout this thesis. Where relevant, specific details are included in subsequent chapters. Details of buffer compositions are provided in the Appendix.

2.1. Tissue Used for Study

2.1.1. Human Tissue

To investigate the expression and distribution of KIS in the human brain, post-mortem tissue was utilised from schizophrenia, bipolar disorder, and control subjects. Normative distribution of KIS was investigated using selected controls from the collections described below, as well as further control tissue supplied by the Stanley Medical Research Institute (SMRI), and tissue collected in Oxford. Brain regions available for study were DLPFC, ACC, superior temporal gyrus (STG), occipital cortex, hippocampus, and cerebellum. For the quantitative studies, tissue sections and mRNA were available from the STG. Tissue sections were also available from the DLPFC, and mRNA samples were available from the ACC and cerebellum. The STG tissue was provided by the National Institute of Mental Health (NIMH, Bethesda, USA) and consisted of schizophrenia and control cases (Table 2.1-2.2). STG mRNA samples were only included if their RNA integrity number (RIN) was greater than or equal to 3.5, age was less than or equal to 80, post mortem interval (PMI) was less than 72 hours, and pH was between 6.0 and 6.9. This was to exclude low quality samples while keeping the diagnostic groups matched for demographic variables (see Lipska et al., 2006). Tissue from the ACC, DLPFC, and cerebellum were provided from the SMRI array collection

and consisted of schizophrenia, bipolar disorder, and control cases. The demographic details of the SMRI array collection were as described previously: (http://www.stanleyresearch.org/dnn/Portals/0/Stanley/Array%20Collection%20Demographic%20Details%20Chart-Final.pdf). However, as one bipolar subject has since been excluded from the collection due to abnormal neuropathology the collection now consists of 35 subjects with schizophrenia, 34 with bipolar disorder, and 35 control subjects (Eastwood et al., 2008). All tissue was collected with the appropriate ethical approval and consent, and diagnoses were made using DSM-IV criteria (Table 1.1). The method of diagnosis used by NIMH for subjects included in the collection was as described previously (Law et al., 2006) and for the SMRI subjects was also as described previously (http://www.stanleyresearch.org/dnn/BrainResearchLaboratorybrBrainCollection/ArrayCollection/tabid/89/Default.aspx).

Human tissue was sectioned in house (by M Walker and L Chen) at 14μm and collected onto Superfrost Plus slides (VWR, Lutterworth, UK), except for the SMRI tissue which was provided as 14μm sections on slides. All sections were stored at -80°C until use.

	Control (N=56)	*Schizophrenia (N=39)*
Sex	41M, 15F	29M, 10F
Race	19C, 31AA, 3H, 3A	15C, 21AA, 2H, 1MD
Age	44.1 (14.9)	45.6 (14.5)
pH	6.52 (0.23)	6.45 (0.24)
PMI	33.7 (14.7)	33.8(13.4)
RIN	5.97 (0.95)	6.09 (1.24)

Table 2.1: Demographics of mRNA samples from the NIMH STG series.
Values shown are mean with standard deviation for continuous variables in brackets. Age is given in years. M, male; F, female; AA, African American; H, Hispanic; A, Asian Pacific; MD, missing data; PMI, post-mortem interval in hours; RIN, RNA integrity number.

	Control (N=75)	*Schizophrenia (N=42)*
Sex	51M, 24F	25M, 17F
Race	23C, 46AA, 3H, 3A	17C, 23AA, 2H
Age	42.1 (15.0)	49.3 (17.1)
pH	6.55 (0.31)	6.38 (0.33)
PMI	32.0 (14.7)	39.6 (19.3)
RIN	5.39 (1.62)	4.40 (1.92)

Table 2.2: Demographics of protein samples from the NIMH STG series.
Values shown are mean with standard deviation for continuous variables in brackets. Age is given in years. M, male; F, female; AA, African American; H, Hispanic; A, Asian Pacific; MD, missing data; PMI, post-mortem interval in hours; RIN, RNA integrity number.

Lymphoblast cell lines were available from 22 schizophrenia (13 male, 9 female) and 39 control subjects (18 male, 21 female). All subjects were Caucasian. Lymphocytes collected from subjects were transformed by infection with Epstein-Barr virus to produce

the lymphoblast cell lines. The lymphocytes were collected and transformed as described previously (Sei et al., 2007).

Adult human RNA samples of frontal cortex, temporal cortex, hippocampus, caudate nucleus, cerebellum, liver, and human foetal brain (Clontech, California, USA), and RNA from the SH-SY5Y human neuroblastoma cell line were also available for study.

2.1.2. Rodent Tissue

2.1.2.1. Antipsychotic Treated Rats

To examine the potential effects of antipsychotic medication on KIS expression in the human brain, brain tissue from male Sprague-Dawley rats (8 weeks, 250-300g) was used. These rats had received an intraperitoneal injection once daily for 14 days of haloperidol (1mg/kg/day) as an example of typical antipsychotic medication, clozapine (25mg/kg/day) as an example of atypical antipsychotics, or saline as a control. The doses chosen are representative of those used in previous gene expression studies (Eastwood et al., 2000; Law et al., 2004a). Animals were sacrificed using a lethal injection of pentobarbitone 6 hours after the final treatment injection. They were then perfused transcardially with phosphate-buffered saline (PBS) and the brains were removed and frozen in isopentane chilled on dry ice. The brains were stored at -80°C until use. Procedures were performed by Dr P Burnet (Department of Psychiatry, Oxford). There were 8 animals in each treatment group.

2.1.2.2. KIS Knockout Mice

The brains of mice which did not express the KIS gene (referred to as KIS knockout, or $KIS^{-/-}$ mice) were supplied from two sources. The National Institutes of Health (NIH, Bethesda, USA, courtesy of E Nabel and M Olive) provided frozen brains from 9 knockout and 9 wildtype control ($KIS^{+/+}$) mice, with 6 males and 3 females in each group. The expression of KIS was prevented in these mice as exon 1 of the KIS gene had been replaced with a neomycin resistance gene by homologous recombination as described previously (Langenickel et al., 2008). Brains were collected on post-natal days 52-55 (P52-55). NIH also provided paraformaldehyde fixed brains from 8 knockout and 8 wildtype mice (all males) which had been collected on P50. The wildtype controls for both the fixed and frozen tissue were not littermates of the knockout mice but are from the same genetic background (C57BL6). Genotyping of these mice was carried out at NIH.

The brains of a second strain of $KIS^{-/-}$ mice were provided by Wyeth (New Jersey, USA, courtesy of Dr. N Brandon). This strain was produced using C57BL/6N mice with exons 2 and 3 of the KIS gene deleted (bases 422 to 906, NM_010633). Frozen brains from 8 wildtype, 7 mice which were heterozygous for the KIS knockout ($KIS^{+/-}$), and 6 knockout mice were provided from this strain. These brains were collected at P42. The animals had been killed using a standard schedule 1 method and the fresh brains were frozen by immersion in isopentane, which had been chilled on dry ice, before storage at -80°C. All of these animals were males and were produced by breeding $KIS^{+/-}$ mice. The animals used were from several litters from various parent animals. Genotyping of these mice was carried out at Wyeth.

Tissue from both series of mice was sectioned in house (by G Bristow, M Walker, and L Chen) at 14μm thickness and sections collected onto Superfrost Plus slides (VWR). Coronal sections were collected at the level of the striatum, hippocampus, and cerebellum. Three sections were collected onto each slide. All sections were stored at -80°C until use.

2.1.2.3. Developmental Mice Series

Normal mouse C57BL/6J brain tissue was available from several ages ranging from P0 to 2 years. There were two mice aged P0, five aged P7, six aged P15, five aged P21, four aged P63, six aged fifteen months, and two aged two years. Coronal sections were available from the level of hippocampus, and for the P63 mice sections were available from the level of the striatum, hippocampus, and cerebellum. The mice were culled using a schedule 1 method and the brain dissected and frozen in isopentane which had been cooled using dry ice (procedures carried out by I Deakin). For P0 tissue the brain was not dissected and the whole head was used. 14μm thick coronal sections from the level of hippocampus (and for the P63 mice sections, from level of the striatum, hippocampus, and cerebellum) were collected onto Superfrost Plus slides (VWR) with three sections on each slide (carried out by L Laatikainen, M Walker, and L Chen). Sections were stored at -80°C until use.

2.2. In Situ Hybridisation Histochemistry

In situ hybridisation histochemistry (ISHH) was used to detect mRNAs of interest within tissue sections in order to determine the quantity and/or distribution of expression of a particular gene. Oligonucleotide probes were designed in the antisense orientation to the

target mRNA sequence, and these probes were labelled with a ^{35}S radioactive tail to facilitate visualisation of the probe. Tissue sections were then incubated with the labelled probe. The probes were complementary to the sequence of interest and so bound to the target mRNA, after which the binding was visualised through detection of the radioactive label.

2.2.1. Section Pre-Treatment

All solutions and equipment used for section pre-treatment were treated before use with diethyl pyrocarbonate (DEPC, Sigma-Aldrich, Poole, UK). DEPC inactivates RNases which may be present in the solution to protect the mRNA from degradation. PBS, triethanolamine (TEA) buffer (see Appendix), and double-distilled water (ddH_2O) were all treated with DEPC to give a final DEPC concentration of 0.1%, and all containers and glassware were also treated overnight with 0.1% DEPC in ddH_2O. Following overnight incubation all solutions and equipment were autoclaved to deactivate the DEPC in order to prevent breakdown of mRNA by DEPC.

Tissue sections, which had been stored at -80°C, were placed at room temperature for 15 minutes before pre-treatment, and then fixed for 5 minutes in a solution of 4% paraformaldehyde in PBS (see Appendix), followed by two washes in PBS. Sections were then soaked for 10 minutes in TEA buffer containing 0.25% acetic anhydride, which neutralizes positive charge on the slide, thereby reducing non-specific binding of the probe. The acetic anhydride was added immediately before use as it is only active for approximately 2 hours once in the solution. After this step the sections were dehydrated by immersion in serial alcohols (70%, 80% (both 1min), 95% (2min), 100% ethanol (1min)). The ethanol was diluted using DEPC treated ddH_2O. The slides were then

placed in chloroform for 10 minutes to remove lipids in order to reduce nonspecific binding, followed by partial rehydration (100% and 95% ethanol, 1min each). Sections were then air dried before immediate use or stored at -20°C until use.

2.2.2. Labeling and Hybridisation

Target mRNA	Probe Sequence
KIS (1) (exon 4)	5' GGC TGG AAT TGC GGC ATT CAC CAC TGC TTT ACT GG
KIS (2) (exon 2)	5' TCC GCA CTC CAC AGG ATG TTT CGT GGC TTG AGG TC
GAPDH*	5' CCT TGA CTG TGC CGT TGA ACT TGC CGT GGG TAG AGT CAT
GAP43*	5' TCG GCT TGT TTA GGC TCC TCC TTG GCT GGG
Spinophilin*	5' CAT CCA CCA AGT CCG CTT CCG AGA AGT CCT CCT TCT TGG A
MAP2*	5' CTA CTT GAA CTA TCC TTG CAG ATA CCT CCT CTG CTG TTT CTC
VGlut1*	5' CGG GGG CCT CGG AGG CTG CAC TGT GCT GTG TGT GGC CCC GTA GGA
Stathmin**	5' TCC AGC TCT TTC ACC TGA ATA TCA GAA GAT GCC ATG TCG AAC AGA A

Table 2.3: Oligonucleotide probe sequences.
* = from Eastwood et al., 2007; ** = modified from Bräuer et al., 2001.

Antisense oligonucleotide probes (Sigma-Aldrich or MWG-Eurofins, Ebersberg, Germany) were supplied lyophilized and were resuspended in nuclease free water (nfH_2O, Promega, Southampton, UK) to a concentration of 2pmol/µl. The probes were 3' labeled with ^{35}S dATP as follows: 8pmol antisense oligonucleotide probe, 0.075mCi ^{35}S deoxyadenosine triphosphate (dATP) (Perkin Elmer, Beaconsfield, UK), terminal transferase buffer (Promega), and 60 units of terminal deoxynucleotide transferase (Promega) were incubated for 30 minutes at 37°C. The reaction was then stopped by adding 100µl TE buffer (see Appendix) and the labelled probe was purified using Nick Columns (GE Healthcare, Chalfont, UK). These columns separated labelled probe from unincorporated ^{35}S dATP by gravity flow chromatography. The solution containing the probe was added to the column and allowed to run through. 400µl TE buffer was then

added and the solution that ran through the column was collected. This was repeated until 4 fractions had been collected. The labelled probe was collected in the second fraction whereas the unincorporated nucleotides were collected in the fourth fraction. 4µl aliquots of the 2nd and 4th fractions were each added to 10ml scintillation fluid (Florasan Safe, VWR), and measured using a scintillation counter (LKB 1211 Minibeta Liquid Scintillation Counter) to establish the quantity of labelled probe and also to determine the efficiency of the labelling. Incorporation of 75% or higher was considered to be successful labelling.

In order for the signal to be quantitative the amount of labelled probe added must saturate the mRNA signal from each section, such that the addition of more probe should not produce an increase in the signal, thereby ensuring that mRNA quantity was the only limiting factor. Pilot studies determined the amount of probe required for saturation by testing a range of quantities of labelled probe. The appropriate volume of labelled probe was diluted in hybridisation buffer (see Appendix) with dithiothreitol (DTT) at a final concentration of 50mM, and the appropriate volume of this solution placed over the sections. DTT is included to minimise formation of non-specific disulphide bonds (Dagerlind et al., 1992). Coverslips were then placed over the sections, which were then incubated overnight in chambers humidified with a solution of 4x saline sodium citrate (4xSSC, see Appendix) and 50% formamide.

The melt temperature (T_m) of probes was calculated from the properties of the probe as follows:

T_m (°C) = 16.6log[M] + (0.41 x GC) + 81.5 – (675 / B) – (0.65 x formamide content)

M is the molar concentration of sodium to a maximum of 0.5, GC is the percentage of nucleotides in the probe that are either guanine or cytosine, B is the total number of nucleotide bases in the probe, and formamide content is the percentage of formamide in the hybridisation buffer. The temperature for incubation (T_i) was 15°C lower than the melt temperature in order to provide conditions which are stringent enough for specificity without loss of signal. The molar concentration of sodium in the buffer was greater than 0.5, and 50% of the buffer was formamide, so T_i of each probe was calculated as:

$$T_i\ (°C) = -4.997 + (0.41 \times GC) + 81.5 - (675 / B) - 32.5 - 15$$

Following the overnight incubation the coverslips were removed by soaking the slides in SSC. 3x20min heated post-hybridisation washes were carried out in SSC, followed by 2x60min SSC washes at room temperature. The slides were rinsed in ddH_2O and air dried. The concentration of SSC used and the T_i and T_w of each probe are listed in Table 2.4.

The temperature of the heated washes (T_w) was calculated based on T_m as follows:

$$T_w\ (°C) = 16.6\log[M] + (0.41 \times GC) + 81.5 - (675 / BP) - 15$$

T_w is again 15°C below melt temperature, and differs from T_i due to the difference in sodium concentration and the absence of formamide. The sodium concentration was dependent on the concentration of SSC used in the wash steps (Table 2.4).

Probe	Length (bp)	GC- Content	Ti (°C)	Tw (°C)	Wash Solution
KIS (1)	35	54%	32	56	1xSSC
KIS (2)	35	57%	32	56	1xSSC
GAPDH	39	54%	33	58	1xSSC
GAP43	30	60%	33	58	0.5xSSC
Spinophilin	40	55%	33	58	1xSSC
MAP2	42	45%	33	55	1xSSC
VGlut1	45	71%	42	55	0.1xSSC
Stathmin	46	43%	32	56	1xSSC

Table 2.4: ISHH incubation and wash conditions.
Bp, base pairs; GC, guanine and cytosine; Ti, incubation temperature; Tw, wash temperature; SSC, saline sodium citrate

Calculations of T_i and T_w (Table 2.4) were based on the formulae described above, although some of the temperatures were modified based on pilot studies and previous publications using these probes (Eastwood et al., 2007). The appropriate SSC concentration was also determined using pilot studies and previous publications (Eastwood et al., 2007).

2.2.3. Visualisation of Radiolabelled Probe Binding

The method used to visualise the binding of the probe was dependent on the purpose of the experiment. Film autoradiography was used to quantify regional gene expression and/or distribution of mRNA of interest, whilst dipping of sections with autoradiographic emulsion was used to characterise the cellular expression of the mRNA of interest.

2.2.3.1. Film Autoradiography

Sections were placed against Biomax MS Film (Sigma-Aldrich) alongside ^{14}C microscales and left in a cassette for the necessary exposure time, after which the hyperfilm was developed (2 minutes in 20% Universal Developer; Ilford, Knutsford, UK) and fixed (2 minutes in 20% Rapid Fixer, Ilford). The ^{14}C microscales were used to calibrate measurements in order to determine the relative abundance of mRNA in terms of ^{35}S nCi/g tissue equivalents. The microscales were used to create a calibration curve and a conversion factor of three was used to convert the ^{14}C values into ^{35}S equivalents (Millar et al., 1989).

2.2.3.2. Dipping with Autoradiographic Emulsion

To examine mRNA expression at the cellular level the slides were coated with autoradiographic emulsion (Hypercoat LM-1, GE Healthcare). This emulsion was sensitive to radioactive emissions and, once developed, dark grains were visible on the slides where the probe had bound, allowing the identification of the particular cells which were expressing the target mRNA.

In complete darkness, 20ml of emulsion was melted in a water bath at 40°C and then added to 10ml ddH_2O with a drop of glycerol. The solution was gently mixed and then the slides were dipped into the emulsion. Slides were then left in complete darkness at room temperature overnight to allow the emulsion to set. The following day the slides were placed in a light tight box with silica gel and stored at 4°C for the necessary exposure time, which was typically three times as long as the sections were exposed to film.

Before developing, the slides and solutions were allowed to equilibrate to room temperature for one hour. The slides were then developed in complete darkness by immersion in 20% Phenisol High Contrast Film Developer (Ilford) for 2 minutes, followed by 30 seconds in 2% glacial acetic acid, and then 5 minutes in 30% sodium thiosulphate. The slides were then soaked in ddH_2O for between one and two hours and then counter stained.

The developed slides were then counter-stained as follows: 1 minute distilled water (dH_2O), 1 minute filtered 0.5% Cresyl Violet Acetate solution (Thermo-Fisher, Massachusetts, USA), dip in 70% industrial methylated spirits (IMS), dip in fresh 70% IMS, 1 minute in 95% IMS containing 0.33% acetic acid, 1 minute in 95% IMS, 1 minute in undiluted IMS, 1 minute in xylene, and finally 5 minutes in a change of xylene. The slides then had a coverslip fixed over them using DPX mountant (VWR).

2.2.4. Experimental Controls

Experimental controls consisted of ISHH with a sense orientation probe and/or ISHH in the presence of 50-fold molar excess of unlabeled probe. The sense orientation probe was used as it demonstrates the level of non-specific binding of a probe with the same GC content as the probe used in the experiments, and the excess unlabelled probe was used to compete for mRNA binding with labelled probe.

2.2.5. Quantification of In Situ Hybridisation Histochemistry

Measurements of ISHH autoradiographs were made using the MCID Elite version 7.0 image analysis system (Interfocus, Haverhill, UK) calibrated to ^{14}C microscales (see

Section 2.2.3.1). In the mouse tissue, signal was measured in the cingulate cortex, somatosensory cortex, visual cortex, dorsolateral striatum, cornu ammonis (CA) 1, CA3, dentate gyrus, and the molecular layer of the cerebellum, as shown in Figure 2.1. Signal for cortical and striatal regions were measured within the boundaries indicated in Figure 2.1, while for the hippocampus and cerebellum, measurements were made from ten to fifteen points across the structure. Measurements were taken from both hemispheres and from all 3 tissue sections on each slide for each region in each mouse. The average of these measurements from each region of each animal was used for analysis. The signal of the control sections (sense probe or excess unlabelled probe, see Section 2.2.4) was used as a measure of background signal, and this background measure was subtracted from the signal measured for all other samples.

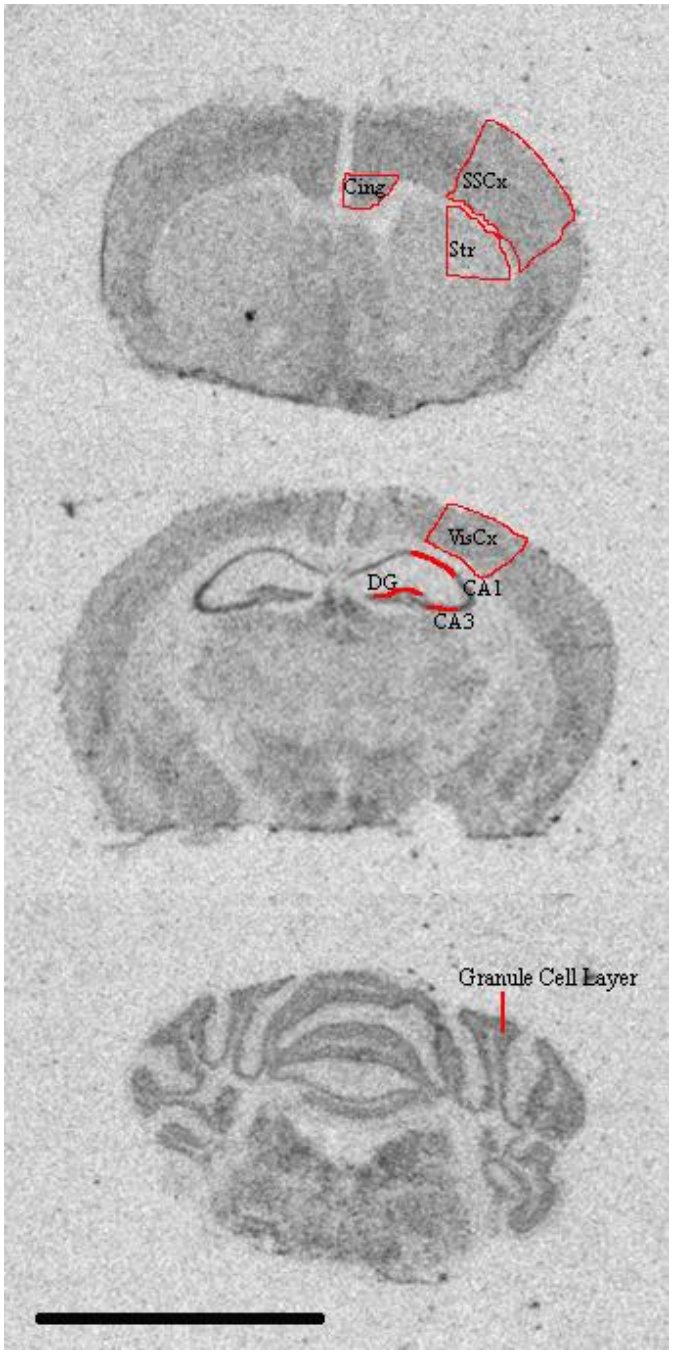

Figure 2.1: Measurements of mice ISHH sections.
Red lines indicate where measurements were made for each region examined. Measurements were made in both hemispheres. SSCx, somatosensory cortex; Cing, cingulate cortex; Str, dorsolateral striatum; VisCx, visual cortex; CA1, cornu ammonis 1; CA3, cornu ammonis 3; DG, dentate gyrus. Scale bar = 5mm

---

2.3. Western Blotting

Western blotting was used to determine the presence and/or quantity of immunoreactivity of an antibody in a particular sample. The proteins were first separated by size using gel electrophoresis, with smaller proteins able to move faster through the gel towards the

anode. The proteins were then transferred to a membrane and incubated with an antibody specific to the protein of interest, so that the binding of this antibody could be visualised and measured. Western blotting was also used to determine whether antibodies detected a single band of the predicted size to investigate specificity before these antibodies were used in other applications.

2.3.1. Protein Extraction

Protein was extracted using protein suspension buffer (see Appendix) or RIPA buffer (Thermo-Fisher), with protease inhibitor (Roche, Welwyn Garden City, UK) to reduce protein degradation. Approximately 1ml of buffer containing protease inhibitor was added for every 0.1g of tissue. Where the phosphorylation state of proteins was to be investigated a phosphatase inhibitor (Roche) was also included in the buffer. The tissue was homogenised using a syringe. Extractions using suspension buffer were boiled for 10 minutes and then centrifuged at 14,000rpm in a bench top centrifuge for 10 minutes. RIPA buffer extractions were centrifuged without boiling. The supernatant containing protein was collected and the cell debris pellet discarded.

2.3.2. Bradford Assays

Protein concentration of extracts was determined by Bradford assay. Bradford reagent changes colour in the presence of protein, and the optical density can be quantified to determine the amount of protein in each sample. Nine bovine serum albumin (BSA) protein standards ranging from 0.8µg/µl to 0µg/µl were used to determine the concentration of the samples. Standards were made up in the same buffer as was used in protein extraction to eliminate the effect of different absorbance of the different buffers.

Extracts and the standards were diluted 1:19 in 1M NaOH. 5µl of each sample was loaded into a 96–well plate in triplicate along with 200µl room temperature Bradford Reagent (Sigma-Aldrich) in each well and incubated at room temperature for 5 minutes. Absorbance was read at 595nm using a SpectraMax 190 plate reader and Softmax Pro 4.0 software (both Molecular Devices, Wokingham, UK). The protein content of each sample was determined in relation to the protein standards.

2.3.3. Sodium Dodecyl Sulphate Polyacrylamide Gel Electrophoresis

Protein samples were denatured by boiling for 10 minutes in protein loading buffer (see Appendix). The samples were then placed on ice for a minimum of 2 minutes immediately after boiling. Protein was separated by size using sodium dodecyl sulphate polyacrylamide gel electrophoresis (SDS-PAGE). The resolving gel (see Appendix) was either a 12% or 15% acrylamide gel, depending on the molecular weight (Mw) of the target protein. The higher percentage gel was used for low Mw targets as the higher percentage improves separation of smaller proteins by slowing the movement of all proteins across the gel. The gels were moulded using a casting system (Mini-Protean 3 Electrophoresis Cell, Bio-Rad, Hemel Hempstead, UK). A layer of isopropanol was placed over the resolving gel to ensure even setting. Once the resolving gel had set the isopropanol was discarded and the stacking gel (see Appendix) added, along with a 10 or 15 lane comb to mould the wells. Pilot studies utilising varying amounts of protein were used to determine the linear range of detection for each protein examined to ensure that the assays were quantitative; typically a protein quantity midway in the linear range was chosen for the quantitative studies. The gels were placed in running buffer (see Appendix) and the appropriate amount of each sample was loaded into the wells.

Approximately 100 volts was passed through the gels until the samples had travelled sufficient distance to separate the proteins, which took typically between 60 and 90 minutes. Kaleidoscope Precision Plus Protein Standard (Bio-Rad) was used in each gel as a molecular size marker.

2.3.4. Protein Transfer

The protein was transferred to a polyvinylidene fluoride (PVDF) membrane using the iBlot Dry Blotting System with PVDF Regular Transfer Stack (both Invitrogen, Paisley, UK) following the manufacturers instructions. Briefly, the anode stack with the PVDF membrane is placed on the bottom and the gel placed on top of the membrane. A piece of filter paper which had been soaked in dH_2O was placed over the gel before the cathode stack was placed on top with the disposable sponge. The transfer was run for 7 minutes at 20 volts.

2.3.5. Western Blotting of PVDF Membrane

The PVDF membranes were soaked in blocking buffer (2% milk in PBS with 0.1% Tween20) for 1 hour at room temperature and probed with primary antibody, diluted to the appropriate concentration (as determined by pilot studies, see Table 2.5) in blocking buffer, for 1 hour at room temperature. Following three 15 minute washes in PBS containing 0.1% Tween20 (PBS-Tw), the membranes were incubated for 30 minutes with the appropriate secondary antibody horseradish peroxidase (HRP) conjugate diluted to 1/5000 in blocking buffer, followed by a further three 15 minute washes in PBS-Tw. The secondary antibody used was either goat anti-rabbit or goat anti-mouse (both Bio-Rad) depending on the species in which the primary antibody was raised (see Table 2.5).

Antibody binding was visualised by electrochemiluminescence (ECL), which produces light in a reaction catalysed by the HRP on the secondary antibody, using an ECL Plus Western Blotting Detection System and Hyperfilm ECL (both GE Healthcare).

Target	Supplier	Catalogue Number	Host Species	Antibody Concentration
KIS	Abcam	Ab38292	Rabbit	1/1000
KIS	Abgent	AP8067a	Rabbit	1/500*
KIS	Caldwell 1999	JH1998	Rabbit	1/10000
Stathmin	Abcam	Ab52906	Rabbit	1/5000
Stathmin (pSer38)	GenScript	A00324	Rabbit	1/500
$p27^{kip1}$	Biosource	AHZ0462	Rabbit	1/1000
$p27^{kip1}$ (pSer10)	Abcam	Ab62364	Rabbit	1/1000
GAPDH	Sigma-Aldrich	G8795	Mouse	1/40000

Table 2.5: Antibody details and concentrations for western blotting.
All antibodies are polyclonal except GAPDH, which is monoclonal. pSer38, phosphorylated on the serine 38 residue; pSer10, phosphorylated on the serine 10 residue; * = Primary antibody incubated at 4°C overnight. Abcam, Cambridge, UK; Abgent, California, USA; GenScript, New Jersey, USA; Biosource, California, USA; The KIS antibody JH1998 is as described in Caldwell et al., 1999.

2.3.6. Quantification of Western Blots

The immunoreactivity of each sample was measured using AlphaEraseFC software (version 3.1.2, Alpha Innotech Corporation, California, USA). A background measure was taken for each sample and subtracted from the immunoreactive signal measured. For quantitative western blot experiments, the immunoreactivity of the test sample was normalised to the housekeeping gene GAPDH, to correct each measurement for any variation in the total amount of protein in each sample which may be caused by uneven transfer to the PVDF membrane or by pipetting errors. GAPDH was measured on the same membrane as the target protein. After the target protein had been detected, the membrane was washed for 2 minutes in methanol, 2 minutes in dH_2O, and 15 minutes in

PBS-Tw. The membrane was then soaked in blocking buffer for 1 hour before being blotted with the GAPDH antibody as described in Section 2.3.5. Both the protein of interest and GAPDH were corrected for background signal before normalisation.

2.3.7. Experimental Controls

Western blot without primary antibody was used as a control for non-specific binding of the secondary antibody. For the KIS antibodies, a recombinant KIS protein (Abnova, Taipei, Taiwan) was also used to test for the specificity of the primary antibody.

2.4. Immunohistochemistry (IHC)

Immunohistochemistry (IHC) uses antibodies to detect and visualise the location of a protein antigen in tissue sections. A KIS antibody was incubated with tissue sections and visualisation of antibody binding was used to examine the cellular distribution of KIS.

2.4.1. Tissue Preparation

Tissue sections of 14μm thickness, stored at -80°C until use, were placed at room temperature for between 30 and 60 minutes. During this time a wax circle (ImmEdge hydrophobic barrier pen, Vector Laboratories, Peterborough, UK) was drawn around the sections and allowed to dry. This forms a barrier which contains the solutions to ensure the sections remain covered during incubations. Sections were then fixed in 4% paraformaldehyde in PBS for 5 minutes before being washed in dH_2O for 5 minutes. Tissue sections were then dehydrated in increasing concentrations of IMS (70%, 95%, and 100%, 1 minute each). The antibody detection system used utilises a peroxidase

enzyme which allows immunoreactivity to be detected by the colour change associated with the peroxidase activity. To ensure the signal detected was the result of antibody binding rather than endogenous enzymes present in the tissue, it was necessary to deplete endogenous peroxidases from the tissue. This was done by placing the slides in solution of 3% hydrogen peroxide (VWR) in methanol for 30 minutes. The slides were then re-hydrated by placing them in decreasing concentrations of IMS (100%, 95%, and 70%, 1 minute each) followed by a 1 minute in dH_2O and 2x5min washes in PBS.

2.4.2. Immunohistochemistry of KIS

Non-specific binding sites were blocked by incubation with 5% normal goat serum in PBS with 0.3% Triton X-100 (PBS-T) for 1 hour at room temperature. The blocking serum used was from the species within which the secondary antibody was raised. The sections were then rinsed in PBS before being incubated at 4°C overnight with the KIS antibody Ab38292 (Abcam, Cambridge, UK) diluted to 1/100 in solution of 1% normal goat serum and PBS-T. The following day the sections were washed in PBS (3x10min) and bound antibody was visualised using the Vectastain elite ABC kit (rabbit IgG) (Vector Laboratories). The ABC kit detects binding of the primary antibody using an avidin and biotinylated HRP macromolecular complex which produces a coloured product localised to the biotinylated secondary antibody. The secondary antibody and reagents A and B were provided in this kit. The slides were incubated in a solution of PBS-T with 1% secondary antibody and 1% normal goat serum for one hour at room temperature and washed in PBS (3x10 minutes). The sections were then incubated in a solution made up of 1% of each of reagents A and B in PBS-T for 1 hour at room temperature, washed in PBS (3x10 minutes), and developed by immersion in a filtered solution of 0.025% diaminobenzidine (DAB) and 0.00018% hydrogen peroxide in PBS

for ten minutes. DAB acts as the substrate for the colour-change reaction. The sections were then washed in PBS (2x2 minutes), rinsed in dH_2O, and dehydrated in IMS (70%, 95%, and 100%, 1 minute each) before being placed in xylene. Coverslips were placed over the slides, fixed in place with DPX.

2.4.3. Experimental Controls

Western blotting was used to determine the specificity of the KIS antibody by confirming that the antibody detected a single protein band of the predicted molecular weight. Control sections which were incubated without the primary antibody were used to indicate any non-specific binding of the secondary antibody.

2.5. Reverse Transcription Polymerase Chain Reaction

Reverse transcription polymerase chain reaction (RT-PCR) allows investigation of the presence and quantity of expression of specific mRNAs. The mRNA is first reverse transcribed to create cDNA, and specific cDNA sequences can then be amplified using thermal cycling and primers targeting the sequence of interest. More of the target cDNA will be produced with each cycle, resulting in exponential amplification of the target sequence which can be visualised using gel electrophoresis (RT-PCR), or through the detection of a fluorescent reporter using quantitative RT-PCR (qPCR).

2.5.1. RNA Extraction

Tissue was homogenised in Tri-reagent, with approximately a 1:10 ratio of tissue to Tri-reagent. 200µl of chloroform (stored at -20°C) was then added for every 1ml of Tri-

reagent, and samples were then vortexed and left at room temperature for 10 minutes before being spun at 14,000rpm in a bench-top centrifuge for 15 minutes. The top phase of the solution containing the RNA was collected and placed into a fresh microcentrifuge tube along with an equal volume of isopropanol to precipitate the RNA. After an overnight incubation at -20°C, the solution was centrifuged at 14,000rpm for 10 minutes to form a pellet of the precipitated RNA. The supernatant was discarded and the pellet washed twice in 70% ethanol. The pellet was then left to dry at room temperature for ten minutes before being re-suspended in nuclease free water (nfH_2O). The concentration of the re-suspended RNA was measured using a NanoDrop ND-1000 Spectrophotometer and NanoDrop 3.0.1 software (NanoDrop Technologies, Delaware, USA). A 50ng/µl aliquot of the RNA was used to measure the RNA integrity number (RIN) of the sample. The RIN provided a measure of the quality of RNA in the sample. The RIN was measured using a Total RNA 6000 Nano LabChip kit, a 2100 Bioanalyzer, and the 2100 Expert software (all Agilent Technologies, Wokingham, UK). The RIN of each sample was calculated by the software by measuring the ratio of the two ribosomal RNA bands and also by the presence or absence of degradation products.

2.5.2. Reverse Transcription

The standard method for reverse transcription was as follows: 2µg RNA was DNase treated by heating to 37°C for 30 minutes followed by 10 minutes at 70°C with 1 unit RNase-free DNase and 24 units ribonuclease inhibitor (both Promega) in each sample. The DNase treatment was used to remove genomic DNA to ensure that cDNA rather than genomic DNA was amplified in subsequent PCR steps. The resulting DNase free RNA was then reverse transcribed by heating at 42°C for 1 hour followed by 10minutes at

70°C with 30ng oligo dT (20xTTP), 200 units M-MLV reverse transcriptase, 24 units ribonuclease inhibitor, 0.5mM of each dNTP (ATP, CTP, GTP, and TTP) in each sample. Oligo dT was used as it binds to the poly A tail which is present at the 3' end of the vast majority of mRNA sequences to provide a primer for the reverse transcriptase to extend from. Using oligo dT also ensures that only intact mRNA is reverse transcribed as the polyA tail is the first point of the mRNA to degrade, whereas alternatives such as random hexamers may reverse transcribe fragmented mRNA.

2.5.3. RT-PCR

RT-PCR was carried out using the appropriate amount of cDNA, as determined by pilot studies, and AmpliTaq PCR beads (GE Healthcare). The PCR beads contain all the necessary enzymes, buffers, and nucleotides required for the PCR. Verti thermal cyclers (Applied Biosystems, Warrington, UK) were used for amplifications. Primers had a final concentration of approximately 1µM. Primer sequences are listed in Table 2.6. Cycling conditions varied depending on the optimal conditions for the primers used in each assay, but the standard conditions were: 95°C for 5 minutes, followed by 35 cycles of 95°C for 30 seconds to melt double stranded cDNA, 60°C for 45 seconds for annealing of primers, and 72°C for 45 seconds for the polymerase to extend a copy of the cDNA from the primers. This is followed by a final extension phase of 72°C for 7 minutes.

Target mRNA	Amplicon Size (bp)	Primer Sequence
KIS (exons 1-2)	117	F: 5’ TGC AGG GTC ACA GAA ACA TC
		R: 5' GCA ATT CCG AAA CAC TGA CA
KIS (exons 1-8)	904	F: 5’ TGC AGG GTC ACA GAA ACA TC
		R: 5’ GCT TTG GAA TCA CCA GCA TT
KIS (exons 4-5)	140	F: 5’ TTG CCA GTA AAG CAG TGG TG
		R: 5’ CAA AAG GAA TGC TAA AGA ATG G
KIS (variant 2)	915	F: 5’ ACC GAA GGT CTG TGT TGA CC
		R: 5’ GCT TTG GAA TCA CCA GCA TT
GAPDH*	147	F: 5' GTG GAC CTC ATG GCC TAC AT
		R: 5' TGT GAG GGA GAT GCT CAG TG
GUSB**	77	F: 5' TCA CTC GAC AGA GAA ACC CCA
		R: 5’ CTC TGG TTT CGT TGG CAA TCC
HPRT**	175	F: 5’ GCC CCA AAA TGG TTA AGG TTG
		R: 5’ TCC ACT TTC GCT GAT GAC ACA
TFRC***	113	F: 5’ TGG GTC TAA GTC TAC AAT GGC TG
		R: 5’ CCC TCA TGA CGA ATC TGT TTG

Table 2.6: PCR primer sequences.
* = from Yoshikawa et al., 2004; ** = from Yamaguchi et al., 2005; *** = from Nishimura et al., 2006; bp, base pairs; F, sequence in forward (sense) direction; R, sequence in reverse (antisense) direction.

2.5.4. Gel Electrophoresis and PCR Product Visualisation

Amplified cDNA was mixed with loading buffer (Sigma-Aldrich) and loaded into a 1.5% agarose TAE gel (1.5g agarose and 5µl ethidium bromide (EtBr) per 100ml TAE running buffer (see Appendix)), and gel electrophoresis was used to separate the amplified cDNA by size. A DNA ladder (123bp ladder, Sigma-Aldrich) was run alongside the samples in each gel. Approximately 100 volts was used for electrophoresis. The amplified cDNA was then visualised using ultra-violet light viewed through AlphaEraseFC software.

Ethidium bromide binds to the double stranded DNA and is visible under ultra-violet light, allowing visualisation of the presence and size of amplified cDNA.

2.5.5. Quantitative Reverse Transcription Polymerase Chain Reaction (qPCR)

qPCR follows the same principles as conventional RT-PCR, but with the addition of a fluorescent reporter which is used to determine the quantity of target cDNA as the reaction proceeds. By measuring how many PCR cycles it takes for the level of fluorescence in each reaction well to reach a threshold, the amount of the target cDNA present initially can be estimated by comparing the threshold cycle (C_t) of each well to a standard curve made up of known cDNA quantities. qPCR is more sensitive than conventional RT-PCR (typically requiring smaller starting quantities of cDNA) and can be used to provide a more accurate measure of mRNA expression. Whilst conventional RT-PCR measures gene expression in the samples based on the end point of the reaction (generally in the plateau phase), qPCR collects data during the progression of the reactions and can determine the point at which samples reach a threshold during the exponential amplification phase, giving a much more accurate quantitative measure (see Figure 2.2).

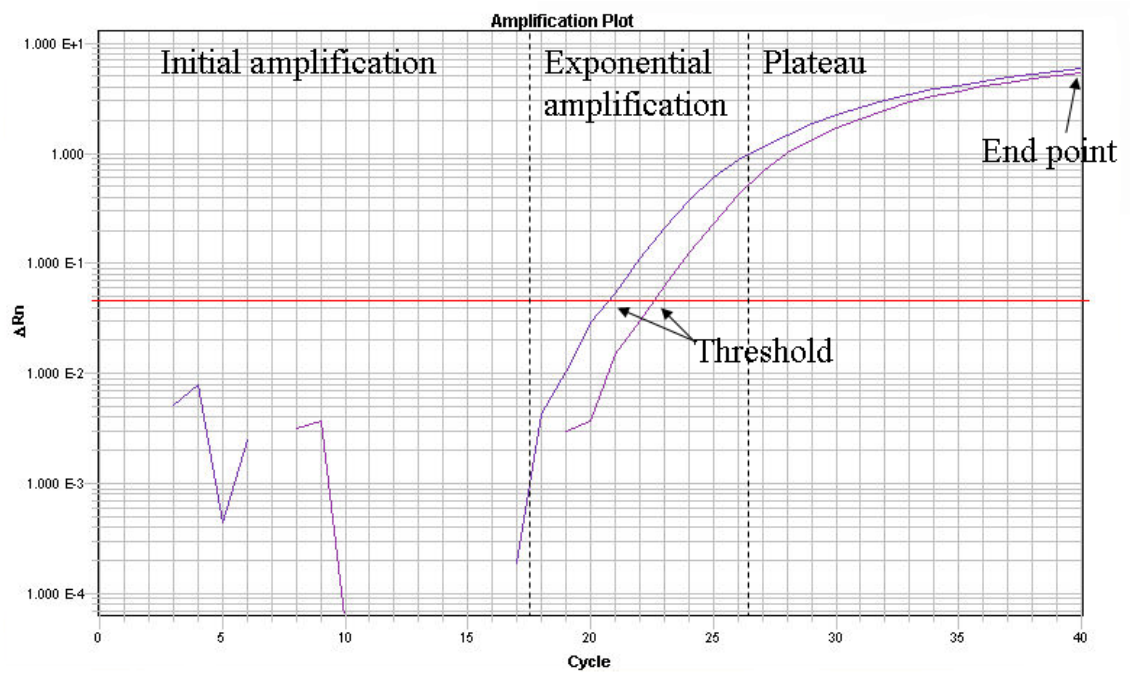

Figure 2.2: Amplification phases of PCR.
Plot shows number of PCR cycles (X axis) against quantity of PCR product (Y axis).

Either TaqMan probes or SYBR Green can be used to provide fluorescence in qPCR assays. TaqMan probes are complementary to a sequence within the target cDNA and located between the target sequences of the primers used for amplification. The probe consists of a fluorescent tag and a non-fluorescent quencher which prevents the fluorescence being released while the probe is intact. During the amplification phase the probe will bind to the target sequence and will be broken down by the exonuclease activity of the Taq polymerase enzyme as the cDNA is amplified. The breakdown of the probe causes the fluorescent tag to be released into the solution, which allows this fluorescence to be detected. SYBR Green is fluorescent in the presence of double stranded DNA and so the more the target cDNA is amplified the more fluorescent signal will be detected. Because the SYBR Green is not specific to the target sequence the primers used must be specific to the desired target and produce only a single PCR product, as any unwanted products caused by non-specific primer binding would cause

an increase in fluorescence and make the measurements inaccurate. For this reason pilot studies were used to determine the appropriate primer pairs to be used, and a dissociation curve was also used to determine if there was only a single product present in all reactions. The dissociation curve was produced at the end of the PCR reaction by gradually changing the temperature of the samples, and as products of different sizes will have different melting points the number of peaks of fluorescence over the temperature range will indicate if multiple products are present.

The qPCR measurements of KIS expression were normalised to one or more housekeeping genes (HKGs). HKGs were selected on the basis that their expression is expected to be consistent between individuals regardless of factors such as age, sex, and disease state. The measurements of the quantity of expression of the gene of interest can be normalised to the expression of these housekeeping genes in order to control for any sampling differences, such as differences in the total amount and/or quality of cDNA (Tunbridge et al., 2010). Where more than one housekeeping gene was used, KIS expression was normalised to the geometric mean of the housekeeping genes in order to increase the accuracy of the normalisation (Vandesompele et al., 2002).

2.5.5.1. qPCR of Human mRNA

RNA expression in humans was measured by qPCR in the STG, ACC, and cerebellum. Reverse transcription of all samples from these samples were as described previously (Section 2.5.2). KIS and four HKGs were quantified using TaqMan Universal PCR Master Mix, No AmpErase UNG (Applied Biosystems) and Taqman assays (Applied Biosystems, KIS: assay Hs01111761_m1; β-2-microglobulin (B2M): assay

Hs99999907_m1; glyceraldehyde-3-phosphate dehydrogenase (GAPDH): assay Hs99999905_m1; glucuronidase, beta (GUSB): assay Hs99999908_m1; transferrin receptor (TFRC): assay Hs00951094_m1). Each reaction contained 10ng (human ACC) or 20ng (human cerebellum and STG) cDNA. The amount of cDNA to be used was determined in pilot studies. Each plate for each brain region included a standard curve ranging from 150 to 2.34375ng cDNA which was made up of a pool of cDNA samples from the brain region being measured. STG samples were quantified using the average of four reactions, ACC and cerebellum were measured in triplicate. Each point of the standard curve was in triplicate on all plates. qPCR conditions were: initial denaturing step of 10 minutes at 95°C, followed by 40 cycles of 15 seconds denaturing at 95°C and 60 seconds of primer annealing/extension at 60°C. Samples were quantified using a standard curve and SDS v2.2.2 software with a 7900HT qPCR system (Applied Biosystems).

2.5.5.2. qPCR of Rat mRNA

RNA was extracted from coronal sections of brain tissue from the anti-psychotic treated rats at the level of the frontal cortex and the cerebellum as described in Section 2.5.1. Reverse transcription was as described in Section 2.5.2. except that 1.3µg RNA, 40ng oligo dT, 267 units M-MLV reverse transcriptase, 32 units ribonuclease inhibitor, and 0.67mM of each dNTP was used. The differences between the reverse transcription methodologies used for human and rat samples were due to low yield in some of the rat RNA extractions which required the use of a larger volume of RNA, necessitating the adjustment of the quantity of the other reagents accordingly.

qPCR of each rat sample was performed in triplicate, with each well containing 7.5ng of cDNA template. The standard curve was made up from a pool of equal amounts from each of the 24 samples and which were diluted serially to give a range of 75ng to 0.59ng of cDNA. qPCR of the standard curve samples were also performed in triplicate.

qPCR of KIS and housekeeping genes mRNAs in rats was performed using powerSYBR Green (Applied Biosystems). The primers used to quantify KIS targeted exons 4-5. GAPDH, GUSB, and hypoxanthine guanine phosphoribosyl transferase (HPRT) were measured as housekeeping genes. All primer sequences are shown in Table 2.6. KIS (exons 4-5), GAPDH, GUSB, and HPRT primers are 100% homologous to the respective transcript sequences in rats (KIS, NM_017293; GAPDH, NM_017008; GUSB, NM_017015; HPRT, NM_012583). Each qPCR reaction well contained 0.2μM of reverse and forward primer for each transcript and 7.5ng cDNA. PCR conditions were identical to those used for human samples (see Section 2.5.5.1) except the anneal/extend temperature for KIS was 58°C, and all SYBR Green assays also had a dissociation curve after the final cycle.

2.5.6. Experimental Controls

PCR in the absence of cDNA, in which nfH_2O was added to the reaction instead of cDNA, was used as a control. Any signal obtained from these samples would provide an indication of cDNA contamination in the reagents. In some experiments RT negative controls were also used, where the reverse transcriptase enzyme was not added to the reverse transcription reaction. Any signal in these samples would indicate the presence of genomic DNA or of cDNA contamination. For qPCR reactions using SYBR Green, confirmation that there was only a single PCR product was carried out using a

dissociation curve of all samples and also by gel electrophoresis of selected samples using a DNA 1000 LabChip kit, a 2100 Bioanalyzer, and 2100 Expert software (all Agilent Technologies).

2.6. Immunoautoradiography

Immunoautoradiography allows quantitative investigation of the immunoreactivity of antibodies directed at proteins of interest in tissue sections using radioactively labelled secondary antibodies. This technique provides information of the distribution of the immunoreactivity which cannot be determined from tissue homogenates, while also allowing more reliable quantification of the immunoreactivity than with IHC as the signal can be measured against ^{14}C microscales in terms of ^{35}S nCi/g tissue equivalents, overcoming the problem of variability of staining intensity found in IHC (Eastwood et al., 1995). Immunoautoradiography was performed on human STG and DLPFC tissue (see Section 2.2.1) to quantify the immunoreactivity of a KIS antibody.

2.6.1. Tissue Preparation and Immunoautoradiography

Frozen tissue sections of 14μm thickness, stored at -80°C until use, were placed at room temperature for one hour. As with IHC (Section 2.4), a wax circle was drawn around the sections and allowed to dry. Tissue sections were then fixed using 4% paraformaldehyde in PBS (5min) and washed in PBS (2x5min). Non-specific binding sites were blocked by incubating sections with 10% donkey serum (Sigma-Aldrich) in PBS-T for 1 hour. Sections were then rinsed in PBS and incubated at 4°C overnight with KIS antibody (Ab38292) diluted to 1/100 with 1% donkey serum in PBS-T. After PBS washes (3x10min) sections were incubated for 1 hour with 0.5μCi/ml ^{35}S-labelled donkey anti-

rabbit IgG (GE Healthcare) in PBS-T with 1% donkey serum, followed by PBS washes (3x10min). Two tissue sections were used from each subject in each brain region.

2.6.2. Experimental Controls

Western blotting was used to determine the specificity of the KIS antibody by confirming that the antibody detected a single protein band of the predicted molecular weight. Control sections which were incubated without the primary antibody were used to indicate any non-specific binding of the secondary antibody.

2.6.3. Visualisation and Measurement

DLPFC sections were placed against Biomax MR Film (Sigma-Aldrich) for 13 days, and STG sections against Hyperfilm ECL (GE Healthcare) for 24 days, both alongside ^{14}C microscales (GE Healthcare). The films were developed as described in Section 2.2.3. Measurements were made using the methods described in Section 2.2.5 with the MCID image analysis system, and calibrated to the ^{14}C microscales. KIS immunoreactivity was measured through the depth of the cortex. Non-specific binding, determined using sections incubated without KIS primary antibody, was subtracted from each measure.

2.7. Immunoblot of Lymphoblast Cell Lines

2.7.1. Immunoblot

Lymphoblast cell lines were maintained in RPMI 1640 (Lonza, Basel, Switzerland), 1% L-glutamine (200mM), and 10% heat inactivated fetal bovine serum (FBS) (Cambrex, New Jersey, USA) until they reached $5x10^5$ cells/ml (logarithmic growth phase). Cell

division should be at a constant rate during this phase. Cell lines were maintained by T Lane. Approximately $10x10^6$ cells were lysed by boiling for 10 minutes in suspension buffer with protease inhibitor (Roche). Protein content was determined by Bradford assay (as in Section 2.3.2). Pilot studies established the linear range over which KIS could be quantified. 2μg of protein (in 40% PBS and 60% suspension buffer) for each case was dried onto Immobilon-P Transfer Membrane (Millipore, Massachusetts, USA) in duplicate. The membranes were soaked for 2 minutes in methanol, 2 minutes in dH_2O, and blocked (1 hour with 2% milk in PBS-Tw), incubated with KIS antibody (Ab38292; 1/1000 diluted with 2% milk in PBS-Tw) for 1 hour at room temperature, washed (3x15min, PBS-Tw), incubated for 30min with Goat anti-Rabbit IgG HRP conjugate (Bio-Rad) at 1/5000 (diluted with 2% milk in PBS-Tw), and washed again (3x15min, PBS-Tw). Antibody binding was visualised using ECL Plus Western Blotting Detection System and Hyperfilm ECL (both GE Healthcare).

2.7.2. Experimental Controls

Western blotting was used to determine the specificity of the KIS antibody by confirming that the antibody detected a single protein band of the predicted molecular weight. Non-specific binding of the secondary antibody was determined in each sample using an immunoblot without the primary antibody.

2.7.3. Immunoblot Measurements

Immunoreactivity was measured using AlphaEraseFC software. Background signal, measured using the control membrane which was not exposed to KIS antibody, was subtracted from the average of the duplicate readings for each subject.

2.8. KIS Genotype Determination

rs7513662 is an intronic A/G single nucleotide polymorphism (SNP) located between exons 4 and 5 of the KIS gene (Figure 1.1). It was chosen for study as it is the only SNP associated with schizophrenia in two individual studies and also when the data from these two studies were combined (Puri et al., 2007; 2008; see Table 1.2). rs7513662 also tags a haplotype block (using an algorithm taken from Gabriel et al., 2002) which covers the entire KIS gene and surrounding sequence (Haploview version 4.0, Broad Institute, USA).

2.8.1. Genomic DNA Extraction

Genomic DNA (gDNA) was extracted from the cerebellum of all subjects in the SMRI array collection and the STG of the subjects in the NIMH series using a Nucleon Genomic DNA Extraction Kit (Tepnel Life Sciences, Manchester, UK) according to the manufacturers' instructions. Briefly, approximately 250mg of post-mortem tissue was homogenised and DNA extracted with a resin (supplied with the extraction kit) before being precipitated and cleaned using ethanol. The DNA pellet was then air dried and dissolved in nfH_2O by placing in a rotary mixer for two hours at room temperature. gDNA was extracted from lymphoblast cell line samples using DNeasy Blood and Tissue kit (Qiagen, Crawley, UK) according to manufacturers instructions.

2.8.2. Genotyping rs7513662 SNP

The genotyping of the rs7513662 SNP was performed using a 7900HT Real-Time PCR system (Applied Biosystems) and a TaqMan SNP Genotyping Assay designed to target

the rs7513662 SNP (Assay ID C___3033929_20, Applied Biosystems). This genotyping assay contained both forward and reverse primers spanning the site of the rs7513662 SNP, and also 2 fluorescent labelled probes, each specific to one of the alleles of the rs7513662 SNP. The probe targeting the A allele was labelled with VIC fluorescence, whereas the probe targeting the G allele was labelled with FAM fluorescence, each of which emitted fluorescence at distinct wavelengths. The genotyping assay worked under the same principle as TaqMan qPCR assays (as described in Section 2.5.5) but as a result of the different fluorescence (FAM or VIC) emitted by each probe the genotype of each sample could be determined by measuring the wavelength of fluorescence released. If VIC was detected then the gDNA contained the A allele, if FAM was detected the gDNA contained the G allele, and if both FAM and VIC were detected the gDNA contained both alleles.

Each reaction well consisted of between 20 and 30ng gDNA, genotyping assay (C___3033929_20), and TaqMan Universal PCR Master Mix, No AmpErase UNG (Applied Biosystems), made up to 5µl with nfH_2O (Promega). The amplification phase consisted of an initial 95°C hold for 10 minutes followed by 40 cycles of 15 seconds at 92°C and 60seconds at 60°C, in accordance with the manufacturer's instructions. After PCR amplification, the fluorescence of each of the samples was analysed using the allelic discrimination function of the SDS 2.2.2 software (Applied Biosystems) to identify the rs7513662 genotype of each sample. All genotypes were confirmed with a duplicate sample. The reproducibility of the genotype results was greater than 99%.

2.9. Stereological Measurements

Stereological measurements were made to determine the volume of brain structures in mice. In this process the volume was calculated by sectioning through the length of the structure and then calculating the area of the structure on the sections at regular intervals. This measurement of area was then multiplied by the distance between the sections measured to provide an estimate of the structures volume. This method is based on the Cavalieri principle, which essentially states that two objects with an equal cross-sectional area over their length will have an equal volume, regardless of their three dimensional shape. The two main methods of measuring the area of the structures are planimetry, which involves tracing around the edges of the structure and using a computer program to calculate the number of pixels within the area traced, or a point counting technique using a two dimensional rectangular grid made up of regularly spaced crosshairs where the number of crosshairs in contact with the region of interest provides an estimate of the area of the structure on the section. Each of these methods produce consistent and accurate measurements, but the point counting method has been shown to be a more efficient technique (Cotter et al., 1999), and as such was the method chosen for use in these studies.

The tissue sections were magnified using the MCID image analysis system, and a grid of crosshairs, spaced in a regular and uniform square array, was placed over the magnified image. The number of crosshairs in contact with the region of interest was counted on sections at regular intervals and the summation of the number of crosshairs was used to calculate the area of the region of interest on each section, corrected for the level of magnification. The sum of the areas across all sections measured was then multiplied by the distance between sections to give the volume of the measured region. Two

measurements were made of each structure on each section, and the average of these two measures was used for analysis.

2.9.1. Tissue Preparation

A selection of brains from KIS$^{-/-}$ and control mice had been fixed in parformaldehyde (see Section 2.1.2.2) and stored in 70% alcohol. Subsequently, brains were placed in 90% alcohol for two hours, followed by three steps in absolute alcohol (two hours in each of the first two steps and one hour in the final step). The brains were then treated in three changes of Histoclear (National Diagnostics, Georgia, USA), firstly for one hour, then overnight, and finally for a further one hour. They were then placed in three changes of paraffin wax (Lambwax pelletized paraffin, Raymond A. Lamb, Eastbourne, UK) at 57ºC for two hours in each step, before being embedded and cut into 14μm thick sections. Tissue preparation was carried out by M Walker. Sections were collected at 420μm intervals over the length of the whole brain, except where the lateral ventricles were visible, in which case sections were collected every 210μm in order to obtain additional sections to allow more accurate measurements of ventricular volume.

2.9.2. Partial Brain Volume

A representative measure of partial brain volume was taken by measuring coronal sections of the brain from the start of the corpus callosum to the end of the granular layer of the dentate gyrus (Figures 21 to 63, Paxinos and Franklin, 2004). The whole area of each section was measured between these points. This representative measure was taken rather than measuring across the whole length of the brain as the sections were often damaged at the very beginning and end of the brain, and so using more consistent

reference points within the brain provided a more reliable measure. The grid used to measure the area of the section was 19mm x 19mm. Corrected for magnification, this equates to 1.2258mm x 1.2258mm on the section, such that each crosshair represented an area of 1.5026mm^2. The distance between each section measured was 0.42mm. The volume was calculated from the area of the section multiplied by the distance between sections, therefore each crosshair represented a volume of 0.63mm^3.

2.9.3. Ventricular Volume

Ventricular volume was estimated by measuring the area of both lateral ventricles and the dorsal third ventricle (Figures 21 to 54; Paxinos and Franklin, 2004). Measurements were taken using a 5mm x 5mm grid. Corrected for magnification, this equates to 0.1786mm x 0.1786mm on the section, such that each crosshair represented an area of 0.03189mm^2. The distance between each section measured was 0.21mm. The volume represented by each crosshair was therefore 0.0066964mm^3.

2.9.4. Striatal Volume

The volume of the striatum was calculated by measuring the area of the caudate putamen and nucleus accumbens from the start of the corpus callosum to the point where the lateral ventricles meet (Figures 21 to 33; Paxinos and Franklin, 2004). The border of the structure measured was defined by the corpus callosum, lateral ventricles, and the cerebral cortex. Measurements were taken using a 5mm x 5mm grid. Corrected for magnification, this equates to 0.1724mm x 0.1724mm on the section, such that each crosshair represented an area of 0.029727mm^2. Measurements were taken every 15 sections, and each section was 0.014mm thick, so the distance between each section

measured was 0.21mm. The volume represented by each crosshair was therefore 0.0062426mm^3.

2.9.5. Hippocampal Formation Volume

The volume of the hippocampal formation was calculated by measuring the area of the hippocampus, the fimbria, and the subiculum over the whole length of the granular layer of the dentate gyrus (Figures 39 to 63; Paxinos and Franklin, 2004). Measurements were taken using a 5mm x 5mm grid. Corrected for magnification, this equates to 0.1786mm x 0.1786mm on the section, such that each crosshair represented an area of 0.03189mm^2. The distance between each section measured was 0.42mm. The volume represented by each crosshair was therefore 0.013393mm^3.

2.10. Statistical Analysis

All statistical analyses were carried out using the SPSS 16 program. Outliers were defined by the SPSS program as being greater than 1.5 times the interquartile range below the 25th percentile value or 1.5 times the interquartile range above 75th percentile value. Following the removal of the outliers, the normality of each set of data was determined by Kolmogorov-Smirnov test. Parametric tests were used where the data were normally distributed (ANOVA and post-hoc t-tests), otherwise nonparametric tests were used (Kruskal-Wallis or Mann-Whitney). A p-value ≤ 0.05 was considered to be significant and $0.1 \geq$ p-value > 0.05 was considered to be a trend.

2.10.1. KIS Expression during Development in Mice

For the investigation of KIS expression during development in mice using ISHH, the background signal measured from the control sections was subtracted from the measurements of KIS mRNA signal. For GAPDH expression a background measure was taken from each slide and subtracted from each measurement from sections on that slide. Each KIS measurement was then normalised to GAPDH by dividing the KIS signal by the GAPDH signal from the same area of the same animal. A univariate ANOVA was used to determine the effect of age on normalised KIS expression, and post-hoc t-tests were used to further investigate the differences between the age groups.

2.10.2. KIS Quantification in Human and Rat Samples

All experiments were performed and measured blind to diagnosis and genotype. Potential influences of continuous variables (such as pH, PMI, RIN, and age) were measured using either the Pearson or Spearman coefficient, depending on the normality of the data. Any variable showing a significant correlation with KIS expression was included as a covariate for that dataset. Categorical variables, such as gender, ethnicity, and smoking status, were also investigated for influence on KIS expression. Diagnostic group, genotype, and diagnosis by genotype interactions were included in the ANOVA, with any significant results investigated further using post-hoc t-tests, where the data were normally distributed. Where the data did not have a normal distribution the effect of diagnostic group and genotype were investigated separately using Kruskal-Wallis or Mann-Whitney tests as appropriate. For qPCR experiments, HKGs were excluded from the analysis if there was any significant difference in their expression between diagnostic groups, and the number of HKGs measured varied between brain regions due to limited mRNA availability. Where more than one HKG was used, the data of KIS expression

was normalised to the geometric mean of the HKGs. Due to the low frequency of the G allele for SNP rs7513662, G/G and A/G subjects were grouped together and compared to A/A subjects.

The data of KIS expression in rats treated with anti-psychotic medication was analysed as described for human samples.

2.10.4. KIS Knockout Mice

All experiments were performed and measured blind to genotype. For the western blot and ISHH experiments, samples were first investigated for the overall effect of genotype (with data from all brain regions combined), with genotype, brain region, and interactions between genotype and region included in the ANOVA. The effect of genotype in each brain region individually was then investigated using post-hoc t-tests. For the western blots each measurement was normalised to GAPDH by dividing the target signal by the GAPDH signal for each sample. For the stereological measurements, each region was tested for the effect of genotype using a univariate ANOVA, and the volume of each brain region was also tested as a percentage of the brain volume.

Chapter 3: Distribution of KIS Expression in Humans and Mice

3.1. Rationale of Experiments

There were two main objectives to the studies described in this chapter. The first was to explore the distribution of KIS mRNA and protein in the adult human brain, and the second was to investigate KIS through development in the mouse brain by examining its expression at several developmental time points.

As discussed earlier (Section 1.2.3), KIS expression in humans, rats, and mice has been found to be at its highest in the brain (Maucuer et al., 1995, 1997; Caldwell et al., 1999; Bièche et al, 2003; Langenickel et al., 2008; Table 1.3). To date, the only available data for KIS expression in the human brain are northern blot analyses and qPCR (Boehm et al., 2002; Bièche et al., 2003), and these data are limited as both only examined the mRNA from the whole brain in comparison to samples from elsewhere in the human body, and neither examined differences in KIS expression between brain regions. The distribution of KIS mRNA has been examined in the rat brain by ISHH in two studies (Caldwell et al., 1999; Bièche et al., 2003).

The first set of studies in this chapter aimed to confirm and expand on current knowledge of the distribution of KIS by using ISHH to detail KIS mRNA distribution in several human brain regions, and also by examining which cell types express KIS in the adult human brain. Further to this, KIS immunoreactivity was examined using IHC in order to determine the distribution of KIS protein. The IHC data of the distribution of KIS

immunoreactivity should complement and enhance the data obtained by ISHH by indicating the location of the translated protein, particularly in regard to its subcellular localisation which may provide clues to the functions of the KIS in adult neurons.

To date only one study has investigated KIS during development, and it found that KIS mRNA expression in the rat brain dramatically increased during development in whole brain mRNA measured using northern blot and qPCR (Bièche et al., 2003). Hence, the second part of this chapter aimed to confirm and extend this finding by using ISHH to quantify KIS mRNA at several ages in mice. Firstly the distribution of KIS mRNA in adult mice was investigated in detail in several brain regions, and KIS mRNA was then quantified in a selection of brain regions at several developmental time points to examine the changes in KIS mRNA expression through neurodevelopment.

3.2. Methods

3.2.1. Tissue Used for Study

KIS distribution in the adult human brain was investigated using post-mortem tissue sections from control subjects who had no known history of any brain disorder. The brain regions included in this study were the STG, ACC, DLPFC, occipital cortex, hippocampus, and cerebellum, which were supplied by NIMH, SMRI, or collected in Oxford. Further details of the tissue used are included in Section 2.1.1.

Tissue sections from the brains of the developmental series of mice were used to investigate the distribution and quantity of KIS expression during development. Details of this tissue can be found in Section 2.1.2.3. Coronal sections of the mouse brains at the

level of the hippocampus were used to investigate expression through development. The ages of the mice ranged from P0 to 2 years. Tissue from animals aged P63 were used to investigate the distribution of KIS in adult mice and included tissue sections at the level of the hippocampus, striatum, and cerebellum.

3.2.2. In Situ Hybridisation Histochemistry

ISHH was used to investigate KIS mRNA distribution in the human brain, allowing characterisation of both the regional and cellular distribution of KIS expression. ISHH was carried out as described in Section 2.2 on the human tissue, using the probe KIS (1), with 1,000,000 counts per minute (cpm) of labelled probe added to each tissue section. Sections were exposed to MS film for 19 days. A selection of tissue sections were emulsion dipped (see Section 2.2.3.2), with an exposure time of 30 days for the STG and 84 days for all other brain regions.

ISHH in mice was carried out as described for human samples above, except that 800,000 cpm of labelled probe were added to each section. Pilot studies established that this amount of probe was saturating for KIS in rodent tissue, in that an increase in the amount of probe did not increase mRNA signal. The mouse sections were exposed to MS film for 14 days (see Section 2.2.3.1), and a selection of the slides were also exposed to autoradiographic emulsion (see Section 2.2.3.2) for 81 days. GAPDH expression was also measured in the developmental mouse tissue as a housekeeping gene to determine if any change in KIS expression found was specific or simply paralleling changes in total mRNA expression at each point. 1,000,000 cpm of labelled probe were added to each section for the GAPDH ISHH and the sections were exposed to MS film for 2 days.

Probe sequences and the incubation and wash conditions for the KIS and GAPDH probes are as described in Section 2.2.2. The brain regions measured in the developmental mouse tissue were the visual cortex and the CA1, CA3, and dentate gyrus regions of the hippocampus for both KIS and GAPDH, using the methods described in Section 2.2.4.

The KIS (1) oligonucleotide probe is 100% complementary to human (NM_175866) and mouse (NM_010633) KIS sequences. The sequence of the KIS probe does not have any more than 50% homology with any other RefSeq transcripts found on BLAST search (NCBI) for humans or mice, and the target sequence is in exon 4 of the KIS mRNA transcript. The GAPDH oligonucleotide probe is 95% complementary to mouse GAPDH (NM_008084).

3.2.3. Immunohistochemistry

IHC was carried out as described in Section 2.4 using human tissue listed in Section 3.2.1.

3.2.4. Western Blotting

Western blotting was used to validate the antibody to be used for IHC. The full methods for the western blot are described in Section 2.3. Western blotting using the KIS antibody Ab38292 was performed using protein extracted from human cerebellum, and also recombinant KIS protein (Abnova), which is identical to 340 of the first 341 amino acids of the human KIS protein. As the recombinant KIS protein has a glutathione S-transferase tag, its molecular weight is 64kDa. Human KIS protein has a predicted molecular weight of 46.5kDa (Maucuer et al., 1997). 30µg human cerebellum protein

(extracted using suspension buffer as described in Section 2.3.1) and 0.075µg recombinant protein were used for the western blot.

3.3. Results

3.3.1. Human KIS Distribution

Using ISHH and IHC, KIS was detected in all brain regions examined. The autoradiograph images of KIS mRNA expression showed greater signal in deep than superficial layers in each cortical area examined (Figure 3.1A-E). There was strong KIS mRNA signal in the dentate gyrus, CA1, CA3, and CA4 regions of the hippocampus (Figure 3.1F), and KIS mRNA expression was also observed in Purkinje cells and in the granule cell layer of the cerebellum (Figure 3.1G). There was negligible mRNA signal in the white matter (Figure 3.1A-E). Minimal background signal was detected after hybridisation with a probe in the sense direction (see Figure 3.1H).

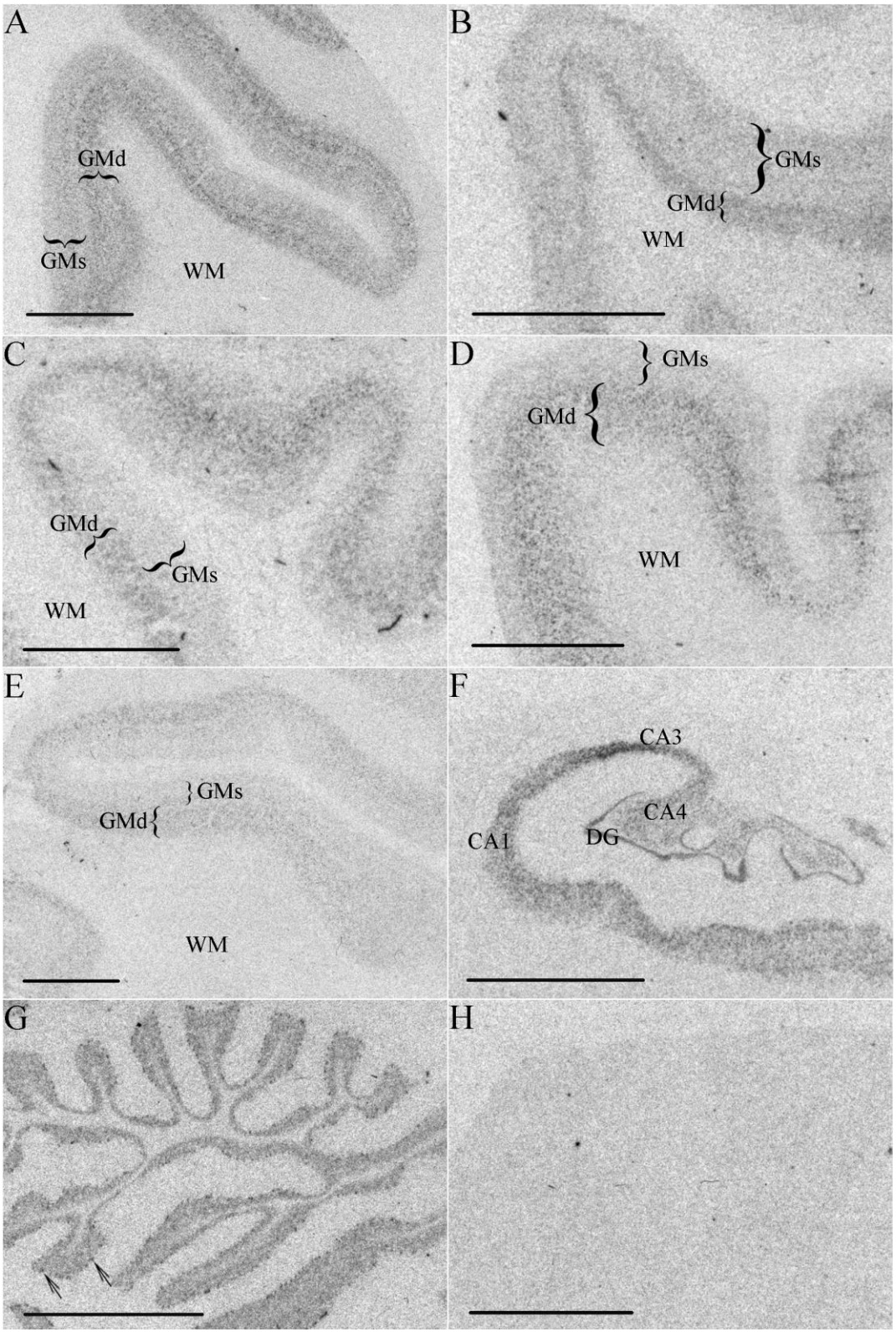

Figure 3.1: ISHH autoradiographs of KIS mRNA distribution in the human brain.
(A) Dorsolateral prefrontal cortex; (B) occipital cortex; (C) superior temporal gyrus; (D) anterior cingulate cortex; (E) superior temporal gyrus; (F) hippocampus; (G) cerebellum (arrows indicate Purkinje cells); (H) cerebellum sense control. CA, cornu ammonis; DG, dentate gyrus; WM, white matter; GMs, superficial layers of grey matter; GMd, deep layers of grey matter. Scale bar = 5mm.

Examination of emulsion-dipped ISHH sections demonstrated that KIS mRNA was expressed sparsely in the cells of the superficial layers of the cortex (Figure 3.2A) but was strongly expressed in the pyramidal cells of the deeper cortical layers (consistent with the film images) and was also present in some of the surrounding smaller cells, which are possibly interneurons (Figure 3.2B). KIS mRNA was widely detected in the hippocampus, particularly in the pyramidal cells of the CA3 region (Figure 3.2C) and the granule cells of the dentate gyrus (Figure 3.2E), and also in both Purkinje cells and granule cells of the cerebellum (Figure 3.2G). No signal was detected in the white matter (not shown), and the sense orientation control probe for ISHH showed minimal signal (Figure 3.2G insert).

The distribution of KIS immunoreactivity corresponded to that of KIS mRNA, as can be seen in the cortex (Figure 3.2A-B inserts), hippocampus (Figure 3.2D and 3.2F) and cerebellum (Figure 3.2H). No KIS immunoreactivity was found in the white matter (not shown), and IHC in the absence of the KIS primary antibody showed minimal staining (Figure 3.2H insert). At the cellular level both nuclear and cytoplasmic KIS immunoreactivity was detected, as can be seen in pyramidal neurons (Figure 3.2B insert and 3.2D) and Purkinje cells, where KIS immunoreactivity appears to extend into some proximal dendrites (Figure 3.2H).

The specificity of the KIS antibody was confirmed by western blot, which showed a single band of the expected size when the antibody was tested against recombinant KIS protein (64kDa; Figure 3.3A) and protein extracted from human cerebellum tissue (46.5kDa; Figure 3.3B).

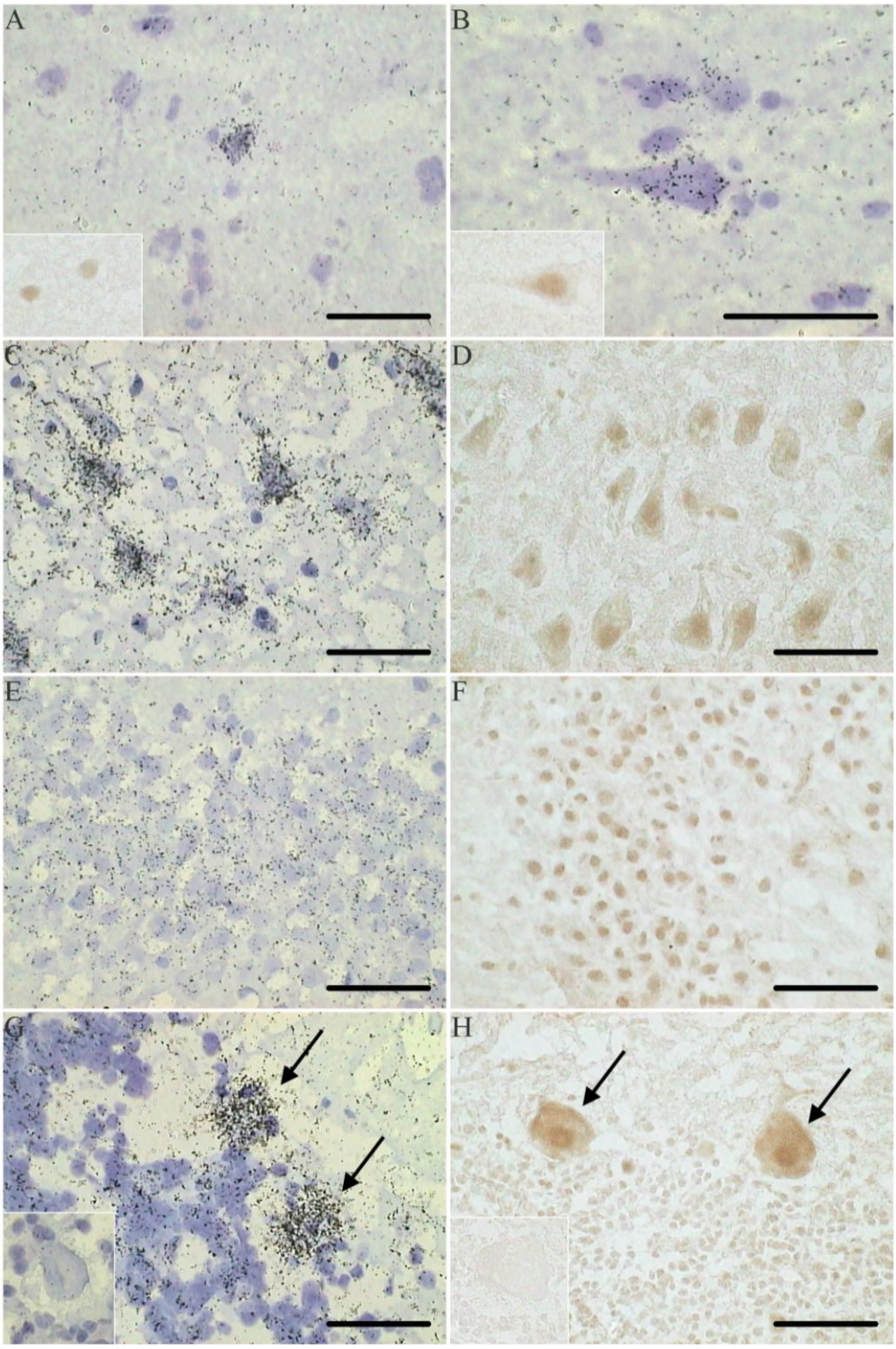

Figure 3.2: Cellular distribution of KIS mRNA and immunoreactivity in human brain.
(A) KIS mRNA and immunoreactivity (insert) in superior temporal gyrus, cortical layer 2; (B) KIS mRNA and immunoreactivity (insert), in superior temporal gyrus, cortical layer 3; (C) KIS mRNA in CA3; (D) KIS immunoreactivity in CA3; (E) KIS mRNA in dentate gyrus; (F) KIS immunoreactivity in dentate gyrus; (G) KIS mRNA in cerebellum, showing Purkinje cells (arrows); insert shows sense control; (H) KIS immunoreactivity in cerebellum, showing Purkinje cells (arrows); insert shows absence of staining after omission of the primary antibody. Scale bar = 50μm.

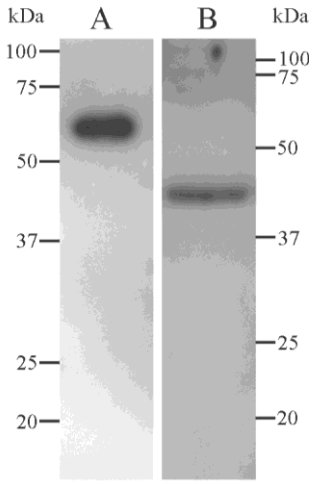

Figure 3.3: Western blot using the anti-KIS antibody (Ab38292).
(A) Recombinant KIS protein with GST tag; (B) Protein extracted from human cerebellum. Molecular weight markers shown are in kilodaltons (kDa).

3.3.2. KIS mRNA Distribution in Mice

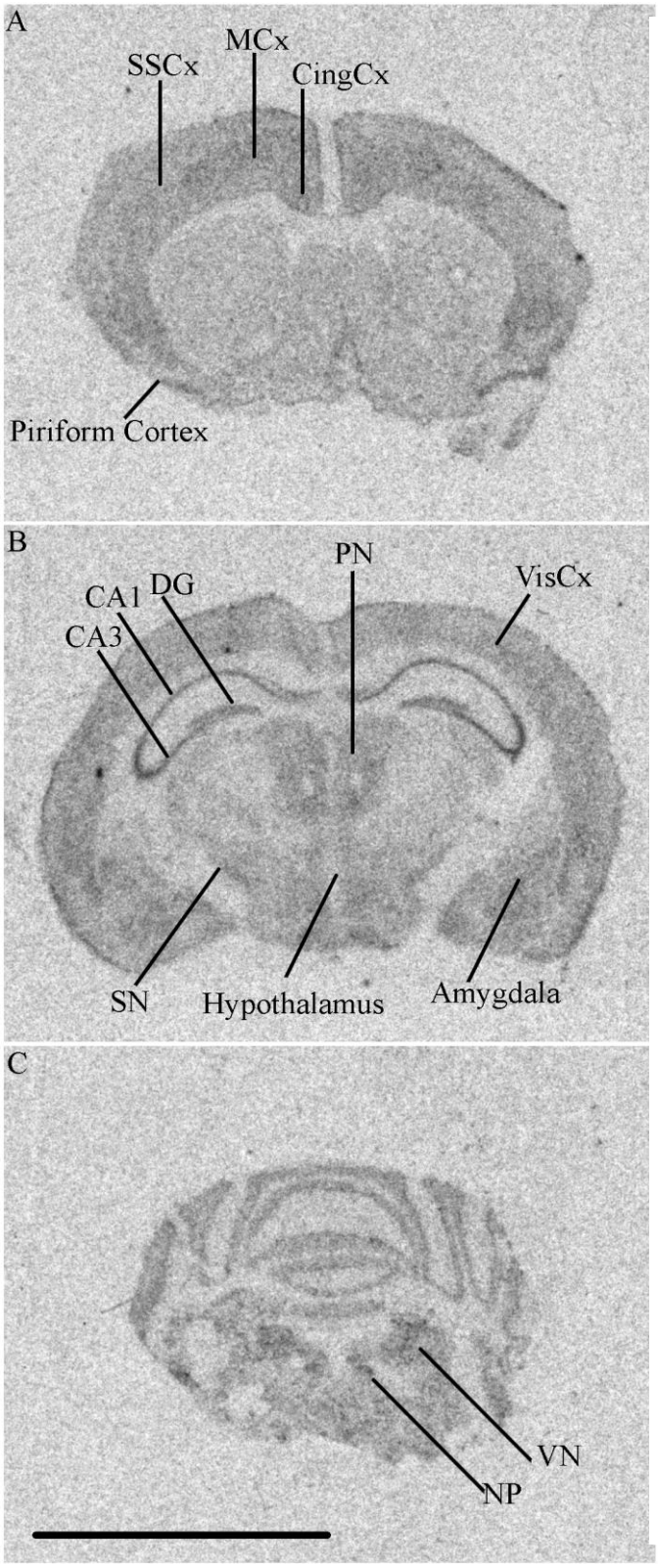

Figure 3.4: ISHH autoradiograph images of KIS mRNA expression in the mouse brain. Shown are coronal sections at the level of (A) the striatum, (B) hippocampus, and (C) cerebellum. Tissue shown is from a mouse at age P63. SSCx, somatosensory cortex; MCx, motor cortex; CingCx, cingulate cortex; VixCx, visual cortex; DG, dentate gyrus; CA1, cornu ammonis 1; CA3, cornu ammonis 3; PN, parafascicular thalamic nucleus; SN, substantia nigra; VN, vestibular nuclei; NP, nucleus prepositus. Scale bar = 5mm.

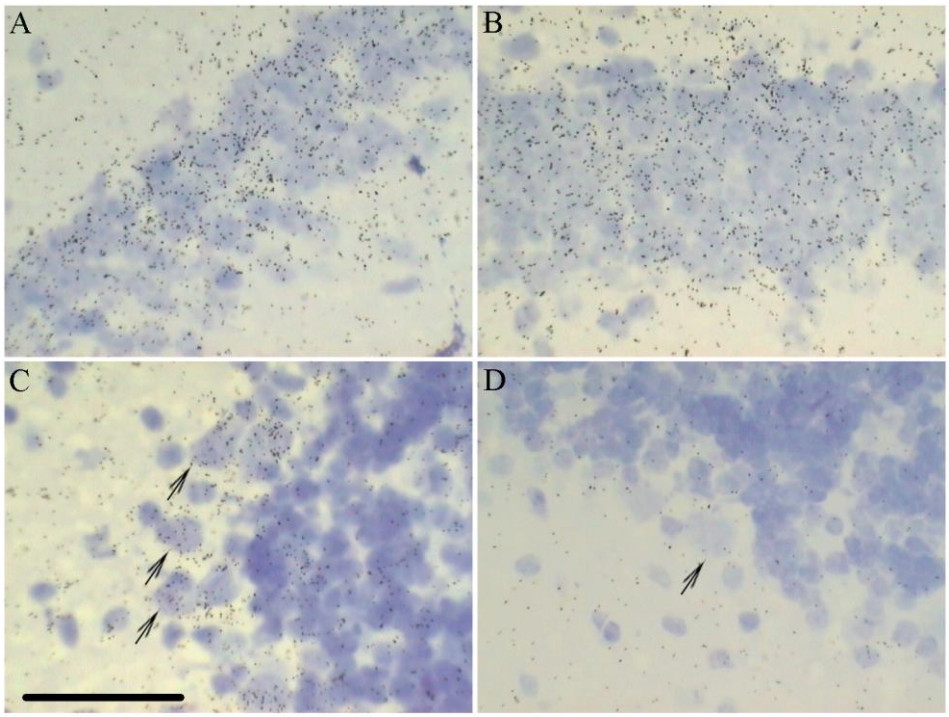

Figure 3.5: Cellular distribution of KIS mRNA in the adult mouse brain.
(A) CA1 region of the hippocampus; (B) dentate gyrus; (C) cerebellum showing Purkinje cells (arrows); (D) sense control cerebellum showing Purkinje cell (arrow). Scale bar = 50μm.

As observed in humans (Section 3.3.1), KIS mRNA was widely expressed in the adult mouse brain (Figure 3.4). KIS mRNA was expressed in all cortical regions examined (Figure 3.4A-B), and was strongly expressed in the dentate gyrus, CA1, and CA3 regions of the hippocampus, as well as in the amygdala, parafascicular thalamic nucleus, substantia nigra, and throughout the hypothalamus (Figure 3.4B, Figure 3.5A-B). KIS mRNA was also expressed in the cerebellum, with signal detected in the granular cell layer and Purkinje cells (Figure 3.4C, Figure 3.5C). High KIS expression was also detected in some of the nuclei of the brain stem, such as the vestibular nuclei and the nucleus prepositus (Figure 3.4C). The sense orientation control probe for ISHH showed minimal signal (Figure 3.5D).

3.3.3. KIS Expression during Development in Mice

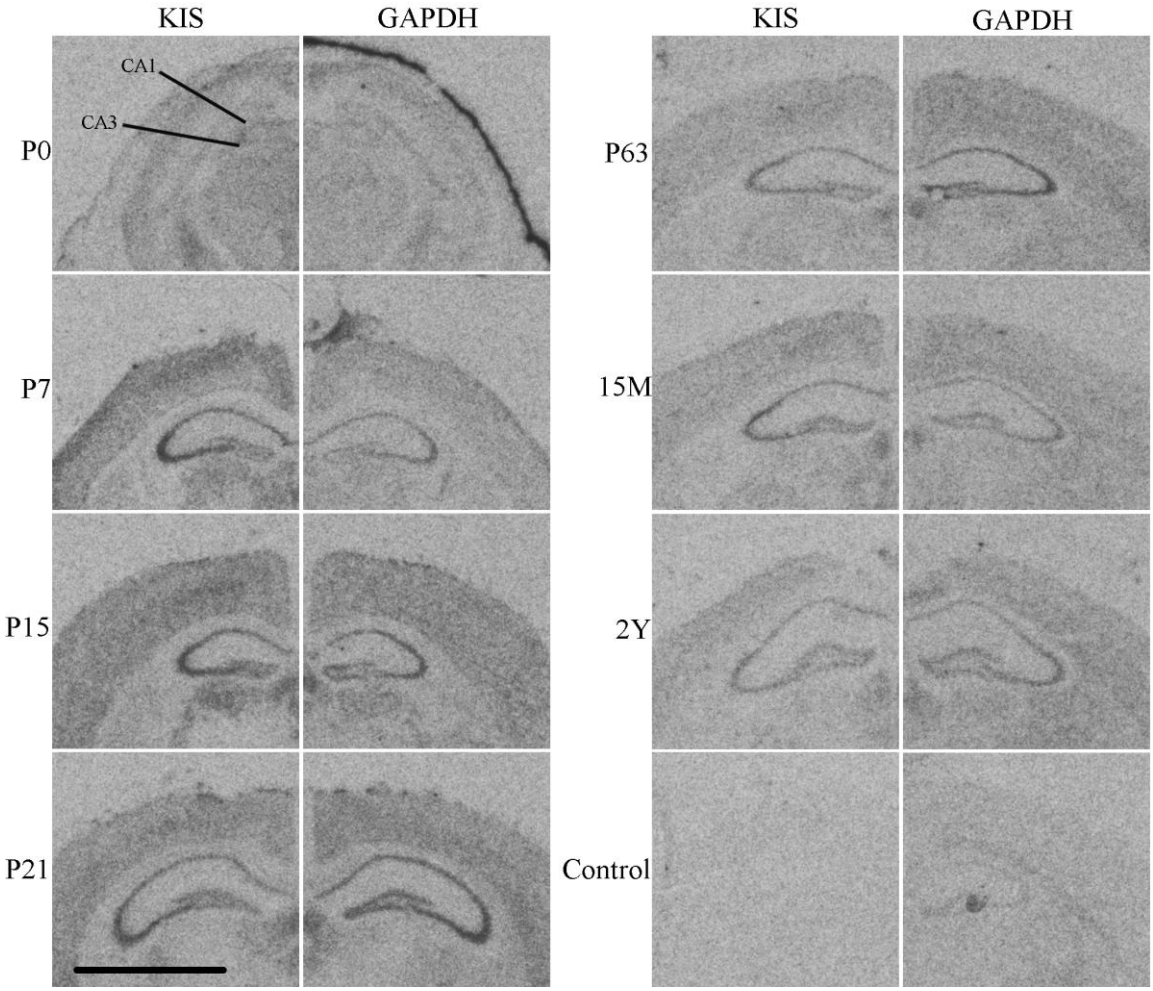

Figure 3.6: ISHH autoradiographs showing KIS and GAPDH mRNA expression in the hippocampus and overlying cortex through development.
P, postnatal day age; M, age in months; Y, age in years. Control section for KIS is from a mouse aged P52 ISHH with a sense orientation probe; control section for GAPDH is from a mouse aged P21 ISHH in the presence of 50-fold molar excess of unlabeled probe (see Section 2.2.4). Scale bar = 2.5mm.

KIS expression, normalised to GAPDH, was highest at P7 before declining sharply to P15 and steadily declining with age, with a slight rise between P63 and 15 months, in all four brain regions examined (Figure 3.6, Table 3.1). KIS expression was significantly different between age groups for all regions measured (Table 3.2). CA1, CA3, and visual cortex showed a rise in KIS expression from P0 to P7, a fall in expression to P63, followed by a rise to 15 months and a further fall to 2 years (Figure 3.7, Tables 3.3-3.6).

Dentate Gyrus

Age	N	KIS	GAPDH	Normalised KIS
P0	0	-	-	-
P7	4	147 ± 18	559 ± 127	0.267 ± 0.020
P15	6	256 ± 15	1627 ± 104	0.170 ± 0.017
P21	3	203 ± 21	1744 ± 147	0.116 ± 0.023
P63	4	144 ± 18	1403 ± 127	0.102 ± 0.020
15 Months	6	126 ± 15	796 ± 104	0.159 ± 0.017
2 Years	2	94	832	0.114

CA3

Age	N	KIS	GAPDH	Normalised KIS
P0	2	143	454	0.313
P7	4	409 ± 42	786 ± 119	0.522 ± 0.017
P15	5	519 ± 38	2257 ± 106	0.227 ± 0.015
P21	4	381 ± 42	2206 ± 119	0.172 ± 0.017
P63	4	206 ± 42	1585 ± 119	0.128 ± 0.017
15 Months	6	168 ± 34	914 ± 97	0.184 ± 0.014
2 Years	2	143	964	0.151

CA1

Age	N	KIS	GAPDH	Normalised KIS
P0	2	165	547	0.301
P7	4	234 ± 19	570 ± 61	0.409 ± 0.014
P15	5	299 ± 17	1673 ± 55	0.178 ± 0.013
P21	4	217 ± 19	1558 ± 61	0.139 ± 0.014
P63	4	182 ± 19	1355 ± 61	0.134 ± 0.014
15 Months	6	120 ± 16	640 ± 50	0.189 ± 0.011
2 Years	2	106	619	0.172

Visual Cortex

Age	N	KIS	GAPDH	Normalised KIS
P0	2	68	319	0.221
P7	3	133 ± 12	338 ± 52	0.394 ± 0.023
P15	6	132 ± 8	671 ± 37	0.203 ± 0.017
P21	4	100 ± 10	697 ± 45	0.144 ± 0.020
P63	4	61 ± 10	549 ± 45	0.109 ± 0.020
15 Months	6	51 ± 8	379 ± 37	0.133 ± 0.017
2 Years	2	34	378	0.089

Table 3.1: The expression of KIS and GAPDH mRNA during development in mice. Values are ^{35}SnCi/g tissue equivalents, mean ± standard error of the mean, except where N=2 for which the mean alone is shown; P, postnatal day.

The dentate gyrus was not measured in the P0 mice as it could not be clearly distinguished from the surrounding regions. KIS expression in the dentate gyrus followed the same pattern as the CA1, CA3, and visual cortex from P7 to 2 years (Figure 3.7, Table 3.1). The visual cortex was not measured in one of the P7 samples as the cortex was too badly damaged for accurate measurement. In the CA1 and CA3 regions one

outlier was removed from each of the P7, P15, and P21 groups, in the visual cortex one outlier was removed from each of the P7 and P21 groups, and in the dentate gyrus one outlier was removed from the P7 group and two were removed from the P21 group.

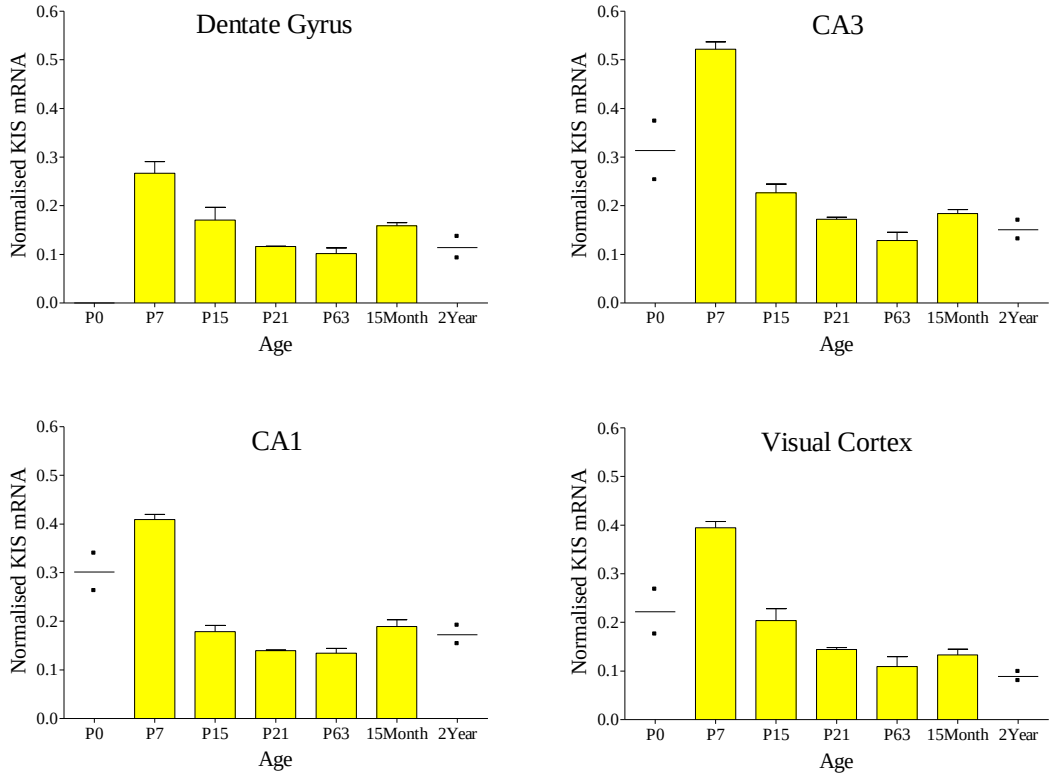

Figure 3.7: KIS mRNA expression in mice during development.
All values are ^{35}SnCi/g tissue equivalents of KIS expression normalised to GAPDH as measured using ISHH. Values shown are mean + standard error of the mean, except where N=2 for which the raw values and mean is shown. P, postnatal day.

Region	Effect of Age	
Dentate Gyrus	$F_{5,19}$=8.41	P<0.001
CA3	$F_{6,20}$=61.89	P<0.001
CA1	$F_{6,20}$=48.26	P<0.001
Visual Cortex	$F_{6,20}$=20.13	P<0.001

Table 3.2: The effect of age on KIS expression.
P-values determined by univariate ANOVA using data of KIS normalised to GAPDH in mice from P0 to 2 years in the CA3, and CA1 regions of the hippocampus and in the visual cortex, and from P7 to 2 years in the dentate gyrus.

Dentate Gyrus	P7	P15	P21	P63	15M	2Y
P7	-	↓**	↓***	↓***	↓**	↓***
P15	↑**	-	(↓)	↓*	-	-
P21	↑***	(↑)	-	-	-	-
P63	↑***	↑*	-	-	↑*	-
15M	↑**	-	-	↓*	-	-
2Y	↑***	-	-	-	-	-

Table 3.3: Post-hoc comparisons of KIS expression normalised to GAPDH over time in the dentate gyrus in mice.
Arrows indicate direction of change relative to the age group noted in the left column. DG, denate gyrus; P, age in postnatal days; M, age in months; Y, age in years; * = p-value<0.05; ** = p-value <0.01; *** = p-value <0.001; Brackets = 0.05< p-value <0.1; - = no significant change or trend.

CA3	P0	P7	P15	P21	P63	15M	2Y
P0	-	↑***	↓**	↓***	↓***	↓***	↓***
P7	↓***	-	↓***	↓***	↓***	↓***	↓***
P15	↑**	↑***	-	↓*	↓***	(↓)	↓*
P21	↑***	↑***	↑*	-	(↓)	-	-
P63	↑***	↑***	↑***	(↑)	-	↑*	-
15M	↑***	↑***	(↑)	-	↓*	-	-
2Y	↑***	↑***	↑*	-	-	-	-

Table 3.4: Post-hoc comparisons of KIS expression normalised to GAPDH over time in the CA3 region of the hippocampus in mice.
Arrows indicate direction of change relative to the age group noted in the left column. P, age in postnatal days; M, age in months; Y, age in years; * = p-value<0.05; ** = p-value <0.01; *** = p-value <0.001; Brackets = 0.05< p-value <0.1; - = no significant change or trend.

CA1	P0	P7	P15	P21	P63	15M	2Y
P0	-	↑***	↓***	↓***	↓***	↓***	↓***
P7	↓***	-	↓***	↓***	↓***	↓***	↓***
P15	↑***	↑***	-	(↓)	↓*	-	-
P21	↑***	↑***	(↑)	-	-	↑*	-
P63	↑***	↑***	↑*	-	-	↑**	-
15M	↑***	↑***	-	↓*	↓**	-	-
2Y	↑***	↑***	-	-	-	-	-

Table 3.5: Post-hoc comparisons of KIS expression normalised to GAPDH over time in the CA1 region of the hippocampus in mice.
Arrows indicate direction of change relative to the age group noted in the left column. P, age in postnatal days; M, age in months; Y, age in years; * = p-value<0.05; ** = p-value <0.01; *** = p-value <0.001; Brackets = 0.05< p-value <0.1; - = no significant change or trend.

Visual Cortex	P0	P7	P15	P21	P63	15M	2Y
P0	-	↑***	-	↓*	↓**	↓*	↓**
P7	↓***	-	↓***	↓***	↓***	↓***	↓***
P15	-	↑***	-	↓*	↓**	↓**	↓**
P21	↑*	↑***	↑*	-	-	-	-
P63	↑**	↑***	↑**	-	-	-	-
15M	↑*	↑***	↑**	-	-	-	-
2Y	↑**	↑***	↑**	-	-	-	-

Table 3.6: Post-hoc comparisons of KIS expression normalised to GAPDH over time in the visual cortex in mice.
Arrows indicate direction of change relative to the age group noted in the left column. P, age in postnatal days; M, age in months; Y, age in years; * = p-value<0.05; ** = p-value <0.01; *** = p-value <0.001; - = no significant change or trend.

3.4. Discussion

The objectives of the studies described in this chapter were to characterise the regional and cellular distribution of KIS mRNA and protein in the adult human brain, to examine the distribution of KIS mRNA expression in the brains of adult mice, and to explore if KIS mRNA expression was developmentally regulated in the mouse brain.

3.4.1. KIS Distribution in the Brains of Adult Humans and Mice

To my knowledge, the distribution of KIS in the human brain has not previously been characterised. Whilst data of the distribution of KIS expression in the mouse brain is available (Allen Brain Atlas, http://www.brain-map.org/), it has not, to my knowledge, been previously described in detail, though previous publications have detailed the distribution of KIS mRNA in the adult rat brain (Caldwell et al., 1999; Biéche et al.,

2003). The findings reported here confirm and expand on the data currently available regarding the distribution of KIS mRNA in the brains of rodents while also providing a detailed investigation of KIS expression and immunoreactivity in the human brain.

In human tissue, KIS mRNA and immunoreactivity were detected through the grey matter of the several cortical regions, particularly in pyramidal neurons of deeper cortical layers and also in some putative interneurons (Figure 3.1A-E, 3.2A-B). KIS expression was observed to be stronger in the deeper cortical layers, when compared to the superficial layers, in all cortical brain regions examined (DLPFC, occipital cortex, ACC, and STG, Figure 3.1A-E). No signal for KIS mRNA or immunoreactivity was detected in the white matter, suggesting that KIS is not expressed in glia, at least in this compartment. KIS expression was detected in dentate gyrus, CA1, CA3, and CA4 regions of the hippocampus (Figure 3.1F, 2C-F), and also in both Purkinje cells and the granule cell layer of the cerebellum (Figure 3.1G, Figure 3.2G-H).

A previous study investigating the distribution of KIS expression in the rat brain using ISHH indicated that KIS is widely expressed with strong expression reported in the hippocampus, amygdala, habenula, hypothalamus, substantia nigra, ventral tegmental area, and in sensory and motor nuclei of the brain stem, with lower levels in the cortex and thalamus (Caldwell et al., 1999), and a second study reported similar results (Bièche et al., 2003). These results are very similar to the findings reported here in mice, suggesting that the distribution of KIS expression is conserved between rodent species. The findings in this study show that KIS is expressed throughout the cortex, hippocampus and cerebellum, and the pattern of expression is common to both mice and humans. The finding that KIS is expressed in neurons in both humans and mice is in

keeping with previous studies which demonstrated KIS mRNA expression in rat neurons by ISHH (Alam et al., 1996; Caldwell et al., 1999). As KIS is present a range of neuron types, including GABAergic neurons (such as the Purkinje cells of the cerebellum), and glutamatergic neurons (such as the granule cells of the dentate gyrus), the findings suggest that KIS expression is not restricted to particular neurons involved in a specific type of signalling.

Subcellular KIS immunoreactivity was strongest in the nucleus, as can be seen in both pyramidal neurons and Purkinje cells (see Figure 3.2B, D, and H). The nuclear localisation of KIS is in agreement with a previous report of KIS immunoreactivity in serum stimulated NIH 3T3 cells (Boehm et al., 2002). In these dividing NIH 3T3 cells the nuclear localisation of KIS is important as phosphorylation of the cyclin dependent kinase inhibitor $p27^{kip1}$ by KIS in the nucleus leads to the export of $p27^{kip1}$ to the cytoplasm, contributing to cell cycle progression (Boehm et al., 2002). However, this particular function of KIS as a promoter of cell cycle progression is unlikely to be its role in post-mitotic neurons. An alternative potential target which may explain the nuclear localisation of KIS is the splicing factor SF1, which is a nuclear protein whose phosphorylation by KIS, at least in vitro, enhances the binding of SF1 to $U2AF^{65}$ protein and the 3' splice site during spliceosome formation (Manceau et al., 2006).

KIS immunoreactivity was also observed in the cytoplasm of the soma (Figure 3.2B, D, and H), extending into the proximal dendrites of some Purkinje cells (Figure 3.2H). A cytoplasmic localisation of KIS is likely to be necessary for an interaction of KIS and the microtubule regulatory protein stathmin (Maucuer et al., 1995, 1997; Langenickel et al.,

2008). KIS in the cytoplasm may also be functioning through its suggested role as a modulator of transport and local translation of β–actin mRNA (Cambray et al., 2009).

The findings reported here of both nuclear and cytoplasmic KIS immunoreactivity are in agreement with previous reports of the subcellular distribution of KIS in cell lines (Alam et al., 1996; Boehm et al., 2002; Manceau et al., 2008; Maucuer et al., 1997), although they do not correspond with another study which reported no nuclear KIS immunoreactivity in neurons of the medulla oblongata in rats (Caldwell et al., 1999). Possible explanations for this difference between the results presented here and the findings of Caldwell et al., 1999, could be the use of a different antibody, the study of differing brain regions, or a species difference. Further investigation to examine these contradictory findings could be carried out using subcellular fractionation of human tissue to determine the subcellular fractions in which KIS protein can be found.

3.4.2. KIS mRNA Expression in the Mouse Brain during Development

In the experiments presented here KIS mRNA expression was measured in mice at several time points ranging from P0 to 2 years. KIS mRNA expression differed significantly with age in all brain regions examined (Table 3.2). Examination of the data showed that KIS mRNA expression in mice in all regions investigated peaks at around P7 before falling sharply to P15, followed by a steady decline as the animals develop into adulthood, with a slight rise between P63 and 15 months. As KIS mRNA expression was normalised to the housekeeping gene GAPDH, it is unlikely that the detected changes in KIS mRNA expression were due to a change in cell number or density, or an overall change in mRNA expression. Housekeeping genes can sometimes be subject to problems of their own, and have been reported to have altered expression in some circumstances,

reducing their reliability as a reference gene (Tunbridge et al., 2010). However, there is currently no reason to think that GAPDH is an inappropriate housekeeping gene for these experiments, and it is useful to note that the signal for un-normalised KIS expression follows a similar profile to that of normalised KIS (Table 3.1).

In rodents, a period of rapid brain development occurs within the first two weeks of birth, and is considered to be developmentally equivalent to the third trimester in humans (Pal et al., 1997). Hence, the peak of KIS expression at around P7 in mice suggests that a similar peak may occur in the brain during the third trimester of human development. This could reflect an important role for KIS in the brain during a period of development (the third trimester) in which a number of factors, such as elevated homocysteine levels, maternal hypertension, and maternal diuretic treatment, have been reported to confer susceptibility to schizophrenia later in life (Brown et al., 2007; Sørensen et al., 2003).

The pattern of KIS expression through development in the mouse brain reported here does not entirely concur with a previous report of the pattern of KIS expression in the rat brain (Bièche et al., 2003). Bièche et al found that KIS expression rose steadily from P0 to P33 when measured by qPCR, with KIS mRNA expression normalised to the housekeeping gene RPLP0, and northern blot, with KIS mRNA expression normalised to GAPDH. This discrepancy in results between the Bièche et al., 2003 study and the results presented here may be due to the differences in the way KIS expression in the brain was quantified. For example, Bièche et al., 2003 used mRNA extracted from the whole brain, whereas in the results presented here KIS expression was measured in specific regions including the dentate gyrus, CA1, and CA3 regions of the hippocampus, and in the visual cortex. The pattern of KIS expression through development may vary between different

brain regions, resulting in a different profile of expression in specific brain regions compared to the profile of expression of the whole brain. However, as the profile of KIS expression here was consistent between the four brain regions measured in this study, this explanation is unlikely to account for the discrepancy between my study and that of Bièche and colleagues. Alternatively, the differences between the studies may reflect a species differences in KIS expression between rats and mice. Furthermore, as the Bièche et al., 2003 study only investigated KIS expression up to P33 (which is before puberty in rats), whereas my study in mice continues up to 2 years old (late adulthood).

3.4.3. Summary

The results presented in this chapter show that KIS is expressed in all of the brain regions examined in humans and mice, appears to be primarily neuronal, and the distribution of KIS expression appears to be highly conserved between species. KIS appears to be developmentally regulated, with a peak at around P7 in mice. These data provide useful information of the basic neurobiology of KIS. However, the data of KIS expression can only lead to limited inferences regarding the function of KIS in the brain.

Chapter 4: Quantitative Studies of KIS Expression

4.1. Rationale of Experiments

As discussed earlier (Section 1.2.1), KIS has been implicated in the pathogenesis of schizophrenia through allelic association of several SNPs within the KIS gene (Puri et al., 2007; 2008). As none of the associated SNPs are within the coding regions of the gene, they are unlikely to affect the structure or activity of the encoded protein. Hence disease susceptibility may be conferred through altered expression of the KIS gene, in keeping with previous studies of other susceptibility genes which suggest that intronic SNPs can affect overall expression of a gene and/or expression of specific splice variants (Kumar et al., 2008; Law et al., 2007; reviewed in Kleinman et al., 2011).

The series of experiments presented in this chapter were designed to examine whether diagnostic group and/or KIS genotype affected KIS expression. KIS mRNA and immunoreactivity was quantified firstly to determine if KIS expression was changed in the disease states of schizophrenia and bipolar disorder when compared to control subjects, and secondly to test the hypothesis that the KIS SNP rs7513662, which has shown the strongest association with schizophrenia across two genetic association studies (Puri et al., 2007; 2008), may impact upon KIS expression. Though there have been no reports implicating the KIS gene in bipolar disorder, cases of bipolar disorder were included in order to examine the disease specificity of any changes found, and also because several schizophrenia genes have also been associated with bipolar disorder (reviewed in Craddock et al., 2006), suggesting there may be common factors in the aetiology of these disorders.

The human brain regions in which KIS expression was investigated were the DLPFC, ACC, STG, and the cerebellum. The brain regions selected for investigation were largely determined by the tissue which was available for these experiments, though each of the brain regions have been implicated in schizophrenia either in terms of their known function in relation to schizophrenia symptoms, or through altered morphology, gene expression, or activity in the disorder (see references below).

The DLPFC is involved in working memory and executive functioning, with deficits in both of these functions present in schizophrenia, and neuroanatomical alterations have been reported in the DLPFC of schizophrenia patients (Lewis, 2009). The ACC is involved in functions such as emotion, affect, and cognition, which are often found to be abnormal in cases of schizophrenia, and abnormal functional activity has been recorded in the anterior cingulate cortex of patients with schizophrenia (Carter et al., 1997; Quintana et al., 2004), in addition to structural alterations such as differences in grey matter volume compared to unaffected controls (Fornito et al., 2009). The STG is believed to be involved in language and communication, and changes in the volume of the STG have been reported in patients with schizophrenia (Hirayasu et al., 1998; Rajarethinam et al., 2000), with the volume of the STG negatively correlating with the severity of hallucinations and thought disorder in schizophrenia (Rajarethinam et al., 2000). The cerebellum has been shown to have a role in cognition (Schmahmann and Sherman, 1998), and abnormalities of functionality, neuroanatomical changes and changes in gene expression in the cerebellum have been reported in schizophrenia patients (Andreasen et al., 2008).

In conjunction with studies in brain regions implicated in schizophrenia, KIS was quantified in lymphoblast cell lines derived from schizophrenia and control cases. Lymphoblast cell lines provide a useful model for investigating genetic or diagnostic differences in gene expression as they are genetically identical to the individuals from which the cell lines was derived but the influence of external factors, such as anti-psychotic medication, substance abuse, and smoking, will be removed as all cell lines will be grown under the same conditions. This means that any differences observed between groups should be solely due to genetic factors. Previous studies investigating schizophrenia have identified changes in expression in lymphoblast cell lines associated with genotype and diagnostic groups (Liu et al., 2007; Sei et al., 2007; Slonimsky et al., 2010). However, the implications of the data collected from the lymphoblast cell lines must be interpreted with caution. The use of lymphoblast cell lines assumes that any genetic influence upon expression in the brain which may contribute to disease symptoms would likewise impinge upon gene expression in non-neuronal tissues, which may not necessarily be true. For example, previous studies have shown that some but not all mRNA transcripts have coordinated expression between the brain and lymphoblast cell lines (Rollins et al., 2010). Further to this, there is good reason to think the regulation of KIS in cell lines may be through a different mechanism to that which regulates KIS expression in post-mitotic neurons in the brain. As discussed in Section 1.2.2.2, KIS is known to have a role in the regulation of the cell cycle through the negative regulation of $p27^{kip1}$ (Boehm et al., 2002). This is likely to be a major function of KIS in the lymphoblast cell lines, but is very unlikely to be the main role of KIS in neurons in the adult brain. FoxM1, which is one of the transcription factors reported to be involved in the regulation of KIS expression during the cell cycle (Petrovic et al., 2008) is not found

in the adult human brain (Liu et al., 2006), providing further indication that there may be different mechanisms which regulate KIS expression in the brain and the blood.

KIS expression was also quantified in rats treated with antipsychotic medication to examine whether these medications affect KIS expression. Antipsychotic medication has been shown to alter the expression of some genes (for example Law et al., 2004a), and so by investigating the effect of antipsychotic administration in rats we can determine whether any changes in KIS expression in humans associated with diagnostic groups might be confounded by the medication.

As well as quantifying the full length KIS mRNA transcript, the possibility of KIS splice variants and whether they might be affected by genotype or diagnosis was also explored. There are recent precedents for novel alternative transcripts in the human brain which are associated with risk genotypes, particularly where the risk genotype is an intronic SNP (Law et al., 2007). If KIS expression is altered by genotype or in disease states, this alteration could be by a change in the quantity of KIS or by alterations in the expression of splice variants of the KIS transcript. These splice variants could alter KIS function by altering the functional domains or the stability of the protein, or by altering its subcellular localisation. As well as the full length KIS transcript (variant 1, NM_175866), three splice variants have been reported (Figure 4.1), although there are no available data on the presence of these variants in the brain. The KIS splice variants include a transcript with an alternative first exon (variant 2, NM_001184763) in which part of the kinase domain is missing, a transcript without the seventh exon (variant 3, NM_144624) in which the skipped exon results in a frame shift leading to an earlier stop codon in exon eight and a truncated UHM domain, and a fourth transcript with a shortened exon one, a

retained intron between exons two and three, and the translation start site in exon three (AL834136) which would be missing most of the kinase domain (Aceview, Genome Biology 2006, 7(Suppl 1):S12). These changes are likely to affect the function of the translated protein.

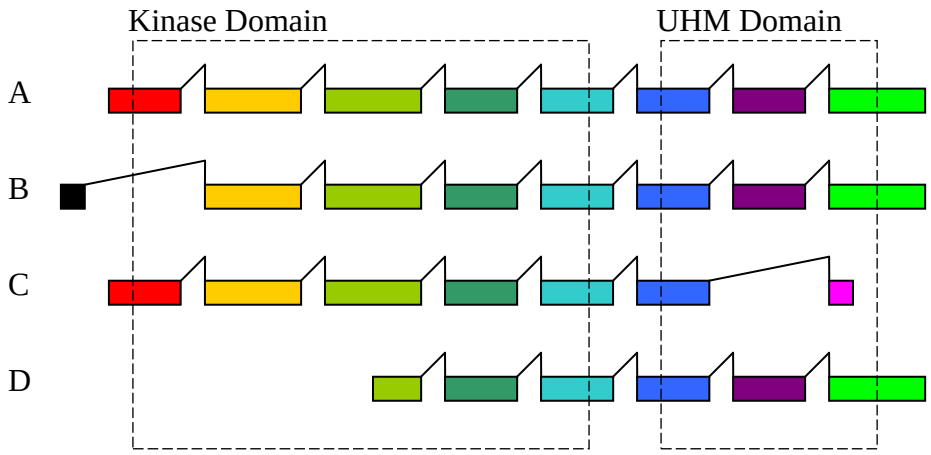

Figure 4.1: Reported splice variants of KIS.
The figures represent the coding regions of the KIS variants, with each box representing an exon. See Figure 1.1B for the full KIS mRNA transcript. Dashed boxes indicate the approximate location of the regions encoding the kinase and UHM domains. (A) Variant 1 (NM_175866); (B) Variant 2 (NM_001184763); (C) Variant 3 (NM_144624); (D) AL834136. Exons are shown in proportion to their size. UHM, U2AF homology motif.

4.2. Methods

4.2.1. Reverse Transcription Polymerase Chain Reaction

4.2.1.1. Quantitative Polymerase Chain Reaction

KIS expression was measured by qPCR in the STG, ACC, and cerebellum of human post-mortem samples provided by NIMH and SMRI. These samples included cases of schizophrenia, bipolar disorder, and unaffected controls, as detailed in Section 2.1.1. RNA preparation and qPCR was performed as described in Section 2.5, using Taqman

assays to measure KIS as well as the housekeeping genes B2M, GAPDH, GUSB, and TFRC.

qPCR was also used to quantify KIS expression in the brains of rats which had been treated with antipsychotic medication using cDNA from the frontal and cerebellar regions of brain. The tissue used is as described in Section 2.1.2.1 and details of the RNA preparation and qPCR methods are described in Section 2.5. The expression of KIS and the housekeeping genes GAPDH, GUSB, and HPRT were measured as detailed in Section 2.5.5.2.

4.2.1.2. Reverse Transcription Polymerase Chain Reaction

RT-PCR was used to investigate the potential presence of KIS splice variants. An outline of PCR methods is included in Section 2.5.3, and primer sequences can be found in Table 2.6.

The KIS transcript variant 1 was detected using primers targeting the first and eighth exons of NM_175866 (KIS (exons 1-8)), with a predicted amplicon size of 904 base pairs. The KIS (exons 1-8) primers should also detect KIS variants 3 and AL834136, which would have predicted sizes of 815 base pairs for variant 3 and 1569 base pairs for the AL834136 variant. The primers for KIS variant 2 targeted the first and eighth exons of the NM_001184763 transcript, which has a different first exon to the other KIS transcripts. The PCR for each of these primer sets was carried out using a “touchdown” PCR program, which involves initial high annealing temperatures for high specificity, with a decrease in annealing temperature in each subsequent cycle to increase the efficiency of amplification of the high specificity products. The PCR conditions were

94°C for 2 minutes, followed by 20 cycles of 94°C for 30 seconds, 70°C for 45 seconds, 72°C for 90 seconds, with the 70°C anneal temperature dropping by 1°C per cycle, and then a further 20 cycles of 94°C for 30 seconds, 55°C for 45 seconds, and 72°C for 90 seconds, and finally 72°C for 7 minutes. Primers were used at a final concentration of 5ng/µl, and each sample included 2.5mM magnesium. The cDNA used was produced using the methods described in Section 2.5.2 from adult human RNA samples, described in Section 2.1.1, of frontal cortex, temporal cortex, hippocampus, caudate nucleus, cerebellum, liver, and also human foetal brain. RNA from the SH-SY5Y human neuroblastoma cell line and a control with nfH_2O in place of cDNA were also included. 80ng of cDNA was included in each reaction. Following the PCR samples were separated using a 1.5% agarose gel.

4.2.2. Immunoautoradiography

KIS immunoreactivity was quantified in the DLPFC and STG using immunoautoradiography, with the methods performed as described in Section 2.6. Immunoautoradiography was chosen to quantify the immunoreactivity in these cases as the use of tissue sections allows separate measurements of grey and white matter which is not possible using tissue homogenates, as used for western blotting. Also, for groups of this size it would not be possible to fit all samples on a single western blot, which may have affected the consistency of measurements.

4.2.3. Immunoblot

KIS immunoreactivity was measured in lymphoblast cell lines by immunoblot, as described in Section 2.7. Lymphoblast cell lines are as described in Section 2.1.1. The

immunoblot was chosen as it allows all samples to be measured on a single membrane, which would not be possible using a western blot due to the large number of samples. An enzyme linked immunosorbant assay (ELISA) was tested as an alternative method but this KIS antibody (Ab38292) was found to be unsuitable for ELISA (data not shown). The KIS immunoblot was determined to be an accurate measurement of immunoreactivity by a pilot study in which the immunoblot was carried out as described in Section 2.7 except that the amount of protein loaded onto the membrane ranged from 0.5µg to 8µg. The specificity of the antibody in humans was confirmed by western blot, which produced a single band of the expected size (Figure 3.3).

4.2.4. SNP Genotyping

The rs7513662 SNP genotype for each sample was determined using methods described in Section 2.8 in order to investigate the effect of genotype on KIS expression. The rs7513662 SNP was chosen for study as it was the most strongly associated with schizophrenia (Puri et al., 2007; 2008), and rs7513662 also tags a haplotype block which contains the other KIS SNPs (rs6427680 and rs10494370) which have been associated with schizophrenia.

4.3. Results

Categorical and continuous variables had no effect on the quantity of KIS except where otherwise stated.

4.3.1. KIS Quantification in Diagnostic Groups

Superior Temporal Gyrus (STG): STG KIS qPCR data were normalised to B2M. Only one housekeeping gene was used due to limited mRNA available for use. One control subject was excluded as an outlier. KIS mRNA signal was normally distributed and correlated with RIN (Pearson correlation, R=0.24, p =0.02) which was thus included as a covariate in the ANOVA. No difference in KIS mRNA was found between diagnostic groups (Table 4.1). The immunoautoradiography data in the STG were normally distributed and the ANOVA showed no significant change by diagnosis in KIS immunoreactivity in the cortex of the STG (Table 4.1).

Anterior Cingulate Cortex (ACC): ACC KIS mRNA qPCR data were normalised to the geometric mean of four HKGs (B2M, GAPDH, GUSB, and TFRC). Two bipolar disorder subjects were excluded from analysis as the samples failed to amplify. Normalised KIS mRNA was normally distributed and correlated with pH (Pearson correlation, R=0.318, p=0.001), which was included as a covariate in the ANOVA. No change in KIS expression between diagnostic groups was found (Table 4.1).

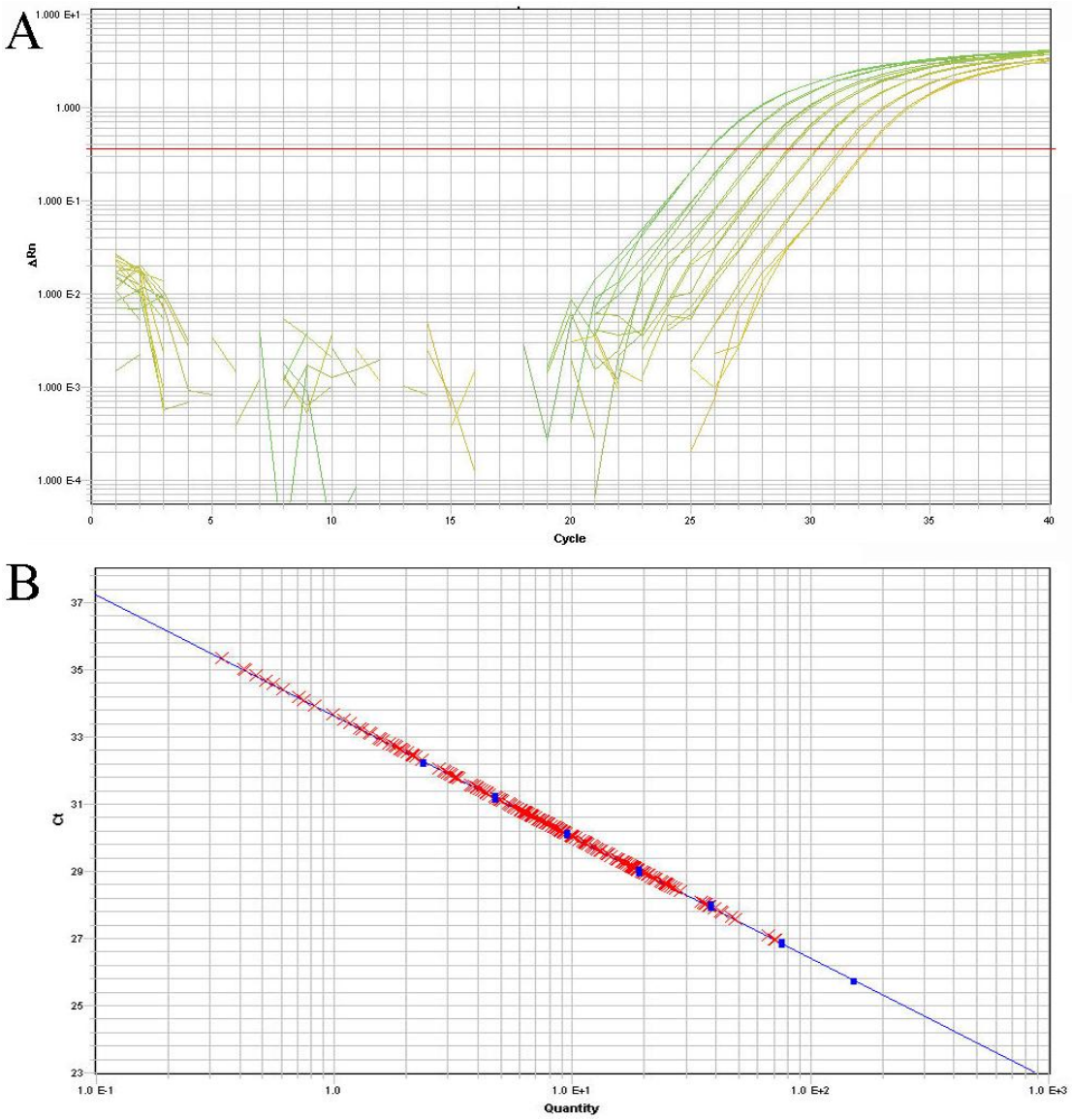

Figure 4.2: Amplification plot and standard curve from qPCR of KIS in the ACC.
(A) Amplification plot showing the cDNA standards with fluorescent signal plotted against the number of cycles for each sample. The red horizontal line indicates the threshold at which the samples were quantified. (B) Standard curve showing the cDNA standards (blue squares) and test samples (red crosses) with quantity of KIS plotted against the threshold cycle.

Cerebellum: One subject from each of the schizophrenia and bipolar disorder groups were excluded from analysis as the samples failed to amplify. Cerebellum KIS qPCR data were normalised to B2M alone, as one-way ANOVA and post-hoc t-tests of GAPDH, GUSB, and TFRC expression each showed significant difference between diagnostic groups (data not shown). KIS normalised to B2M was not normally

distributed so the data were analysed using Kruskal-Wallis test, which showed no effect of diagnosis (Table 4.1).

Dorsolateral Prefrontal Cortex (DLPFC): The immunoautoradiography data in the DLPFC were normally distributed and the ANOVA showed no significant change by diagnosis in the quantity of KIS in the cortex (Table 4.1).

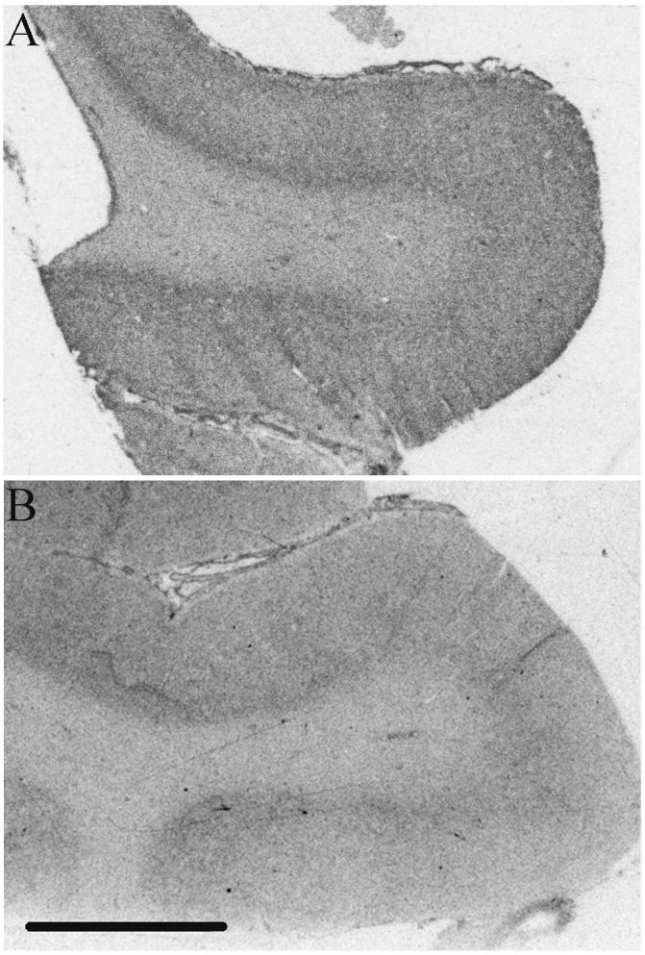

Figure 4.3: Representative examples of KIS immunoautoradiography.
(A) Dorsolateral prefrontal cortex; (B) Superior temporal gyrus. Scale bar = 5 mm.

Lymphoblast Cell Lines: Pilot studies confirmed that the immunoblot was quantitative (Figure 4.4). Data from the immunoblot of KIS in lymphoblast cell lines were normally

distributed and the ANOVA showed no difference in levels of KIS between the schizophrenia and control groups (Table 4.1).

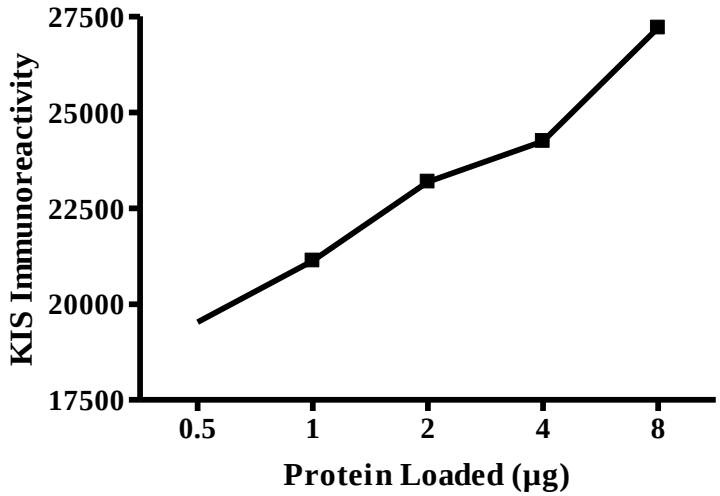

Figure 4.4: Pilot study result demonstrating the quantitative nature of KIS immunoreactivity in lymphoblast cell lines using immunoblot.
KIS immunoreactivity is shown in units of optical density corrected for background signal.

mRNA	Control	Schizophrenia	Bipolar Disorder		
STG[1]	0.73 ± 0.06	0.70 ± 0.07	n/a	$F_{1,89}$=0.134	P=0.716
N	55	39			
ACC[2]	1.29 ± 0.15	1.01 ± 0.08	1.25 ± 0.09	$F_{2,95}$=1.575	P=0.212
N	35	35	32		
Cerebellum[3]	2.94 ± 0.45	2.86 ± 0.38	2.51 ± 0.36	-	P=0.666
N	35	34	33		
Immunoreactivity					
STG	175 ± 4	168 ± 6	n/a	$F_{1,113}$=0.835	P=0.363
N	75	42			
DLPFC	272 ± 6	270 ± 5	275 ± 7	$F_{2,98}$= 0.072	P=0.930
N	35	35	34		
Lymphoblast	8729 ± 330	7797 ± 616	n/a	$F_{1,57}$=2.027	P=0.160
N	39	22			

Table 4.1: KIS mRNA expression and immunoreactivity in schizophrenia, and bipolar disorder, and unaffected controls.
KIS mRNA data are shown normalised to housekeeping gene(s). Immunoreactivity values in the STG and DLPFC are ^{35}SnCi/g tissue equivalents. Immunoreactivity values for lymphoblasts are units of optical density corrected for background signal. Values are mean ± standard error of the mean. STG, superior temporal gyrus; ACC, anterior cingulate cortex; DLPFC, dorsolateral prefrontal cortex. [1] = RIN included as covariate, [2] = pH included as covariate, [3] = Kruskal-Wallis test.

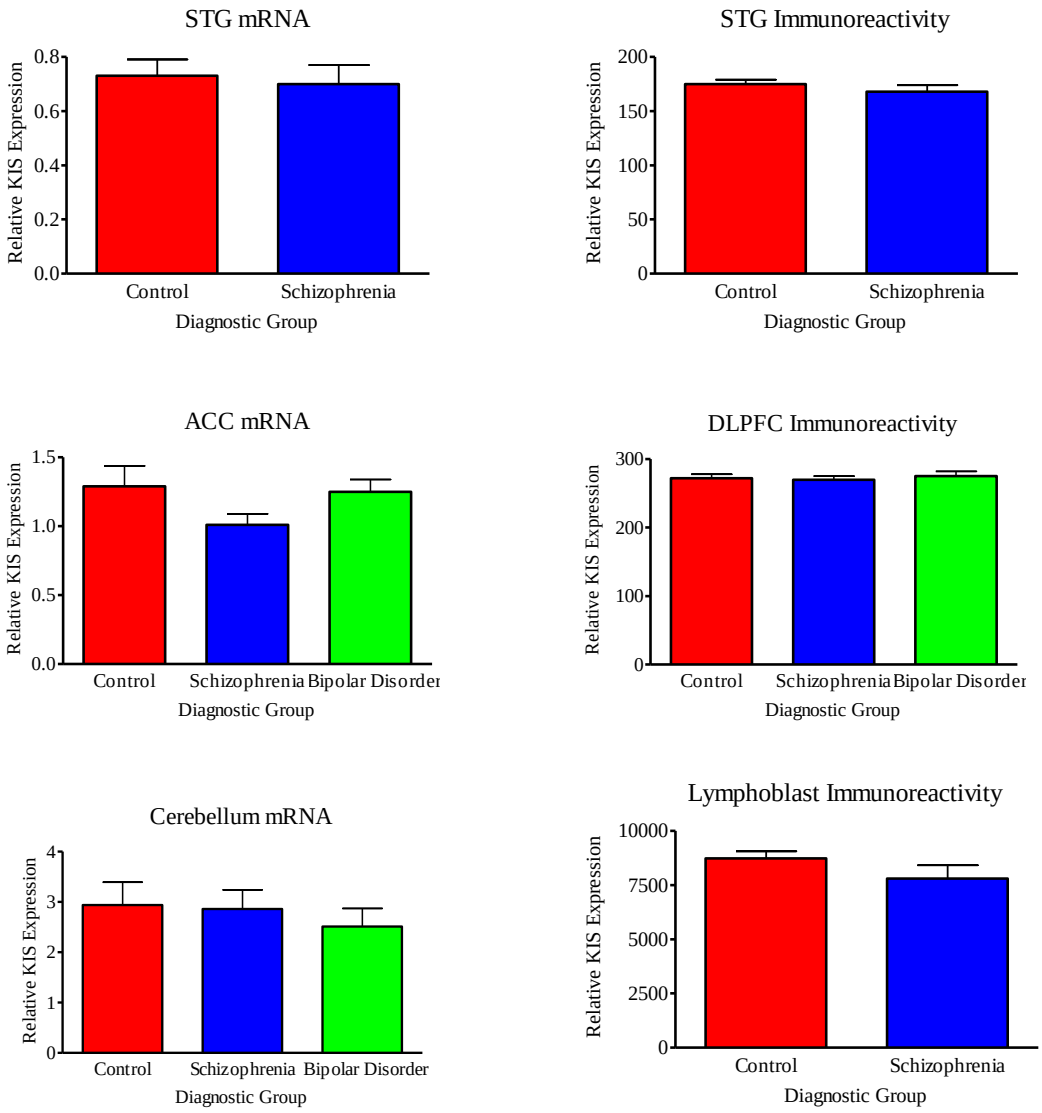

Figure 4.5: KIS expression in diagnostic groups.
KIS mRNA was quantified using qPCR in the STG, ACC and cerebellum. KIS mRNA expression values are normalised to the expression of housekeeping gene(s). KIS immunoreactivity was quantified using immunoautoradiography in the DLPFC and STG with values shown in ^{35}SnCi/g tissue equivalents. Immunoreactivity in lymphoblast cell lines was quantified using immunoblot, units are optical density corrected for background signal. Histogram shows mean value plus standard error of the mean. STG, superior temporal gyrus; ACC, anterior cingulate cortex; DLPFC, dorsolateral prefrontal cortex.

4.3.2. Genotype and KIS Expression

The distribution of genotypes of the rs7513662 SNP (Figure 4.6) were in Hardy-Weinberg equilibrium for all groups (Rodriguez et al., 2009). No significant effect of

rs7513662 genotype on KIS mRNA or protein was found in any brain region or in lymphoblast cell lines (Table 4.2), although there was a trend (p=0.089) for an increase in KIS immunoreactivity in the DLPFC of subjects who carried at least one G-allele. STG and cerebellum data were normalised to B2M, ACC data were normalised to the geometric mean of four housekeeping genes, as described in Section 4.3.1. There were no significant interactions of diagnosis with genotype (Table 4.3).

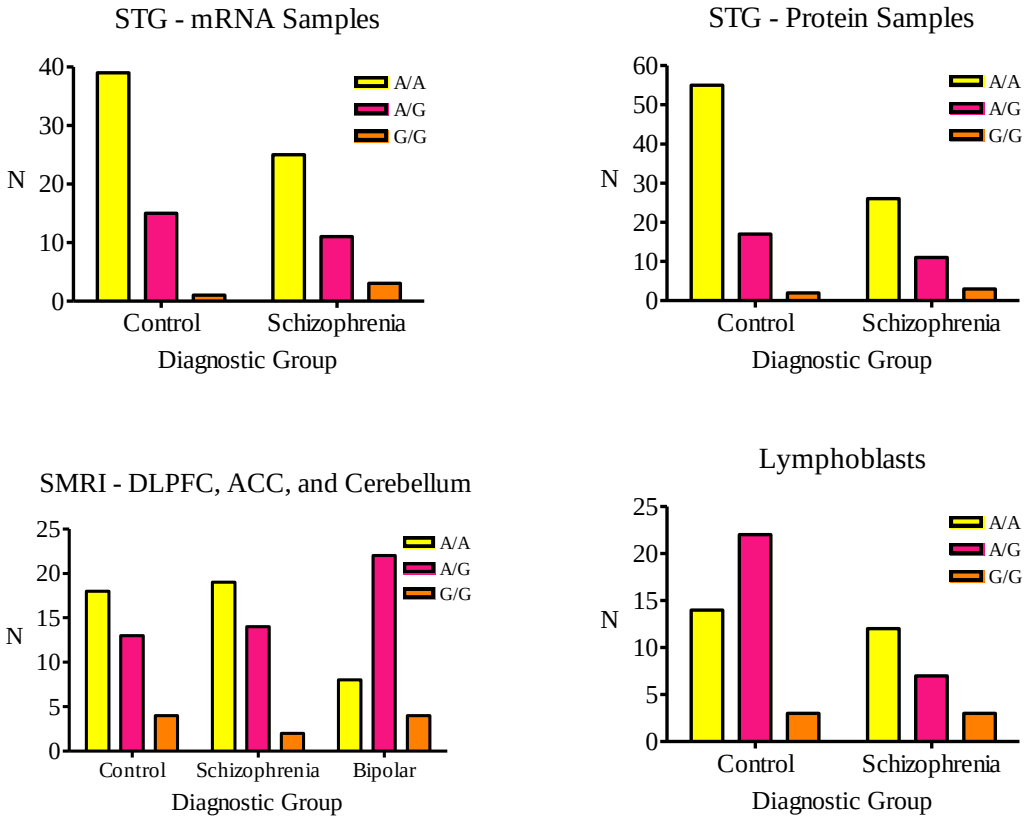

Figure 4.6: Number of subjects in each of the KIS SNP rs7513662 genotype groups in human samples used in quantification studies.
STG, superior temporal gyrus; DLPFC, dorsolateral prefrontal cortex; ACC, anterior cingulate cortex; SMRI, Stanley Medical Research Institute.

mRNA	A/A	A/G or G/G		
STG[1]	0.71 ± 0.05	0.72 ± 0.09	$F_{1,89}$=0.189	P=0.665
N	64	30		
ACC[2]	1.19 ± 0.11	1.18 ± 0.08	$F_{1,95}$=0.000	P=0.985
N	45	57		
Cerebellum[3]	3.06 ± 0.37	2.55 ± 0.28	-	P=0.322
N	45	57		
Immunoreactivity				
STG	174 ± 4	170 ± 7	$F_{1,113}$=0.231	P=0.632
N	82	35		
DLPFC	264 ± 6	278 ± 4	$F_{1,98}$=2.95	P=0.089
N	45	59		
Lymphoblast	8294 ± 562	8466 ± 348	$F_{1,57}$=0.005	P=0.942
N	26	35		

Table 4.2: KIS mRNA and immunoreactivity in rs7513662 SNP genotype groups.
KIS mRNA data were normalised to housekeeping gene(s), immunoreactivity values in the STG and DLPFC are ^{35}SnCi/g tissue equivalents. Immunoreactivity values for lymphoblasts are units of optical density corrected for background signal. Values are mean ± standard error of the mean. STG, superior temporal gyrus; ACC, anterior cingulate cortex; DLPFC, dorsolateral prefrontal cortex. [1] = RIN included as covariate, [2] = pH included as covariate, [3] = Mann-Whitney test.

Genotype x Diagnosis					
mRNA			Immunoreactivity		
STG[1]	$F_{1,89}$=0.036	P=0.850	STG	$F_{1,113}$=0.002	P=0.964
ACC[2]	$F_{2,95}$=0.275	P=0.760	DLPFC	$F_{2,98}$=0.341	P=0.712
			Lymphoblast	$F_{1,57}$=0.062	P=0.804

Table 4.3: Investigation of KIS rs7513662 genotype by diagnostic group interactions on KIS expression in human samples.
KIS mRNA was quantified using qPCR in the STG and ACC, KIS protein was quantified using immunoautoradiography in the DLPFC and STG and using immunoblot in lymphoblast cell lines. [1] = RIN included as covariate, [2] = pH included as covariate. STG, superior temporal gyrus; ACC, anterior cingulate cortex; DLPFC, dorsolateral prefrontal cortex.

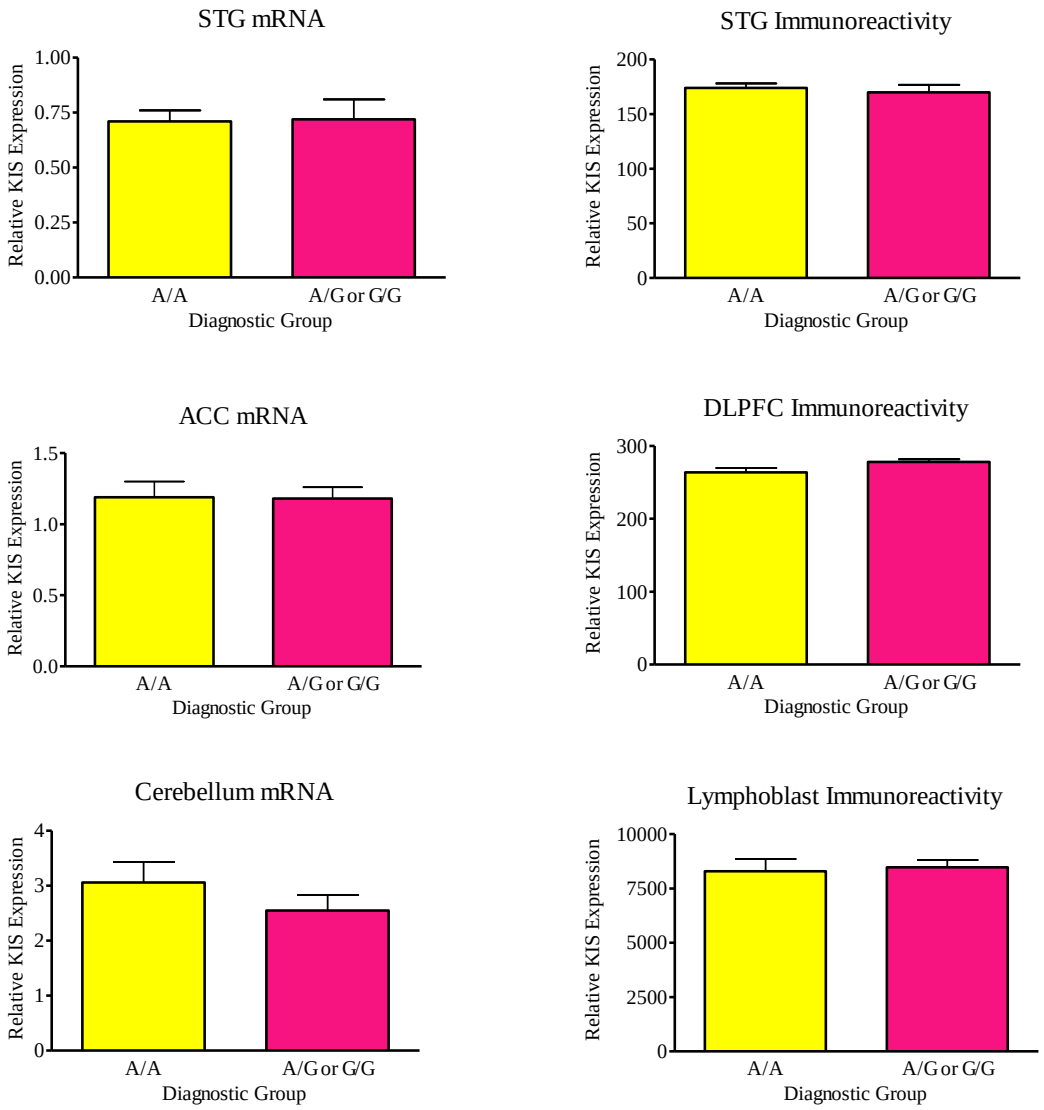

Figure 4.7: KIS expression in KIS SNP rs7513662 genotype groups.
KIS mRNA was quantified using qPCR in the STG, ACC and cerebellum. KIS mRNA expression values are normalised to the expression of housekeeping gene(s). KIS immunoreactivity was quantified using immunoautoradiography in the DLPFC and STG with values shown in ^{35}SnCi/g tissue equivalents. Immunoreactivity in lymphoblast cell lines was quantified using immunoblot, units are optical density corrected for background signal. Histograms show mean value plus standard error of the mean. STG, superior temporal gyrus; ACC, anterior cingulate cortex; DLPFC, dorsolateral prefrontal cortex..

4.3.3. Effect of Antipsychotic Medication on KIS Expression

KIS mRNA in the frontal and cerebellar regions of rat brain was measured by qPCR and normalised to the geometric mean of three HKGs (GAPDH, GUSB, and HPRT). The data were normally distributed and ANOVA showed no effect of antipsychotic treatment (Table 4.4). The dissociation curve and gel electrophoresis confirmed there was a single PCR product of the expected size (Figure 4.8).

	Saline	Haloperidol	Clozapine		
Frontal	0.84 ± 0.16	0.80 ± 0.14	0.95 ± 0.10	$F_{2,21}$=0.319	P=0.731
Cerebellum	1.19 ± 0.15	1.01 ± 0.13	0.90 ± 0.07	$F_{2,21}$=1.537	P=0.238

Table 4.4: KIS mRNA expression after antipsychotic administration in rats.
Samples were measured by qPCR, values shown are KIS mRNA normalised to geometric mean of HKGs, mean ± standard error of the mean. Eight samples are included in each group.

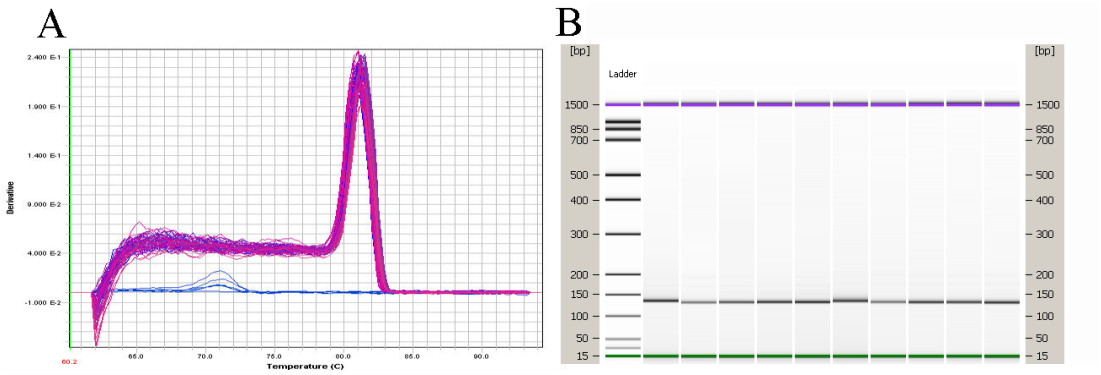

Figure 4.8: Dissociation curve and PCR product from qPCR of rat KIS.
(A) Dissociation curve from qPCR of cDNA from the rat cerebellum showing the level of fluorescence detected at different temperatures after qPCR. The single peak confirms there was a single PCR product. (B) PCR product from a selection of qPCR reactions of cDNA from frontal and cerebellum samples showing the PCR product was of the expected size of 140 base pairs (bp).

4.3.4. KIS Splice Variants

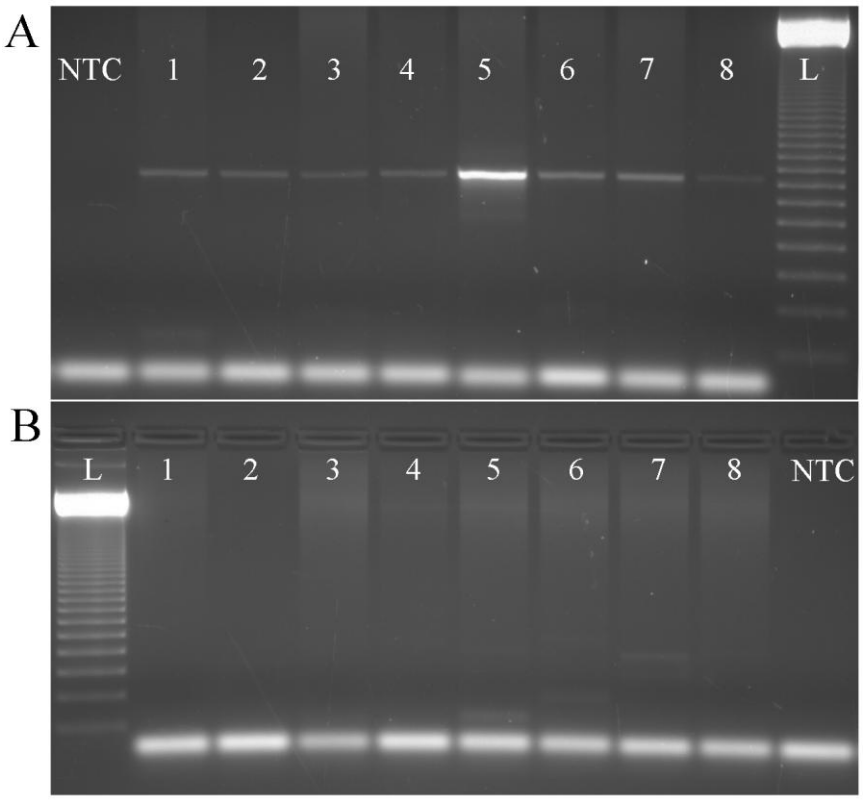

Figure 4.9: Tests for the expression of potential KIS splice variants in human tissues using RT-PCR.
(A) RT-PCR using primers complementary to exons 1 and 8 of KIS variants 1, 3, and AL834136; (B) RT-PCR using primers complementary to exons 1 and 8 of KIS variant 2. All cDNA used is from human samples; (L) DNA ladder, the lowest band represents 123 base pairs and each band above it is 123 base pairs larger than the previous band; (1) Liver; (2) Temporal cortex; (3) Foetal brain; (4) Hippocampus; (5) SH-SY5Y cell line; (6) Frontal cortex; (7) Caudate nucleus; (8) Cerebellum; (NTC) No template control.

Figure 4.9 shows the results of PCR amplification of human samples using the touchdown PCR method. The full length transcript of KIS variant 1 was detected at the expected size of 904 base pairs in all samples investigated (Figure 4.9A). The predicted size of the KIS variant 2 amplicon was 915 base pairs, using primers which were complementary to the eighth exon and the alternative first exon of this variant. There is no indication of a PCR product of this size in any of the samples, although faint bands do

appear in lanes 5, 6, and 7 (Figure 4.9B), but as these bands are all smaller than 500 base pairs and therefore not of the predicted size they are likely to be non-specific.

The primers for KIS (exons 1-8) used to identify KIS variant 1 were also complementary to variant 3 and the AL834136 variant of KIS and should have been able to detect these transcripts. The transcript for variant 3 would be missing exon 7 and would be predicted to be 89 base pairs smaller than the variant 1 transcript. The KIS AL834136 variant transcript retains an intron between exons 2 and 3 and as such would be predicted to be 665 base pairs larger than variant 1. There was no indication that either of these predicted bands were present in any sample (Figure 4.9A).

4.4. Discussion

4.4.1. KIS Expression in Schizophrenia

No significant difference between diagnostic groups was found in KIS mRNA or immunoreactivity in a post-mortem series of STG tissue comprised of schizophrenia and matched control subjects, or in a further post-mortem series of ACC, cerebellum, and DLPFC tissue that included control, schizophrenia, and bipolar disorder subjects. KIS immunoreactivity in lymphoblast cell lines derived from schizophrenia and control subjects also showed no effect of diagnosis. The data in schizophrenia cases are unlikely to have been confounded by medication since there was no evidence of a change in KIS expression in rats treated with typical or atypical antipsychotic medication, and no measure of KIS mRNA or protein in human tissue showed correlation with the patients' antipsychotic history (data not shown). Therefore, these results do not offer any

supporting evidence for a potential role for KIS in the pathophysiology of schizophrenia in these samples.

The quantification studies in the human brain presented here determined the level of KIS expression in adult post-mortem samples. Though no changes in KIS expression were found, this does not rule out the possibility that differences in KIS expression earlier in life, particularly during neurodevelopment, could confer susceptibility to schizophrenia in adulthood. KIS phosphorylation target $p27^{kip1}$ is thought to play an important role in proliferation, differentiation, and migration of cortical neurons in mice (Goto et al., 2004; Nguyen et al., 2006a) which, along with the evidence for the involvement of KIS in neurite outgrowth (Cambray et al., 2009), indicates that KIS activity is likely to be important for normal brain development. Both the results presented in Chapter 3 of this thesis and the work of Bièche et al., 2003 indicate that KIS expression is developmentally regulated and changes during neurodevelopment. It could be that alterations in KIS expression through neurodevelopment could increase susceptibility to schizophrenia and such changes may not be detected in a post-mortem study of this kind.

As discussed earlier (Section 4.1), the lymphoblast data may be limited in terms of investigating KIS in psychiatric disorders as the mechanisms which regulates KIS expression in cell lines may differ from the mechanisms of regulation in the brain. However, as no significant difference in KIS expression was found between diagnostic groups in any brain region, the negative results in the lymphoblast cell lines are more likely to be genuine rather than indicative of a flaw in the use of lymphoblast cell lines in quantifying gene expression in schizophrenia.

4.4.2. Genotype and KIS Expression

The SNP rs7513662 has been associated with schizophrenia in two separate studies, with the G-allele of this SNP found to be less common in cases of schizophrenia compared to controls (Puri et al., 2007; 2008). A recent study in a Bulgarian population failed to replicate this, although they did report equivocal association with a decrease in frequency of the A-allele in schizophrenia (Betcheva et al., 2009). The results presented here show a trend indicating an increase in KIS immunoreactivity in the DLPFC of subjects with at least one G-allele ($p=0.089$), but no significant effect of genotype on KIS mRNA or immunoreactivity was found in any brain region or in lymphoblast protein. Hence, these results do not provide any evidence to support the hypothesis that altered expression is the mechanism through which the rs7513662 SNP could confer susceptibility to schizophrenia. As discussed earlier (Section 4.4.1), the lack of effect in the lymphoblast cell lines may reflect differences in the mechanisms of regulation of the KIS gene in dividing cells compared to the brain, but as no significant effect of genotype was found in any tissue investigated this is unlikely to have been relevant in this study.

The results presented in this thesis do not rule out the possibility that the SNPs within the KIS gene may regulate expression and/or increase schizophrenia susceptibility in some cases. The initial association of KIS with schizophrenia was in a London based sample (Puri et al., 2007), and this was replicated in a Scottish population (Puri et al., 2008), with an equivocal association reported in a Bulgarian sample (Betcheva et al., 2009). The human samples used in the experiments presented here were from the USA, with most of the STG samples being from African Americans (Tables 2.1 and 2.2). The samples from SMRI were mostly Caucasian, but risk genes may vary even within sub-populations of

European descent, and so it is possible that KIS may be a schizophrenia susceptibility gene in particular populations.

No splice variants were detected in the human brain, or indeed in a human cell line or liver sample. It may be relevant that there was no positive control available for the KIS variant 2 transcript, but there is no reason to think that the primers used would not detect this transcript if it were present. KIS variant 1 was detected in all samples, and the primers used to detect KIS variant 1 were also complementary to variants 3 and the AL834136 variant, but there was no evidence of these variants detected. This does not represent an exhaustive search for KIS splice variants, and there may be as yet unknown splice variants of the KIS gene in the human brain. It may also be that splice variants of KIS are more prominently expressed through development, though this possibility is less likely considering the finding reported here that none of the reported KIS variants examined in this study were detected in a sample of human foetal brain (Figure 4.9). The failure to detect any of the reported splice variants of KIS in the brain indicates that the rs7513662 genotype is unlikely to regulate altered splicing of the KIS gene, at least in the brain regions examined here. The possibility of KIS splice variants could be further investigated using 5' or 3' RACE (rapid amplification of PCR ends) to identify as yet unknown splice variants. As this technique amplifies from a point within the transcript to either the 5' or 3' end, thereby removing the need to know the exact sequence of any potential transcripts (required to design primers for RT-PCR), 5' or 3' race would facilitate the detection the full length transcript and additionally any variants which may be present.

Due to the low frequency of the G-allele of rs7513662, the data of homozygous G and heterozygous subjects were combined and compared to the homozygous A group for analysis. It is possible that this investigation did not have enough power to detect a genotype effect due to the low number of G-allele homozygotes, or that rs7513662 may be involved in the expression of an as yet unknown splice variant of KIS, or is in linkage disequilibrium with a coding SNP which affects KIS activity rather than expression, although no such coding SNPs have yet been identified. Nevertheless, these results suggest that the SNP rs7513662 does not influence KIS expression, and as such the biological basis for any genetic involvement of KIS in schizophrenia remains unknown.

4.4.3. Summary

The main objectives of the experiments described in this chapter were to investigate the expression of KIS in schizophrenia and with regard to the intronic KIS SNP rs7513662 which showed the strongest association with schizophrenia (Puri et al., 2007; 2008). The failure to find any differences in KIS expression between diagnostic groups weakens the case for KIS as a schizophrenia susceptibility gene, and the absence of any effect of SNP genotype on KIS means that these experiments have not indicated any mechanism by which the rs7513662 SNP may regulate the KIS gene and thereby confer schizophrenia susceptibility.

Chapter 5: Characterisation of KIS Knockout Mice

5.1. Rationale of Experiments

In this chapter, some of the potential functions of KIS are explored using KIS knockout mice. By determining what abnormalities arise from the absence of KIS in the brain, it may be possible to infer the likely functions of KIS. Cautious extrapolation of the results in mice to the human brain is supported by the fact that mouse KIS is highly homologous to human KIS: it is the same size, contains the same number of exons, and its distribution in the brain is very similar to that of human KIS (see Chapter 3). Hence, any conclusions drawn from this study regarding the function of KIS in the mouse brain are likely to provide an accurate indication of the role of KIS in the human brain.

Three main parameters were measured in these studies. The total quantity and phosphorylation state of a selection of reported KIS targets were quantified, the expression of a selection of molecular markers were also quantified, and the volumes of several structures within the brain was investigated using stereological measurements.

To my knowledge, published work on KIS knockout mice is currently limited to the effects of KIS knockout in mouse embryonic fibroblasts and vascular smooth muscle cells, where the main findings were that there was reduced stathmin degradation (and therefore increased stathmin levels), reduced cell proliferation, and increased cell migration (Langenickel et al., 2008; see Section 1.2.2.3 for more detail). The effect of blocking KIS expression using siRNA has been examined in cultured cortical neurons, where the main finding was that there was a reduction in both the number and the length of neurites in the absence of KIS (Cambray et al., 2009).

Tissue from two strains of KIS knockout mice were used in these experiments, provided by NIH and Wyeth (see Section 2.1.2.2). There were several reasons for including both strains of mice in these studies. Measurements of two strains of $KIS^{-/-}$ mice allow the possibility of confirming any findings in one strain in a second independently produced strain. The strain from NIH has already been verified and included in a publication (Langenickel et al., 2008), and it was possible to examine both fixed and frozen brain tissue from these mice. The tissue provided by NIH included only knockout and wildtype mice, whereas the strain from Wyeth also included heterozygous knockout mice ($KIS^{+/-}$) which allows investigation of the effects of a reduction of KIS as well as the absence of KIS expression.

The effects that the absence of KIS has on the quantity of reported KIS targets and also their phosphorylation states were examined to try to identify which of these targets are relevant to the function of KIS in the adult brain. Of the proteins reported to interact with and be phosphorylated by KIS, stathmin and $p27^{kip1}$ were chosen for study in these experiments. These proteins were selected as they have both been shown to interact with KIS (Maucuer et al., 1995; Maucuer et al., 1997; Boehm et al., 2002; Langenickel et al., 2008) and the site phosphorylated by KIS on each of these proteins is known, with serine 10 phosphorylated on $p27^{kip1}$ (Boehm et al., 2002) and serine 38 on stathmin (Langenickel et al., 2008).

Stathmin was particularly of interest as it was through the interaction of KIS and stathmin that KIS was first discovered (Maucuer et al., 1995), and, as discussed above, an increase in stathmin has been reported in KIS knockout mice (Langenickel et al.,

2008). This is the same strain of knockout mice provided by NIH which have been used in the experiments presented here. KIS has been shown to phosphorylate $p27^{kip1}$ on its serine 10 residue during the G_1 phase of the cell cycle (Boehm et al., 2002; see Section 1.2.2.2 for further details), although to my knowledge there are no data available regarding the effect of KIS on $p27^{kip1}$ in quiescent cells.

There have also been reports of stathmin and $p27^{kip1}$ interacting with each other (Baldassarre et al., 2005), and both have been implicated in regulation of the cell cycle (Marklund et al., 1994; Rubin et al., 2004; Boehm et al., 2002) and in cell migration (Jin et al., 2004; Langenickel et al., 2008; Nguyen et al., 2006a). The interactions of stathmin and $p27^{kip1}$ indicate that KIS may have a complex regulatory role on these cellular functions.

The molecular markers measured in the KIS knockout mice were growth associated protein 43 (GAP43), vesicular glutamate transporter 1 (VGlut1), microtubule associated protein 2 (MAP2), spinophilin, and stathmin. GAP43 was measured here as a marker of neuronal plasticity (Benowitz et al., 1997). VGlut1 was measured as a marker of glutamatergic synapses and neurons as it is associated with synaptic vesicles, has functions in glutamate transport, and it is exclusively found in glutamatergic terminals (Bellocchio et al., 1998; 2000), and VGlut1 expression has been shown to be related to the amount of glutamate released from the presynaptic terminal (Wojcik et al., 2004; Wilson et al., 2005). MAP2 was measured as it is a neuron specific cytosketetal protein which is enriched in dendrites (Pollard et al., 1994). Spinophilin was measured as a marker of dendritic spines (Feng et al., 2000). Stathmin was also measured here as it is a known target of KIS (Maucuer et al., 1995, 1997; Langenickel et al., 2008) which is also

associated with microtubules (Belmont et al., 1996), and so should provide an indication of the level of microtubule stability and also whether knockout of the KIS gene affects the turnover of this protein. These molecular markers together provide some indication of pre- and post-synaptic functioning, and any changes in their expression in the KIS knockout mice may reflect a role for KIS in such processes, or their developmental origins.

Moreover, these genes were chosen for study since the expression of each of them has been reported to be altered in schizophrenia (GAP43 (Eastwood and Harrison, 1998; Paz et al., 2006), VGlut1 (Eastwood and Harrison, 2005), MAP2 (Rosoklija et al., 2005), spinophilin (Law et al., 2004b), stathmin (Clark et al., 2006)). Thus, any changes found in the expression of these genes in the KIS knockout mice may potentially be of relevance to the possible role of KIS in schizophrenia susceptibility.

Complementing these molecular studies, stereological measurements were made to investigate the effect of KIS knockout on the volume of selected brain structures. As KIS has a role in the regulation of the cell cycle as well as potentially in other facets of neuronal development, as detailed earlier in this chapter, the absence of KIS may have an impact on regional or total brain volume. Mice which do not express $p27^{kip1}$, which is regulated by KIS (Boehm et al., 2002), have been found to have increased brain volumes compared to their wildtype controls (Fero et al., 1996). Investigating whether there are changes in brain volume, or the volume of particular structures within the brain, in $KIS^{-/-}$ mice should contribute to determining the importance of KIS in maintaining normal brain morphology.

5.2. Methods

The brains from two series of knockout mice were available for this study. Frozen tissue was provided by Wyeth which included wildtype, heterozygous, and knockout mice, and both frozen and fixed tissue provided by NIH including wildtype and knockout mice only, as detailed in Section 2.1.2.2. Only male mice were included in the quantitative studies to avoid any effect of sex differences and variation associated with the oestrous cycle on gene expression.

5.2.1. PCR

5.2.1.1. RT-PCR

RT-PCR was used to confirm the absence of KIS mRNA expression. RNA was extracted from coronal sections of the frontal brain region of the frozen tissue and RIN was measured as described in Section 2.5.1 for each animal from both strains of mice. The RIN of all RNA samples was greater than 7.7. Reverse transcription was performed as described in Section 2.5.2. For the NIH mice, RT-PCR was carried out using 50ng cDNA template from each sample as described in Section 2.5.3 except that there were 30 cycles and an annealing temperature of 64°C was used. The PCR conditions were determined by pilot studies (data not shown). The KIS transcript was targeted using a forward primer complementary to exon 1 and reverse primer complementary to exon 2 (KIS (exons 1-2), see Table 2.6). KIS (exons 1-2) primers homology to the mouse KIS transcript (NM_010633) is 95% for the forward primer and 100% for the reverse primer. PCR of KIS exons 1 and 2 in the Wyeth mice was as described for NIH mice except that 35 cycles were included in the PCR. The increase in the number of cycles compared to the NIH mice was due to difficulties detecting KIS expression at lower cycle numbers in

these samples. TFRC expression was also measured as a control for total cDNA quantity and reverse transcription efficiency in both mouse brain series. PCR conditions for TFRC were as used for KIS as described above, using TFRC primers listed in Table 2.6. TFRC primers each have 95% homology to the mouse TFRC transcript (NM_011638).

5.2.1.2. qPCR

For the mice provided by Wyeth, qPCR was used to further confirm the absence of KIS expression in $KIS^{-/-}$ mice, and also to give a more accurate measure of the difference in KIS expression between $KIS^{-/+}$ and $KIS^{+/+}$ mice. The primer sets for KIS (exons 1-2) and the TFRC housekeeping gene (see Table 2.6), all at a final concentration of 0.2µM, were used along with SYBRgreen. Cycling conditions were as described in Section 2.5.5.2 with an anneal/extend temperature of 58°C. Each sample was measured in triplicate for each assay with 7.5ng cDNA in each well. A standard curve ranging from 37.5ng to 0.586ng of cDNA was made up of a pool of all $KIS^{-/+}$ and $KIS^{+/+}$ samples. $KIS^{-/-}$ samples were not included in the standard curve as the absence of KIS in these samples would be likely to affect the reliability of the standard curve for the KIS assay.

All samples from both knockout mice series were measured by qPCR using the primer set KIS (exons 4-5). Both the forward and reverse primers are 100% homologous to mouse KIS (NM_010633). This second primer set was used as they target a region of the transcript downstream of the knockout, whereas the KIS (exons 1-2) primer set targets the region which has been knocked out in both series of mice (Figure 5.1). Hence qPCR using the KIS (exons 4-5) primers should indicate if any truncated transcripts of KIS are still produced in the knockout mice. qPCR conditions are as described above for the KIS

(exons 1-2) qPCR assay, but with KIS$^{+/+}$ samples from the NIH mice also included in the standard curve. TFRC was also measured as a housekeeping gene.

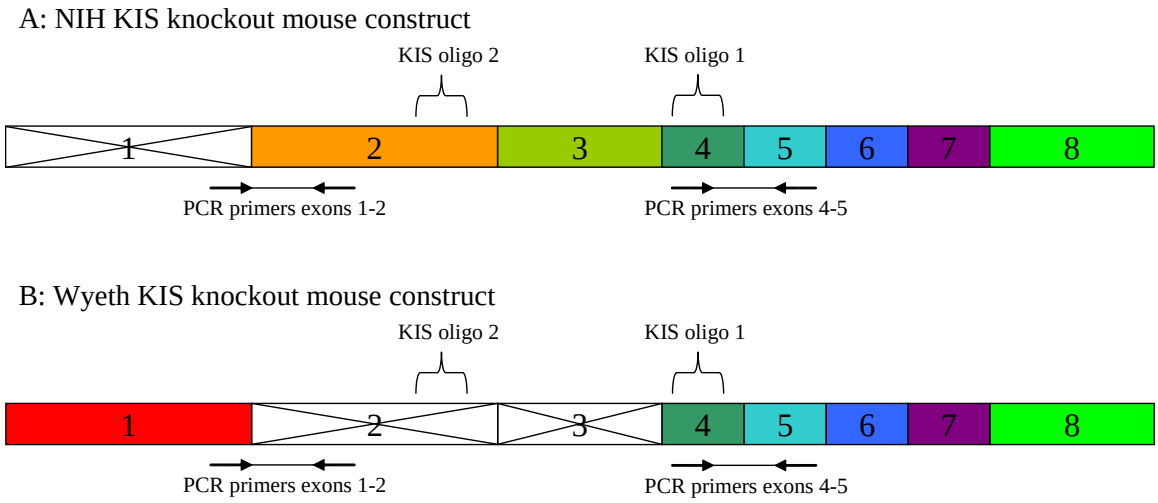

Figure 5.1: Schematic of the NIH and Wyeth KIS knockout mouse constructs.
The exons which have been deleted in each construct are marked. The regions of the transcript targeted by the oligonucleotide probes and PCR primers are also marked. Arrows indicate the location and direction of the primers.

5.2.2. In Situ Hybridisation Histochemistry

ISHH was used to further confirm the absence of KIS mRNA expression using the probe KIS (1) (Table 2.3) with 900,000 cpm of labelled probe per section (methods detailed in Section 2.2). Tissue sections from the level of the striatum of two KIS$^{+/+}$ and two KIS$^{-/-}$ mice from the NIH series were used. The slides were exposed to film for 16 days. ISHH of coronal sections at the level of the striatum, hippocampus, and cerebellum from all mice in the Wyeth series using the KIS (1) oligonucleotide probe was as performed in the NIH series but with 800,000 cpm of labelled probe per section and exposed to film for 14 days. The KIS (2) oligonucleotide probe (Table 2.3) was also used to confirm KIS knockout, with 800,000 cpm per section used on hippocampal sections from both the NIH and Wyeth KIS knockout series. Two animals of each genotype were included from

each series. The sections were exposed to film for 14 days. Two different probes were used to confirm KIS knockout in order to provide examples of ISHH where the probe targets the sequence which has been knocked out as well the sequence downstream of the knockout. Measurements were taken using methods described in Section 2.2.5, with background signal determined using the sense control sections.

The KIS (1) oligonucleotide probe is 100% complementary to the mouse KIS sequence (NM_010633), with the target sequence in exon 4 of the KIS mRNA transcript, and the KIS (2) probe is 97% homologous to mouse KIS, and targets exon 2 (Figure 5.1). The sequences of the both KIS probes do not have any more than 55% homology with any other RefSeq transcripts found on BLAST search (NCBI) for mouse.

ISHH was also used to measure the mRNA expression of GAP43, VGlut1, MAP2, spinophilin, and stathmin in the mice. These oligonucleotide probes (Table 2.3) are all 100% complementary to mouse transcripts of these genes (GAP43, NM_008083; VGlut1, NM_182993; MAP2, NM_008632; spinophilin, NM_172261; stathmin, NM_019641). Specificity of all probes was confirmed by BLAST search (NCBI), which confirmed probes showed less than 50% homology to any sequence other than the target transcript in mice. Methods were as described in Section 2.2, with 800,000 counts of labelled probe added to each tissue section. Slides were exposed to film for 4 days for GAP43, 2 days for VGlut1, 4 days for MAP2, 9 days for spinophilin, and 3 days for stathmin. Probe sequences and conditions of incubations and washes are detailed in Section 2.2.2, and measurements were taken using methods described in Section 2.2.5.

5.2.3. Western Blot

Western blots were used to determine the presence or absence of KIS protein in the knockout mice samples and the wildtype controls. The KIS antibodies used were Ab38292, AP8067a, and JH1998, as detailed in Table 2.5. The antibodies were raised against antigens encoded by a sequence in exons 4 and 5 of the KIS gene for Ab38292, exon 1 for AP8057a, and the full length of KIS for JH1998. The antibodies were tested against protein samples from the level of the striatum, which had been extracted using suspension buffer (see Section 2.3.1), from the NIH KIS mice series, with 20µg protein loaded into each well. Ab38292 was also tested against samples from the Wyeth KIS mice series which had been extracted from the level of the striatum using RIPA buffer (see Section 2.3.1), with 10µg protein loaded into each well. AP8067a and JH1998 antibodies were also tested against 0.075µg of recombinant KIS protein (Abnova).

Western blot was also used to measure the immunoreactivity of stathmin and $p27^{kip1}$ antibodies in the mice, and antibodies specific to stathmin which has been phosphorylated on serine 38 and $p27^{kip1}$ phosphorylated on serine 10 were used to quantify the level of phosphorylation of these proteins. The western blots were carried out as described in Section 2.3, with protein extracted from coronal sections at the level of the striatum, hippocampus, and cerebellum of the frozen tissue for each animal using RIPA buffer with protease and phosphatase inhibitors. GAPDH was also measured in all samples as a housekeeping gene. Details of the antibodies and the concentrations at which they were used are described in Table 2.5. The western blots were measured as described in Section 2.3.6.

5.2.4. Stereological Measurements

Volumes of the lateral and dorsal third ventricles, hippocampal formation, striatum, and a representative measure of the whole brain were estimated from point counting of sections using Cavalieri theorem as described in Section 2.9. The tissue used was fixed KIS knockout and wildtype mouse brains from NIH as detailed in Section 2.1.2.2. Fixed tissue was used for the stereological measurements as it maintains better morphology than frozen tissue.

5.3. Investigations of KIS Expression in Knockout Mice

The remainder of this chapter is presented in two sections. This section presents the results and discussion of the experiments investigating the level of KIS expression in the two KIS knockout mice series. The results of the quantification studies using these knockout mice will be presented and discussed in Section 5.4.

5.3.1. Results

5.3.1.1. RT-PCR

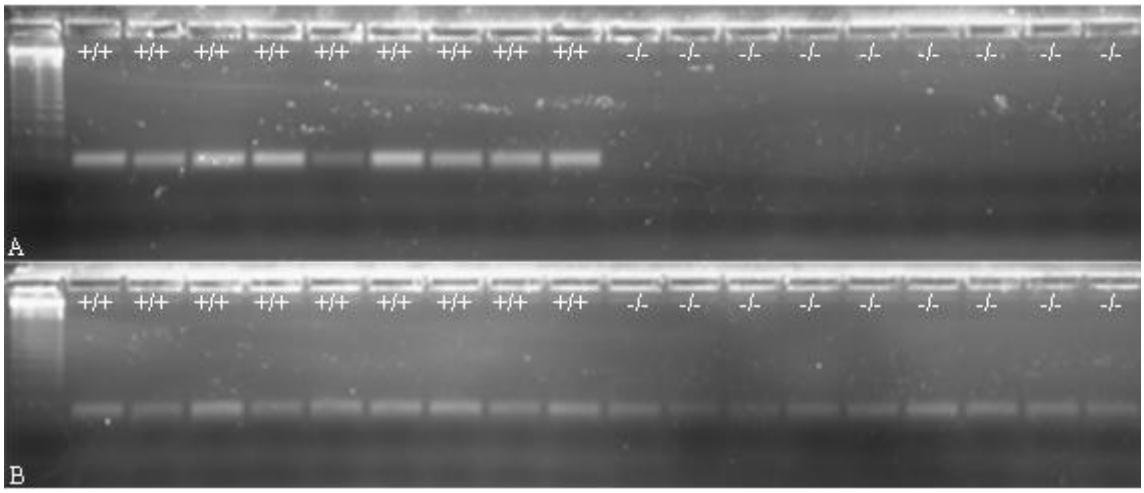

Figure 5.2: RT-PCR of KIS in the NIH KIS knockout mouse series.
(A) KIS exons 1-2, (B) TFRC. TFRC samples correspond to KIS samples directly above.
+/+, wildtype mouse; -/-, knockout mouse.

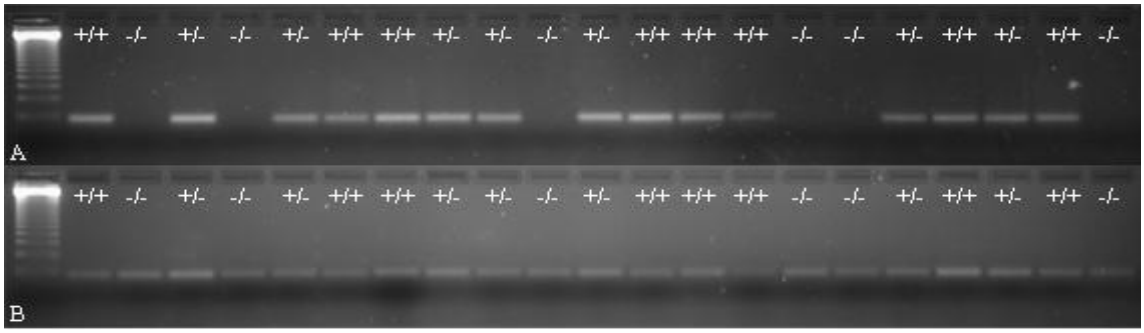

Figure 5.3: RT-PCR of KIS in the Wyeth KIS knockout mouse series.
(A) KIS exons 1-2, (B) TFRC. TFRC samples correspond to KIS samples directly above.
+/+, wildtype mouse; +/- heterozygous knockout mouse; -/-, knockout mouse.

The absence of KIS expression in KIS knockout mice was confirmed in the NIH (Figure 5.2A) and Wyeth (Figure 5.3A) series using primers targeting exons 1 and 2 of the KIS transcript, which show a single PCR product of the expected size for KIS (117bp) in all wildtype and heterozygous mice but no evidence of a PCR product in the knockout mice for either series. TFRC was used as a housekeeping gene to control for the amount and quality of cDNA present, and a PCR product of the expected size for TFRC (113bp) was observed in all samples of the NIH (Figure 5.2B) and Wyeth (Figure 5.3B) series.

qPCR of the samples from the Wyeth mice with the primers for KIS (exons 1-2) normalised to TFRC demonstrated that there was a significant effect of genotype on KIS expression (univariate ANOVA effect of genotype $p<0.001$, post-hoc t-tests: wildtype-knockout $p<0.001$; wildtype-heterozygous $p=0.002$; heterozygous-knockout $p=0.001$), with the heterozygous group showing around 50% of the level of KIS expression of the wildtype group and the knockout group again showing no KIS expression (Figure 5.4).

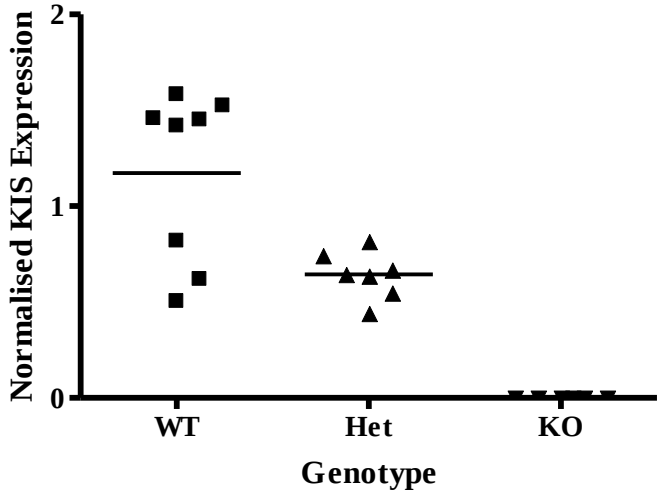

Figure 5.4: qPCR of KIS exons 1-2 in Wyeth KIS knockout mice series.
All measures are normalised to TFRC expression. WT, wildtype; Het, heterozygous knockouts; KO, knockout.

When qPCR was carried out using primers targeting exons 4-5 of KIS there was again an overall effect of genotype on KIS expression in the Wyeth series (univariate ANOVA effect of genotype p=0.001, post-hoc t-tests: wildtype-knockout p<0.001; wildtype-heterozygous p=0.040; heterozygous-knockout p=0.027); however, some KIS mRNA was still detected in the knockout mice (Figure 5.5). In the NIH series, KIS expression is detected in all wildtype samples and there was, as expected, no detectable KIS expression in the knockout mice (Figure 5.5), and there was a significant effect of genotype on KIS expression (Mann-Whitney, p<0.001).

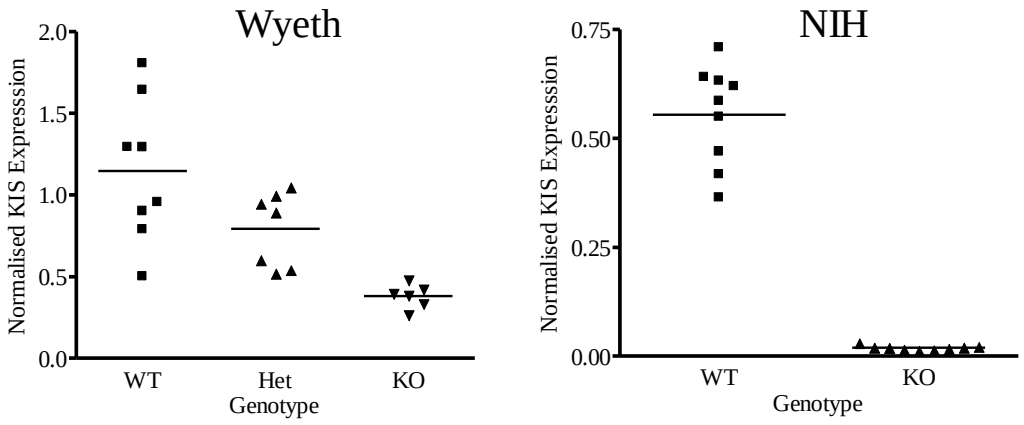

Figure 5.5: qPCR of KIS exons 4-5 in Wyeth and NIH KIS knockout mice series.
All measures are normalised to TFRC expression. WT, wildtype; Het, heterozygous knockouts; KO, knockout.

5.3.1.2. In Situ Hybridisation Histochemistry

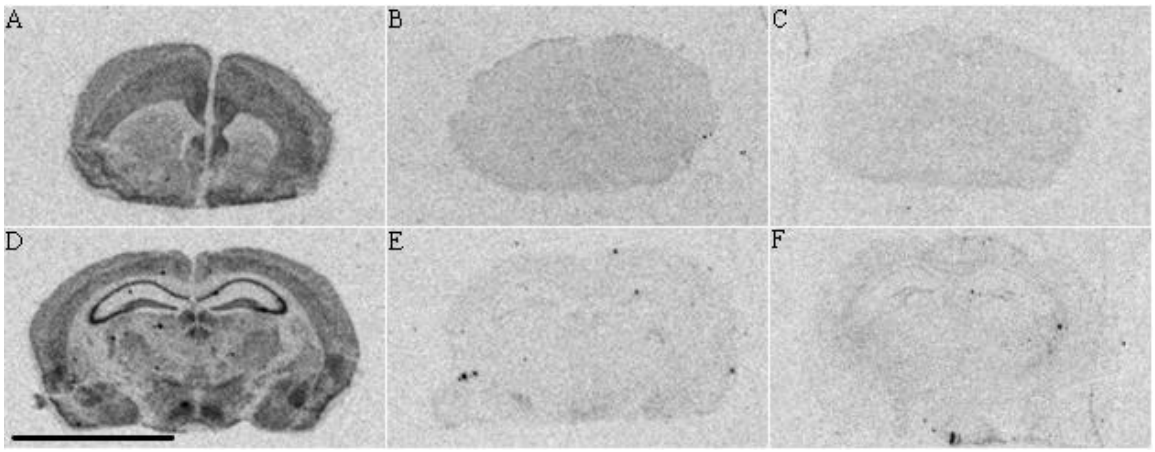

Figure 5.6: ISHH of NIH KIS knockout mice and wiltdtype controls.
(A-C) coronal sections at the level of the striatum; (A-B) KIS (1) oligonucleotide probe; (A) wildtype; (B) knockout; (C) wildtype with KIS (1) sense control oligonucleotide probe; (D-F) coronal sections at the level of the hippocampus; (D-E) KIS (2) oligonucleotide probe; (D) wildtype; (E) knockout, (F) wildtype with excess of unlabeled KIS (2) oligonucleotide probe;. See Figures 2.1 and 3.4 for labelling of brain regions. Scale bar = 5mm.

ISHH of KIS expression in tissue from the NIH KIS knockout series shows normal KIS expression in wildtype mouse brain (Figure 5.6A) and no signal in the knockout mouse brains (Figure 5.6B) when using the KIS (1) oligonucleotide probe, which targets a sequence in exon 4 of the KIS transcript. The same result is found when using the KIS (2) oligonucleotide probe, which targets exon 2 of the KIS transcript (Figure 5.6D-E). The signal observed in the tissue sections from the knockout mice is similar to that of the control section for both oligonucleotide probes (Figures 5.6C and 5.6F).

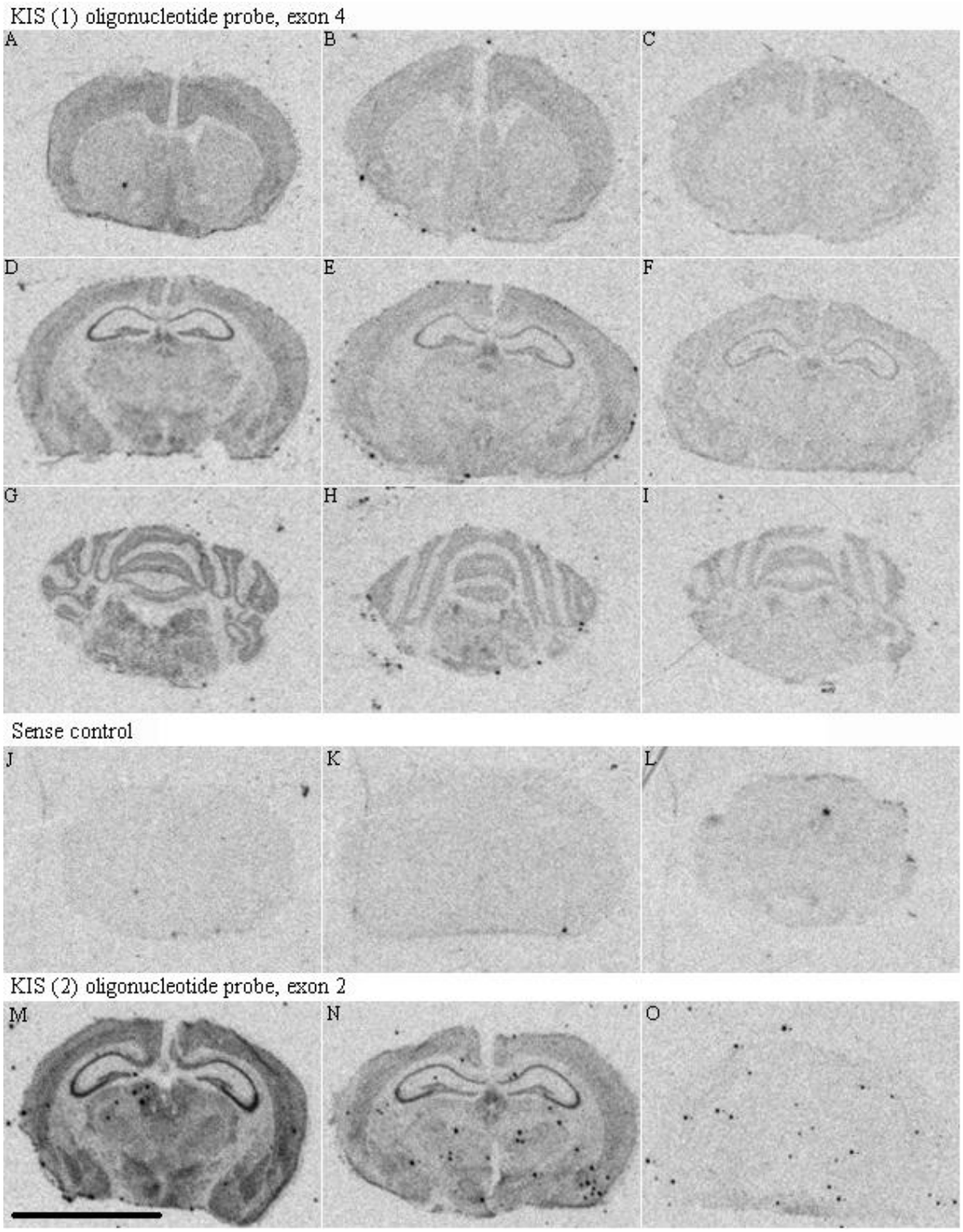

Figure 5.7: ISHH of KIS expression in Wyeth knockout mouse series.
(A-I) KIS (1) oligonucleotide probe; (J-L) KIS (1) sense control oligonucleotide probe; (M-O) KIS (2) oligonucleotide probe; (A, D, G, J, K, L, M) wildtype; (B, E, H, N) heterozygous for KIS knockout; (C, F, I, O) KIS knockout; Shown are coronal sections at the level of (A-C) striatum; (D-F, M-O) hippocampus; (G-I) cerebellum. See Figures 2.1 and 3.4 for labelling of brain regions. Scale bar = 5mm.

ISHH of KIS expression in tissue from the Wyeth KIS knockout series using the KIS (1) oligonucleotide probe shows normal KIS expression in wildtype sections at the level of the striatum (Figure 5.7A), hippocampus (Figure 5.7D), and cerebellum (Figure 5.7G). KIS mRNA is also detected in the knockout mouse tissue (Figures 5.7C, 5.7F, and 5.7I) at levels higher than the background as defined by the sense probe (Figures 5.7J-L), although the expression is lower than in wildtypes. Quantification of the signal confirms that in all brain regions measured KIS expression is highest in wildtype tissue, lowest in knockout tissue, and expression in heterozygote mice is intermediate (Figure 5.8).

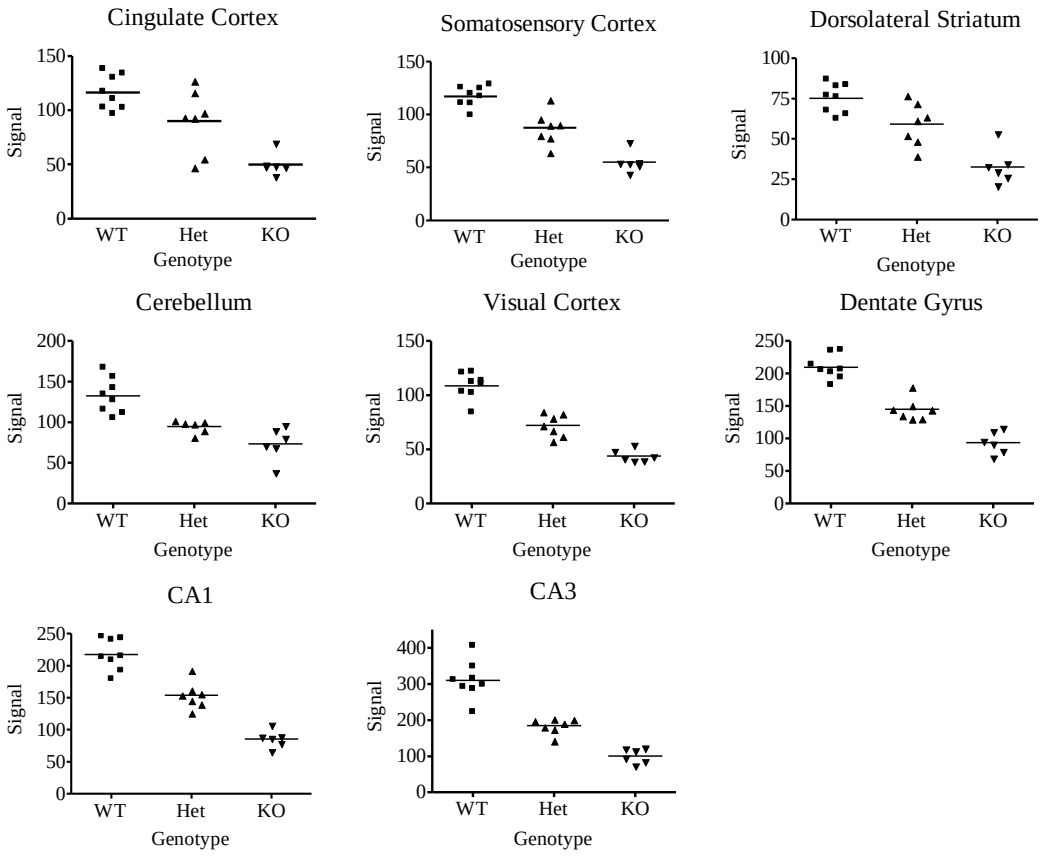

Figure 5.8: Quantification of KIS ISHH in Wyeth KIS knockout mouse series.
Values are from ISHH using the KIS (1) oligonucleotide probe. Signal indicates relative abundance of mRNA in terms of ^{35}S nCi/g, with background signal subtracted. Horizontal line indicates the mean value for each group. CA1, cornu ammonis 1; CA3, cornu ammonis 3; WT, wildtype; Het, heterozygote; KO, knockout.

Results using the KIS (2) probe for ISHH in the Wyeth mouse tissue are similar to those observed in the NIH series of mice (Figure 5.6), with normal KIS expression in wildtype mice (Figure 5.7M) and no apparent signal in the knockout mice (Figure 5.7O). The heterozygote mice show an intermediate level of KIS expression (Figure 5.7N).

5.3.1.3. Western Blot

Confirmation of the absence of KIS protein in both series of KIS knockout mice was attempted first by using the KIS antibody Ab38292. However, no difference was observed between the knockout and wildtype samples (Figure 5.9). This was unexpected, especially with the previous results having shown the absence of complete KIS mRNA transcript in these samples (Sections 5.3.1.1 and 5.3.1.2). In order to determine if there was a problem with the Ab38292 antibody, a selection of alternative antibodies were tested. The antibodies were first tested against the recombinant KIS protein (as described in Section 3.2.4). The antibodies JH1998 and AP8067a detected the recombinant KIS sample at the expected size (Figure 5.10A and 5.10C) and were tested against the KIS knockout mice (Figure 5.10B and 5.10D). As with the Ab38292 antibody, a band was detected approximately at the expected size in the western blot of mouse protein samples, but no difference in signal intensity was observed between the NIH KIS knockout and wildtype mice. Identical results were found when these antibodies were tested in the Wyeth KIS knockout mice (data not shown). These experiments have therefore failed to confirm the absence of KIS protein in the KIS knockout mice.

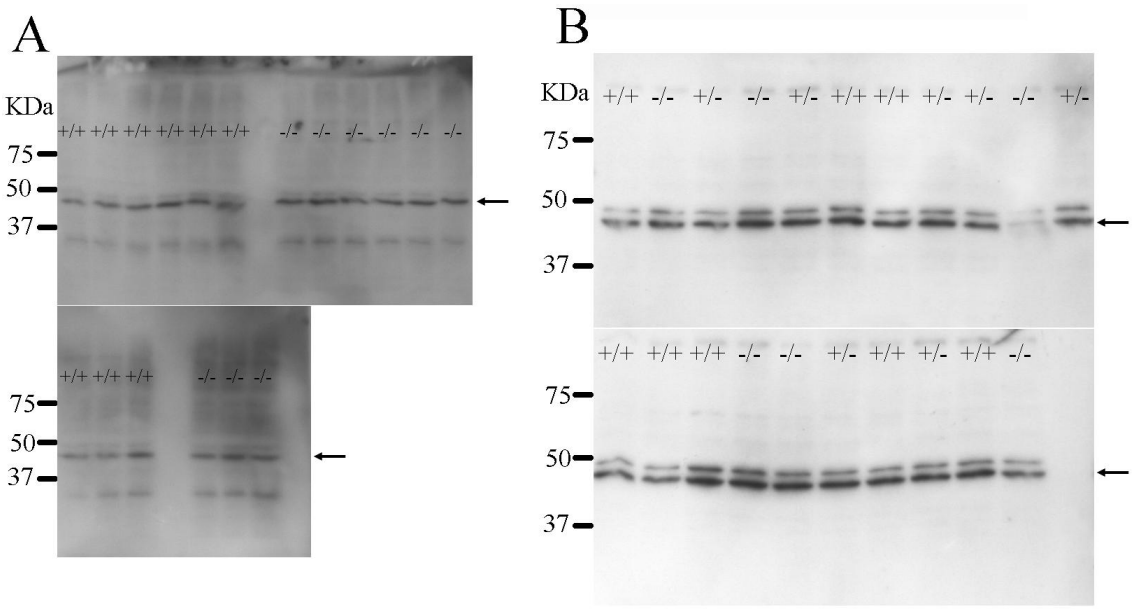

Figure 5.9: Western blot in KIS knockout mice using the Ab38292 KIS antibody.
(A) NIH series. (B) Wyeth series. Arrows indicate the band at the predicted size of KIS (46.5kDa). +/+, wildtype; +/-, heterozygous KIS knockout; -/- homozygous KIS knockout; KDa, kilodaltons.

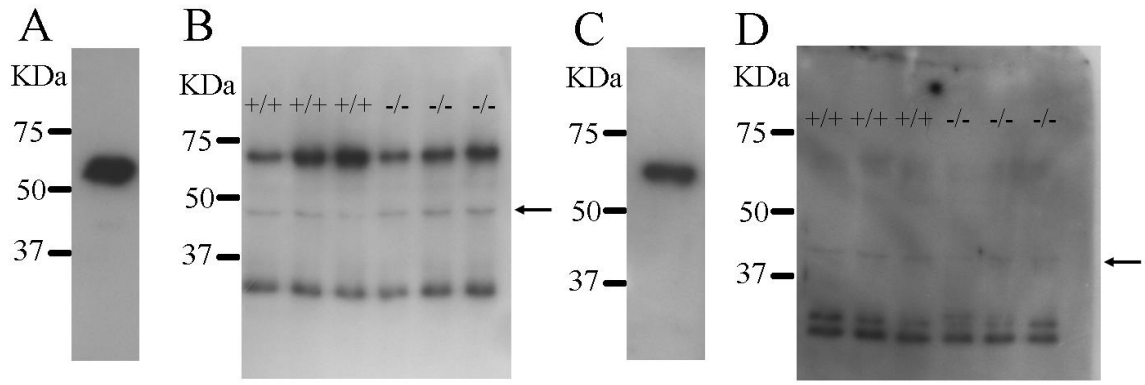

Figure 5.10: Western blot of KIS in KIS knockout mice using alternative KIS antibodies.
All samples from the NIH KIS knockout mice series. (A) Antibody JH1998, recombinant KIS protein; (B) Antibody JH1998, NIH KIS knockout mice series; (C) Antibody AP8067a, recombinant KIS protein; (D) Antibody AP8067a, NIH KIS knockout mice series. Arrows indicate the band closest to the predicted size of KIS (46.5kDa). Recombinant KIS protein has a predicted size of 64kDa. +/+, wildtype; -/-, KIS knockout; KDa, kilodaltons.

5.3.2. Discussion: KIS Expression in Knockout Mice

The absence of KIS mRNA transcript was confirmed in both the NIH and Wyeth KIS knockout mice, both using qPCR and RT-PCR with primers spanning exons 1 and 2 (Figures 5.2 and 5.3). In this respect, both lines are bona fide knockouts. However, some of the tests carried out on particular regions of the mRNA transcript were inconclusive. When the qPCR was repeated using primers targeting exons 4 and 5, the results remained negative for the NIH knockout mice but KIS mRNA was detected in the Wyeth knockout mice (Figure 5.5). Similar results were found in the ISHH experiments (Figures 5.6 and 5.7), in that the NIH mice gave the expected result, with no evidence of KIS mRNA with either oligonucleotide probe (Figure 5.6), and in the Wyeth mice the oligonucleotide probe targeting exon 2 also showed the expected absence of signal in the knockout mice (Figure 5.7M-O). However, the exon 4 oligonucleotide probe did show some signal in all genotype groups in the Wyeth mice (Figure 5.7A-I).

These results are potentially due to the knockout construct in each of these mice. The mice provided by NIH were produced by replacing the first exon of the KIS gene with another gene (Langenickel et al., 2008), while the mice from Wyeth were produced by deleting the 2nd and 3rd exons of the KIS gene (Figure 5.1). It appears that while the NIH construct has prevented the transcription of the any form of the KIS gene, the mice from Wyeth mice still produced some form of KIS transcript, although any transcript produced does not contain the deleted 2nd and 3rd exons. Indeed, subsequent correspondence with Wyeth revealed that they had identical findings in these mice (personal correspondence). The reduced quantity of KIS in the Wyeth mice which were heterozygous or homozygous for the KIS knockout may reflect alterations in regulation of transcription or of mRNA stability in the resultant truncated transcript. The truncated transcript would be

missing 485 base pairs compared to the full length version, which would result in a frame shift and would be very unlikely to produce a functioning protein, if indeed any protein was translated at all.

	NIH KIS Knockout Mice	Wyeth KIS Knockout Mice
RT-PCR		
Exons 1-2	Knockout confirmed	Knockout confirmed
Exons 4-5	Knockout confirmed	Transcript detected
ISHH		
Exon 2	Knockout confirmed	Knockout confirmed
Exon 4	Knockout confirmed	Transcript detected
Western Blot		
Ab38292	Protein detected	Protein detected
JH1998	Protein detected	Protein detected
AP8067a	Protein detected	Protein detected

Table 5.1: Summary of attempts to confirm KIS knockout in NIH and Wyeth series of KIS knockout mice.

In addition to the transcript issues (which questioned the validity of the Wyeth but not the NIH mice), both series of mice revealed unexpected findings in terms of KIS protein, as assessed by western blotting. The results discussed above indicated that neither series of knockout mice should be producing a full length KIS protein (i.e. the NIH mice should have no protein, and any protein in the Wyeth mice would be smaller than normal KIS, if detectable at all). However, a selection of different KIS antibodies, which all robustly detected a band of the expected size when tested against recombinant KIS protein, all showed bands of comparable size and intensity in NIH and Wyeth knockout mice

compared to wildtypes. The antibodies tested included the one which had been used to confirm the KIS knockout at NIH (AP8067a; Langenickel et al., 2008). Subsequent correspondence with those who worked with these mice at NIH revealed that they had also had problems with confirming the KIS knockout by western blot, and had only successfully used the western blot to confirm the knockout in vascular smooth muscle cell extracts, but had been unable to in embryonic fibroblast samples (personal correspondence). Correspondence with Wyeth showed that they had also been unable to confirm the KIS knockout in their series of mice using the JH1998 KIS antibody (personal correspondence). This information was not available until after the experiments reported here were carried out.

There are two possible explanations for these western blot results. The first is that the mice are true knockouts but that the antibodies are not specific and are detecting another protein. This possibility is supported by the absence of full length KIS mRNA transcript in both series of knockout mice – a finding which would often be taken as the 'gold standard' and sufficient evidence of the knockout status. And, although part of the KIS transcript was detected in the Wyeth knockout mice, even if this partial transcript were translated it would have produced a truncated KIS protein which would be predicted to have a frame shift, and so if any protein did result from this transcript it would be shorter than full length KIS, and therefore the western blots would indicate a different size, and it would be unlikely to be a suitable antigen for the KIS antibodies anyway. However, all three of the antibodies tested here detected a band at the expected size in the recombinant KIS sample (Figures 3.3 and 5.10), which should have contained only the KIS protein. While this does not confirm the antibodies detect KIS alone, it does at least confirm they do detect KIS. As stated earlier, these antibodies target various points on the KIS protein

(a sequence spanning exons 4 and 5 of the KIS gene for Ab38292, exon 1 for AP8057a, and the full length of KIS for JH1998), reducing the likelihood that they would all cross-react with another antigen. Further to this, the JH1998 KIS antibody, which failed to detect any difference between the KIS knockout and wildtype mice in this study (Figure 5.10A), has been shown to be able to detect changes in abundance of KIS when KIS expression was upregulated in AtT20 cell lines (Francone et al., 2010).

The second possible explanation is that the antibodies are specific for KIS, and that the mice are not true knockouts. However, the absence of the KIS mRNA transcript (which was unequivocal in the NIH mice at least), raises the question of where the protein is coming from. One possibility is that there is an as yet unidentified KIS homologue elsewhere in the genome, but this would have to produce a protein homologous enough to KIS for the KIS antibodies, which target several different points of the protein, all to bind to it, but not so homologous that the KIS PCR primers and oligonucleotide probes would detect its transcript.

Had these experiments stopped with the RT-PCR confirmation of the absence of KIS expression using the primers targeting exons 1 and 2 of the KIS transcript (Figures 5.2-5.3), this confirmation of the KIS knockout would not have been questioned. However the further results of qPCR, ISHH, and western blotting cannot be ignored. The implications of the KIS Ab38292 antibody failing to detect any difference in KIS protein between the wildtype and KIS knockout mice on the results previously obtained in human tissues using this antibody (Chapters 3 and 4), and precedents of similar problems encountered in other knockout mice, will be further discussed in Chapter 6.

Given the somewhat equivocal findings in the Wyeth mice, it was decided to do the experimental work solely on the NIH mice, about which there was at the time no reason to doubt their knockout status based on mRNA expression (Table 5.1). The issues raised by the KIS western blot data and their impact on data interpretation is considered in Section 6.2, after the results of the molecular and morphological studies have been presented.

5.4. Quantification Studies in KIS Knockout Mice

5.4.1. Results

5.4.1.1. Quantity and Phosphorylation State of KIS Targets

Examples of each of the western blots are shown in Figure 5.11. Two bands were visible in the $p27^{kip1}$ western (Figure 5.11C). The higher of the two was measured as it is closest to the expected size for this protein (27kDa).

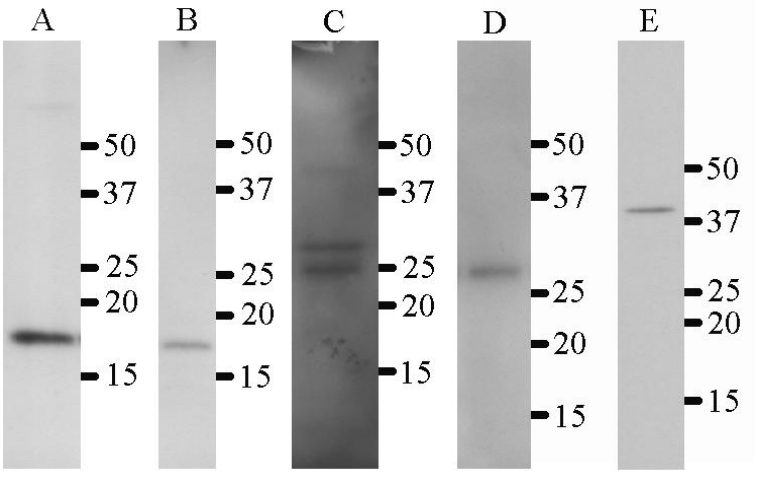

Figure 5.11: Example images of stathmin, $p27^{kip1}$, and GAPDH western blots.
(A) Stathmin; (B) stathmin phosphorylated on serine 38; (C) $p27^{kip1}$; (D) $p27^{kip1}$ phosphorylated on serine 10; (E) GAPDH. Size markers are in kilodaltons.

Protein	Effect of Genotype		Genotype x Brain Region	
Stathmin	$F_{1,29}$=2.334	P=0.137	$F_{2,29}$=0.631	P=0.539
Phosphorylated Stathmin	$F_{1,18}$=0.016	P=0.899	$F_{1,18}$=0.004	P=0.951
$p27^{kip1}$	$F_{1,28}$=0.673	P=0.419	$F_{2,28}$=0.024	P=0.977
Phosphorylated $p27^{kip1}$	$F_{1,27}$=0.138	P=0.714	$F_{2,27}$=3.678	P=0.039*

Table 5.2: The effect of genotype on KIS targets in NIH KIS knockout mice as measured by western blot.
The interaction of genotype and brain region is also shown. The proteins measured were stathmin, stathmin phosphorylated on the serine 38 residue, $p27^{kip1}$, and $p27^{kip1}$ phosphorylated on the serine 10 residue. All data were normalised to GAPDH. * = $p<0.05$.

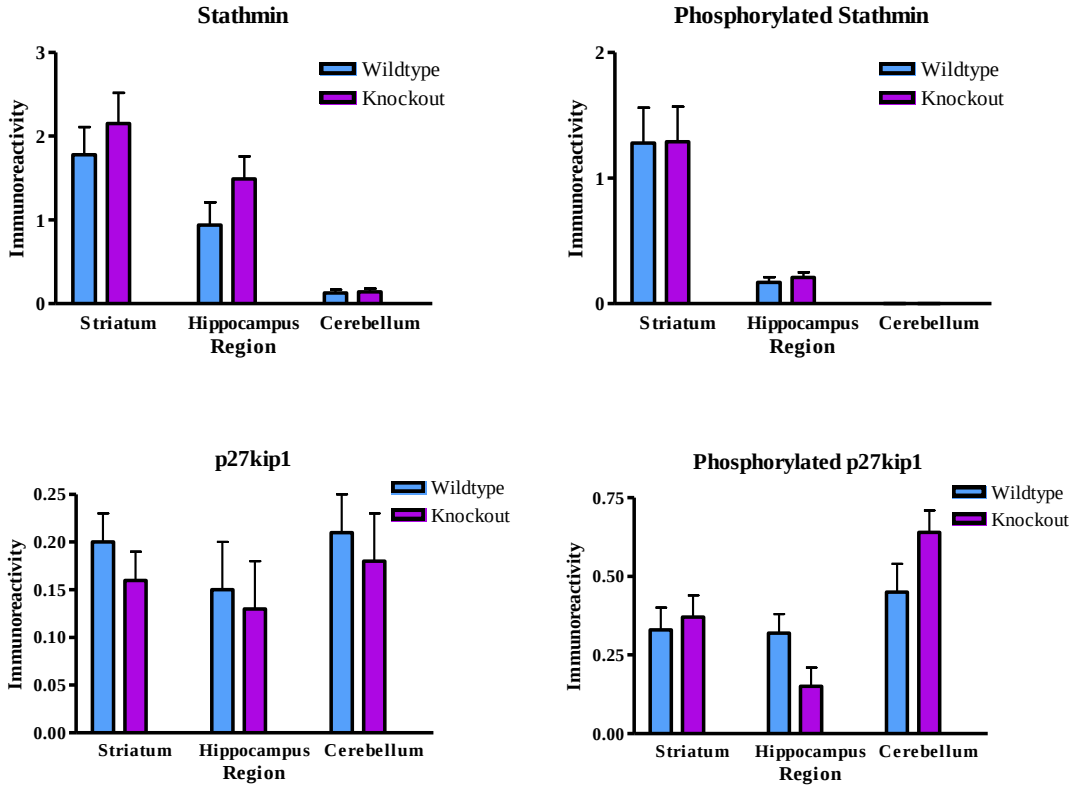

Figure 5.12: Immunoreactivity of KIS targets in the NIH KIS knockout mice series as measured by western blot.
All samples are normalised to GAPDH. Mean value is shown plus standard error of the mean. Stathmin phosphorylation was measured on the serine 38 residue and $p27^{kip1}$ phosphorylation was measured on the serine 10 residue.

The protein samples included in these studies were extracted from coronal tissue sections at the level of the striatum, hippocampus, and cerebellum. One of the knockout mouse samples from the level of the striatum was excluded from all experiments due to problems in protein extraction from this sample. One outlier (see Section 2.10) was removed from the phosphorylated stathmin striatum and the $p27^{kip1}$ cerebellum groups, and two outliers were removed from the phosphorylated $p27^{kip1}$ cerebellum group. After omissions, all of the data were normally distributed and the ANOVA showed no significant effect of genotype in any of the proteins measured when all brain regions are combined (Table 5.2) and post-hoc tests showed no differences in each region individually (Figure 5.12). There was a trend for an increase of phosphorylated $p27^{kip1}$ at the level of the hippocampus (Table A4), and phosphorylated $p27^{kip1}$ also showed a significant interaction of region and genotype (Table 5.2). However there was a significant effect of genotype on the quantity of GAPDH in these samples (data not shown) and this seems to be driving these effects. Tables of these results are included in the Appendix.

5.4.1.2. Quantification of Molecular Markers

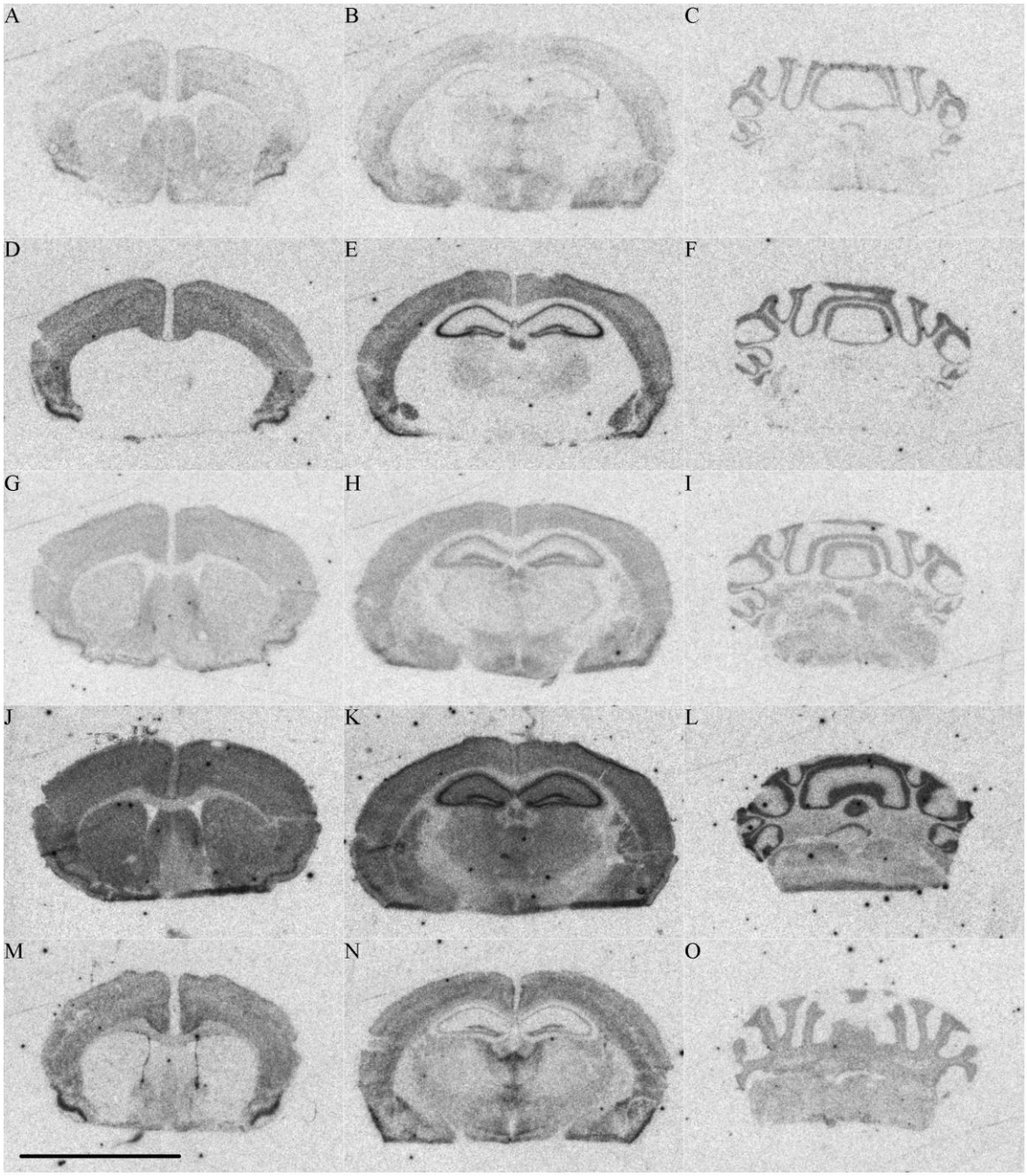

Figure 5.13: ISHH autoradiograph examples of GAP43, VGlut1, MAP2, spinophilin, and stathmin expression in adult mice.
(A-C) GAP43; (D-F) VGlut1; (G-I) MAP2; (J-L) Spinophilin; (M-O) Stathmin. All rows show, from left to right, examples of coronal tissue sections at the level of the striatum, hippocampus, and cerebellum, and all images shown are tissue sections from a wildtype mouse from the NIH KIS knockout mice series. See Figures 2.1 and 3.4 for labelling of brain regions. Scale bar = 5mm.

The mRNA expression of GAP43, VGlut1, MAP2, spinophilin, and stathmin were measured using ISHH in the somatosensory cortex, cingulate cortex, dorsolateral striatum, visual cortex, CA1, CA3, dentate gyrus, and the molecular layer of the cerebellum of the NIH KIS knockout mice and wildtype controls. Although GAP43 was present in the dentate gyrus the signal was not strong enough to be measured accurately (Figure 5.13B), and VGlut1 was not detected in the striatum (Figure 5.13D), as predicted from previous studies (Eastwood et al., 2007).

One cerebellum sample from a knockout mouse was missing from the VGlut1 and MAP2 groups, and one cingulate cortex sample from a knockout mouse was missing from the VGlut1 and spinophilin groups as damage to the tissue prevented accurate measurements. One knockout mouse sample was removed from each of the GAP43 cingulate cortex and spinophilin somatosensory cortex knockout mouse groups, and one wildtype mouse sample was removed from each of the MAP2 somatosensory cortex, CA1, CA3, and dentate gyrus groups, as they were outliers.

Firstly the overall effect of genotype on the selected mRNAs was examined by comparing the mean of all measurements in all brain regions for each genotype. There was a significant change in VGlut1 ($p=0.004$) and stathmin ($p=0.005$) mRNAs in the knockout mice, as well as trend of changes in spinophilin ($p=0.099$) and GAP43 mRNA ($p=0.08$) (Table 5.3). No significant change in overall MAP2 mRNA expression was found, although there was a significant effect of genotype and brain region interaction on MAP2 expression ($p=0.001$) (Table 5.3). Follow up analyses were performed which revealed the localisation and direction of the changes indicated by these ANOVA results,

as shown in Figures 5.14-5.18, summarised in Table 5.4, and tables of these results are included in the Appendix.

Total mRNA				
Target Gene	Effect of Genotype		Genotype x Brain Region	
GAP43	$F_{1,70}$=3.148	P=0.080	$F_{6,70}$=1.112	P=0.365
VGlut1	$F_{1,68}$=9.105	P=0.004*	$F_{6,68}$=0.539	P=0.777
MAP2	$F_{1,79}$=1.770	P=0.187	$F_{7,79}$=4.143	P=0.001*
Spinophilin	$F_{1,79}$=2.787	P=0.099	$F_{7,79}$=0.738	P=0.640
Stathmin	$F_{1,80}$=8.395	P=0.005*	$F_{7,80}$=0.316	P=0.316

Table 5.3: The effect of genotype on the expression of molecular markers in NIH KIS knockout mice as measured by ISHH.
The interactions of genotype with brain region are also shown. mRNA quantities were measured as ^{35}SnCi/g tissue equivalents. * = p<0.05.

Investigation of gene expression by brain region indicated several significant changes in the KIS knockout mice. These were: a decrease in GAP43 mRNA expression in CA1 (p=0.022, Figure 5.14), an increase in VGlut1 mRNA expression in the visual cortex (p=0.028, Figure 5.15), an increase in MAP2 mRNA expression in the somatosensory cortex, dorsolateral striatum, and the cerebellum (p=0.006, p=0.018, p=0.007 respectively, Figure 5.16), an increase in spinophilin mRNA in the dorsolateral striatum (p<0.001, Figure 5.17), and an increase in stathmin mRNA in the dorsolateral striatum (p=0.042, Figure 5.18). There was also a trend of an increase in stathmin mRNA expression in the somatosensory cortex (p=0.055).

	GAP43	VGlut1	MAP2	Spinophilin	Stathmin
SSCx	↔	↔	↑*	↔	↑
Cing Cx	↔	↔	↔	↔	↔
Visual Cx	↔	↑*	↔	↔	↔
Striatum	↔	-	↑*	↑*	↑*
CA1	↓*	↔	↔	↔	↔
CA3	↔	↔	↔	↔	↔
DG	-	↔	↔	↔	↔
Cerebellum	↔	↔	↑*	↔	↔

Table 5.4: Summary of changes in mRNA expression of molecular markers in NIH KIS knockout mice series.
↔ = no significant change; ↓* = significant ($p<0.05$) decrease in knockout mice compared to wildtype; ↑* = significant ($p<0.05$) increase in knockout mice compared to wildtype; ↑ = trend increase in knockout mice compared to wildtype; - = not measured; SSCx, somatosensory cortex; Cing Cx, cingulate cortex; Visual Cx, visual cortex; striatum, dorsolateral striatum; DG, dentate gyrus.

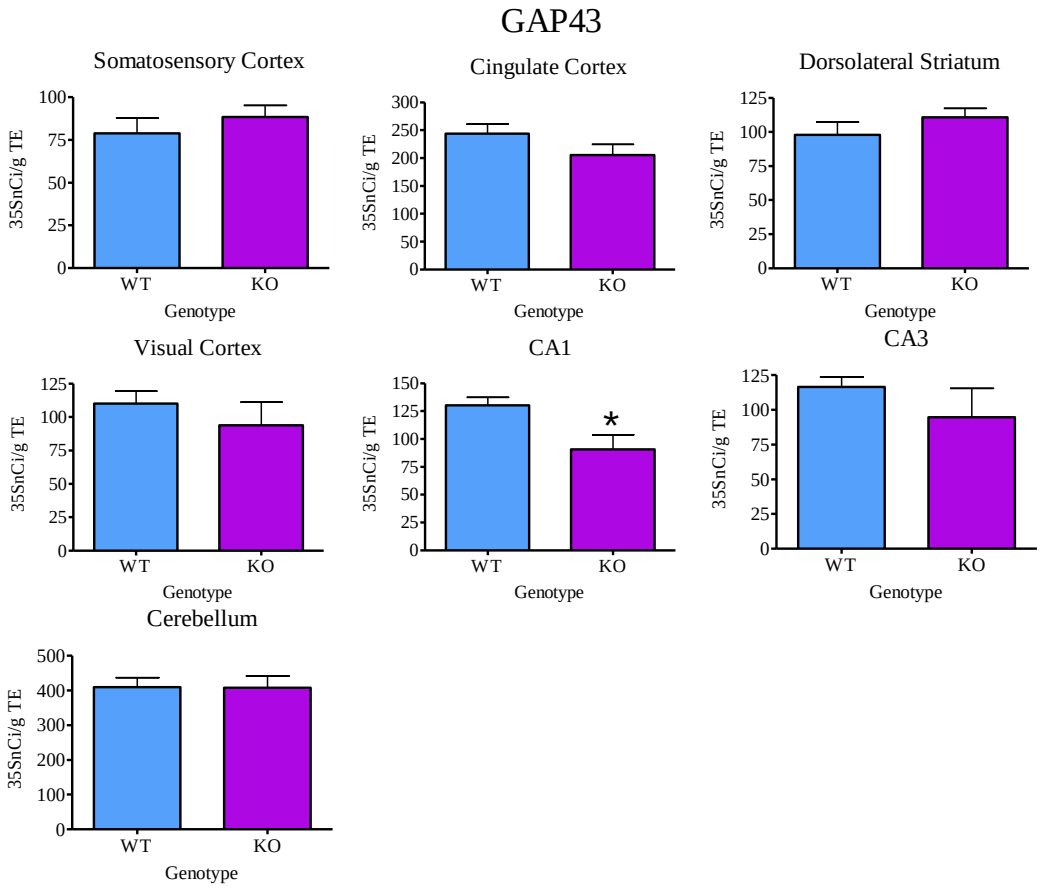

Figure 5.14: mRNA expression of GAP43 in NIH KIS knockout and wildtype control mice.
Mean value plus standard error of the mean are shown. WT, wildtype; KO, knockout; TE, Tissue equivalents. * = $p<0.05$.

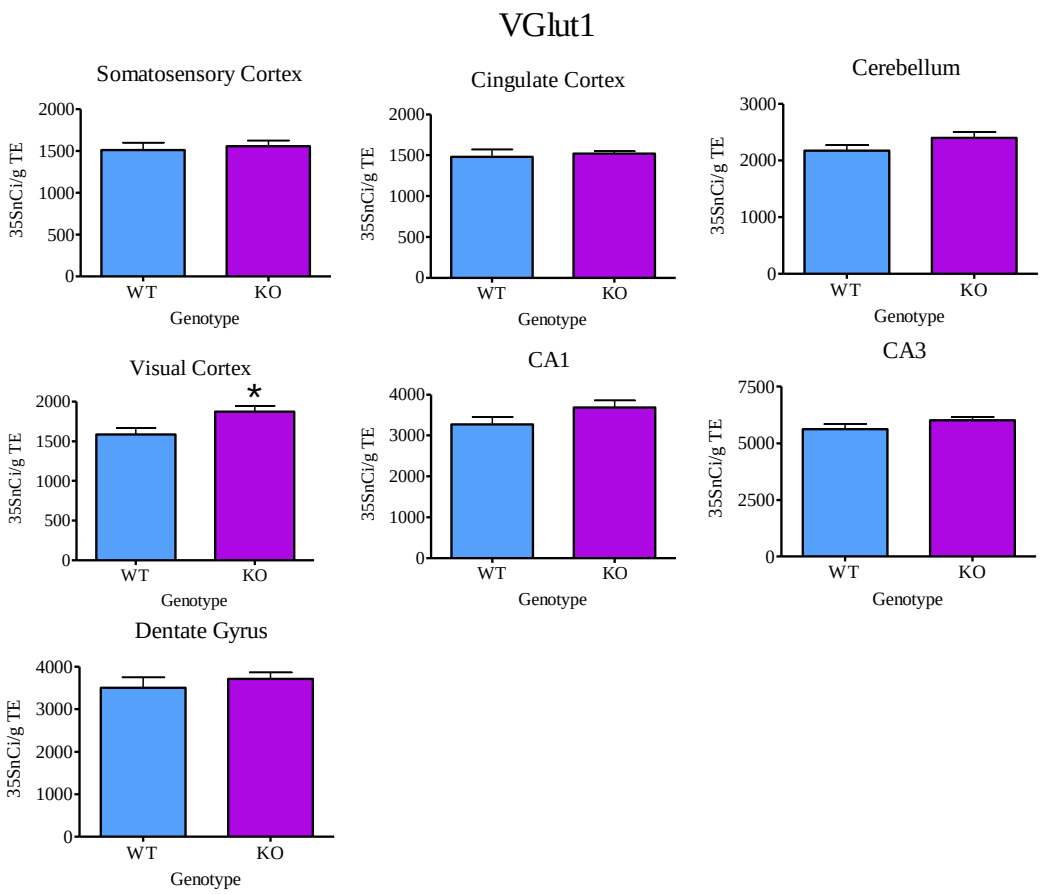

Figure 5.15: mRNA expression of VGlut1 in NIH KIS knockout and wildtype control mice.
Mean value plus standard error of the mean are shown. WT, wildtype; KO, knockout; TE, Tissue equivalents. * = $p<0.05$.

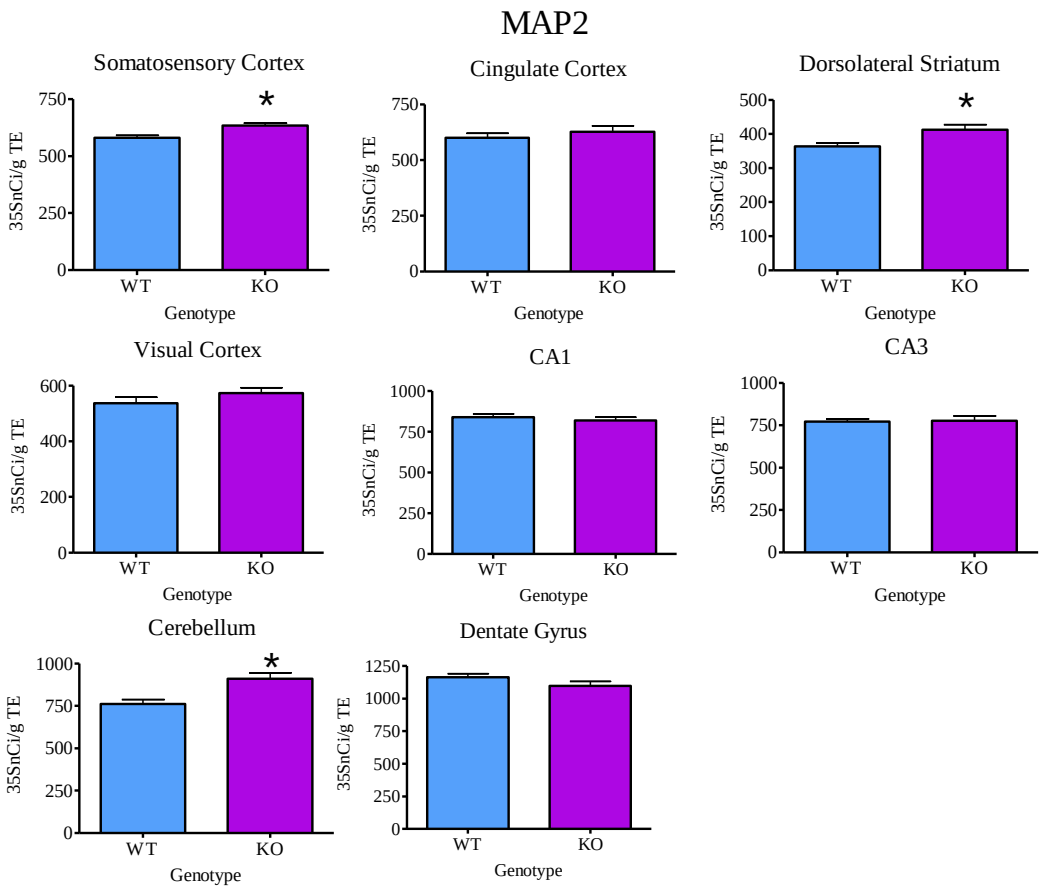

Figure 5.16: mRNA expression of MAP2 in NIH KIS knockout and wildtype control mice.
Mean value plus standard error of the mean are shown. WT, wildtype; KO, knockout; TE, Tissue equivalents. * = $p<0.05$.

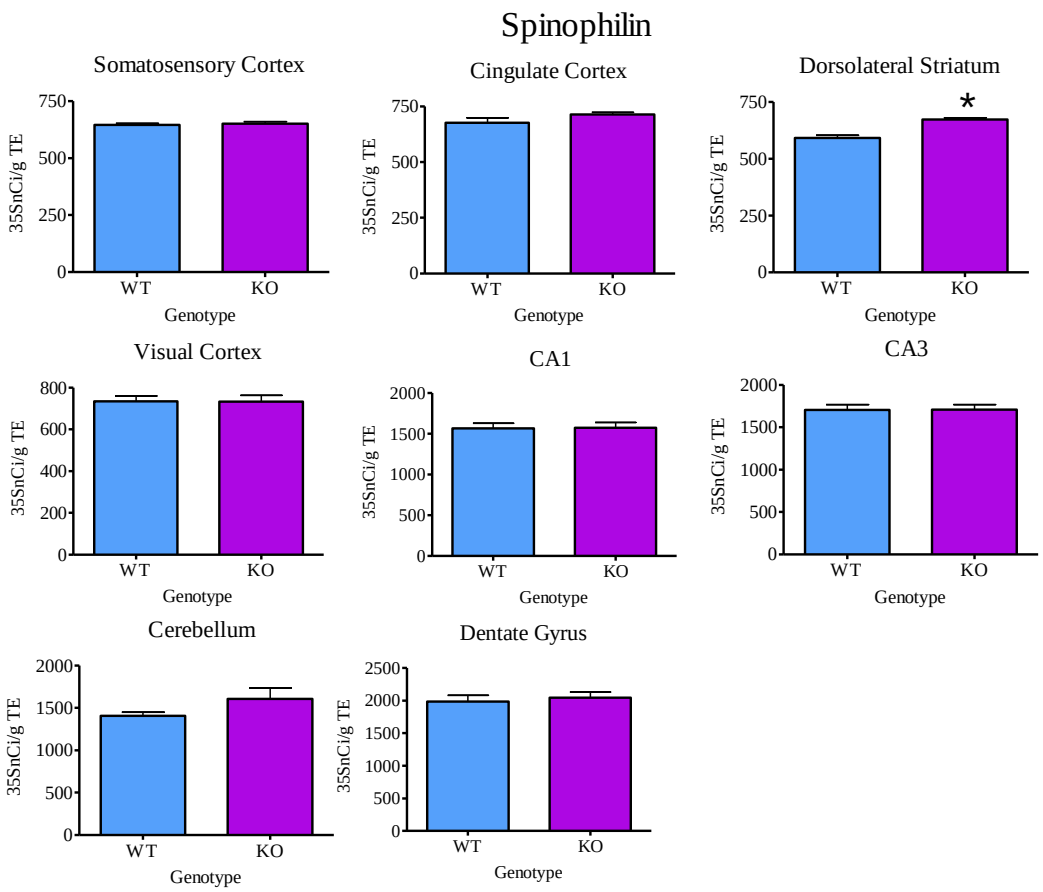

Figure 5.17: mRNA expression of spinophilin in NIH KIS knockout and wildtype control mice.
Mean value plus standard error of the mean are shown. WT, wildtype; KO, knockout; TE, Tissue equivalents. * = $p<0.05$.

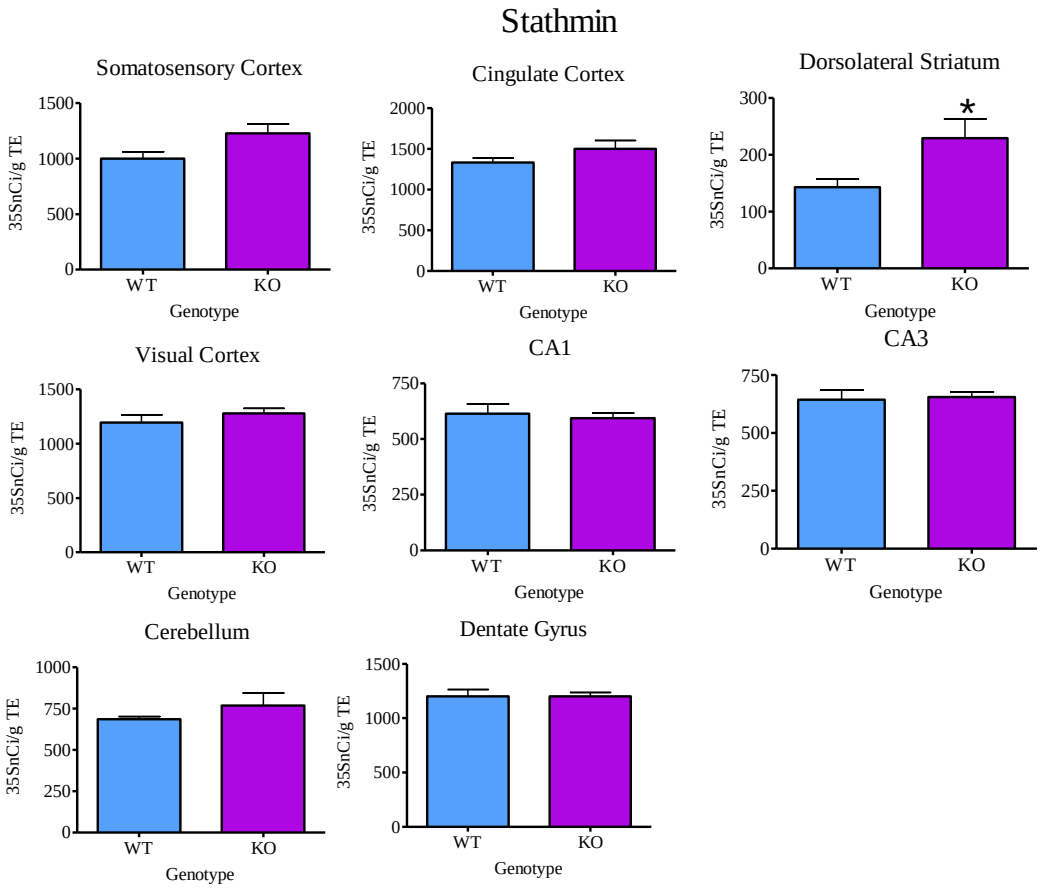

Figure 5.18: mRNA expression of stathmin in NIH KIS knockout and wildtype control mice.
Mean value plus standard error of the mean are shown. WT, wildtype; KO, knockout; TE, Tissue equivalents. * = $p<0.05$.

5.4.1.3. Stereological Measures

Two outliers were excluded from the striatum knockout mouse group. There were no differences in the estimated volumes of the ventricles, striatum, hippocampal formation, and the representative measure of total brain volume between knockout and wildtype mice (Figure 5.19). There was however a borderline significant reduction ($p=0.05$) in the relative volume of the hippocampal formation in the knockout mice brains as a percentage of total brain volume (Figure 5.20). Tables of these results are included in the Appendix.

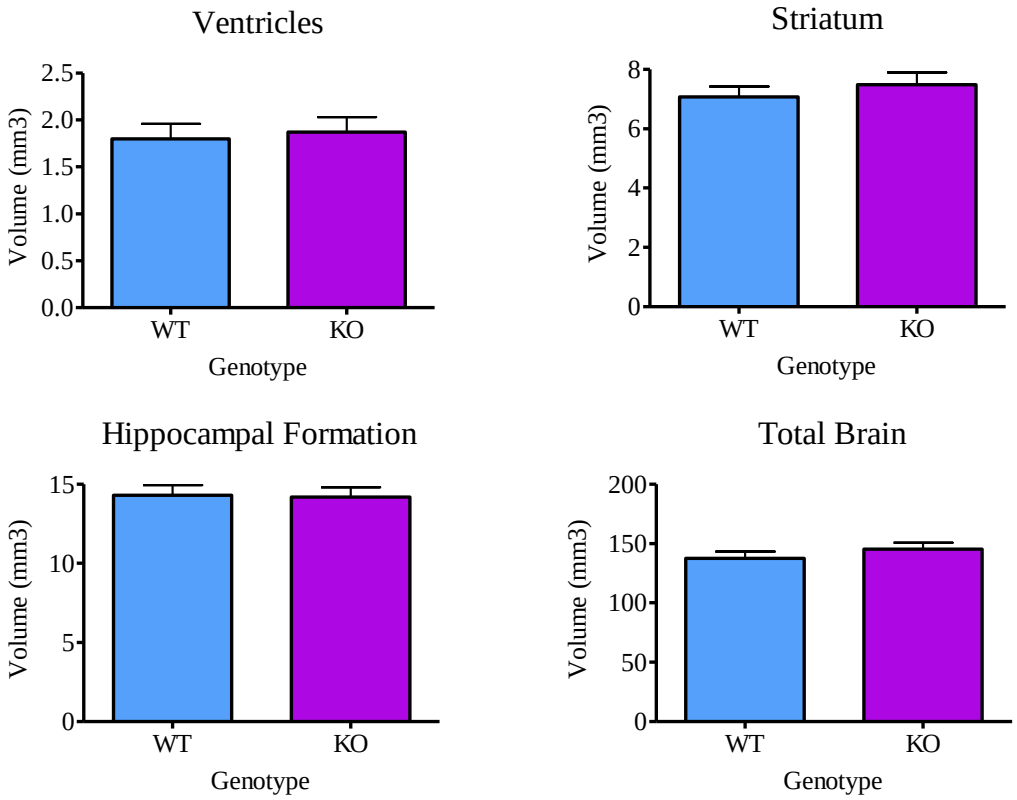

Figure 5.19: Stereological measures of the volumes of brain structures in NIH KIS knockout mice.
Mean value plus standard error of the mean are shown. Measurements of the ventricles were taken from the lateral and dorsal third ventricle. Total brain refers to a representative measure of the brain volume from the beginning of the corpus callosum to the end of the dentate gyrus. WT, wildtype; KO, knockout.

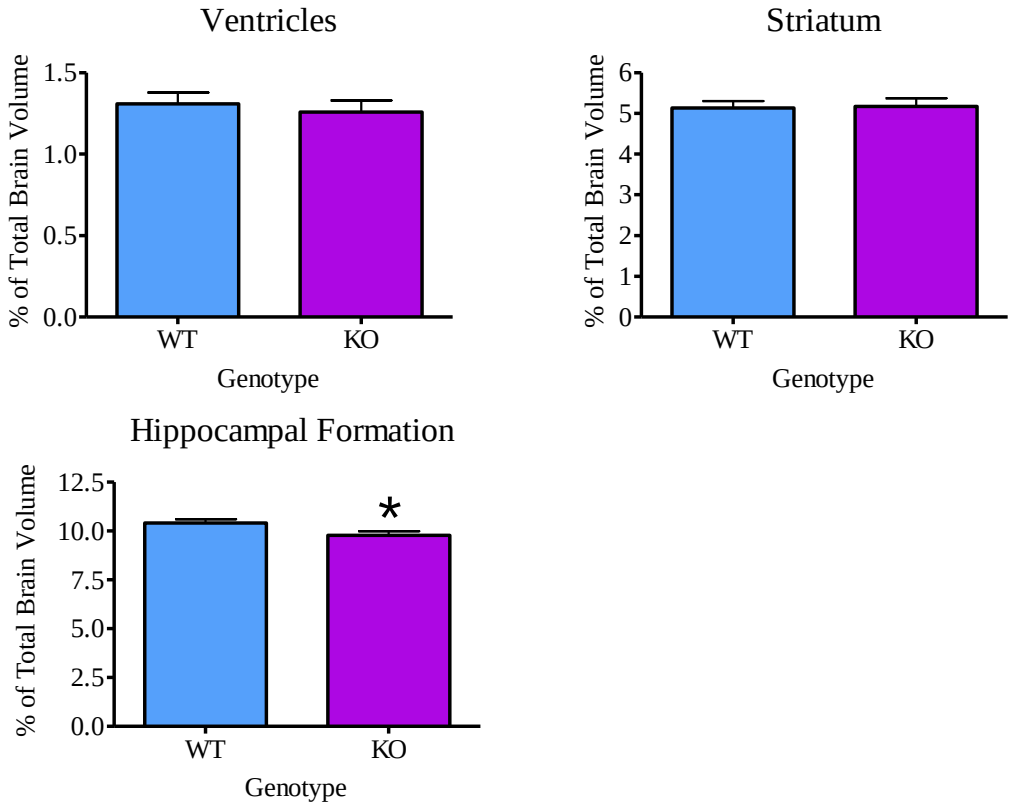

Figure 5.20: Stereological measures of the volumes of brain structures in NIH KIS knockout mice as a percentage of total brain volume.
Total brain refers to a representative measure of the brain volume from the beginning of the corpus callosum to the end of the dentate gyrus. Mean values plus standard error of the mean are shown. WT, wildtype; KO, knockout. * = $p \leq 0.05$.

5.4.2. Discussion: Quantification Studies in KIS Knockout Mice

The remaining discussion of the results described in Sections 5.4.1.1-5.4.1.3 presumes that the NIH mice are true knockouts, although interpretation of the following results should bear in mind that this may not be true (see Section 5.3.2).

5.4.2.1. The Function of KIS in the Adult Rodent Brain

Neither stathmin nor $p27^{kip1}$ were found to be significantly changed in quantity in the KIS knockout mice when compared to the wildtype mice. There was also no change found in the amount stathmin or $p27^{kip1}$ which was phosphorylated on the residues which are targeted by KIS. It was hypothesised, as KIS has been previously shown to phosphorylate both stathmin (Maucuer et al., 1997; Langenickel et al., 2008) and $p27^{kip1}$ (Boehm et al., 2002), that the absence of KIS would lead to a decrease in phosphorylation of these proteins. Phosphorylation has also been shown to lead to the inactivation or breakdown of both stathmin (Larsson et al., 1997; Langenickel et al., 2008; Manna et al., 2009) and $p27^{kip1}$ (Boehm et al., 2002), and so it was also thought possible that the total quantity of these proteins may be higher in the KIS knockout mice. A previous study using the same series of KIS knockout mice from NIH found an increase in the amount of stathmin in cultured cells derived from the knockout mice (Langenickel et al., 2008), however this was not the case in the brain regions of the KIS knockout mice used here. It may be worth noting that the mean quantity of stathmin was higher in the knockout mice than the wildtype in all three brain regions examined (Figure 5.12), although this does not approach significance either in the individual brain regions (Table A1) or when all brain regions were combined (Table 5.2).

It is possible that there is some redundancy in function for KIS, in that KIS may be the main, but probably not the only, kinase to phosphorylate these proteins. A cyclin dependant kinase (CDK-1) has been found to phosphorylate stathmin on the serine 38 residue (Nakamura et al., 2006) and the serine/threonine kinase Akt1 can phosphorylate $p27^{kip1}$ on the serine 10 residue (Nacusi et al., 2006). KIS may phosphorylate stathmin

and/or $p27^{kip1}$ in normal circumstances, but in the absence of KIS an alternative kinase may increase in activity or expression to maintain normal levels of phosphorylation. There are several other potential KIS targets, such as PAM, SF1, MBP, and synapsin, which may be affected by the KIS knockout, but these proteins were not investigated in this study for a combination of reasons which included insufficient information of the site phosphorylated by KIS, and the lack of a reliable antibody.

Though stathmin was detected in the cerebellum, no signal for stathmin phosphorylated on the serine 38 residue was detected in the cerebellum of either knockout or wildtype mice, indicating that despite the presence of both KIS and stathmin, stathmin is not phosphorylated on the serine 38 residue in the cerebellum. The quantity of stathmin detected in the cerebellum samples appears to be considerably lower than at the level of either the striatum or hippocampus (Figure 5.12), so the failure to detect phosphorylated stathmin may be a reflection of this. Alternatively the absence of phosphorylated stathmin in the cerebellum in both genotype groups, combined with unchanged levels of phosphorylated stathmin in other brain regions, may provide further evidence that the phosphorylation of stathmin is not the function of KIS in the cerebellum.

5.4.2.2. The Effect of KIS Knockout on Molecular Markers and Brain Structure Volumes

KIS knockout mice showed significantly higher expression of VGlut1 and stathmin, a trend of higher expression of spinophilin, and a trend of lower expression in GAP43. Significant results from the post-hoc analysis of these mRNA expression data found that in the knockout mice GAP43 was lower in CA1, VGlut1 was higher in the visual cortex, spinophilin and stathmin were both higher in the dorsolateral striatum, and there was a

trend of an increase in stathmin in the somatosensory cortex. Although there was no overall effect of genotype for MAP2, there was a significant interaction of genotype and brain region and post-hoc analysis showed that MAP2 mRNA expression was higher in the somatosensory cortex, dorsolateral striatum, and cerebellum.

The overall decrease in GAP43 mRNA could reflect reduced synaptic plasticity (Benowitz et al., 1997), and may be linked to the role of both KIS and GAP43 regulation of neurites, as overexpression of GAP43 has been shown to increase neurite outgrowth (Aigner et al., 1995), and a reduction of KIS causes a decrease in neurite outgrowth (Cambray et al., 2009). The increase in VGlut1 mRNA suggests that the KIS knockout mice may have increased glutamatergic signalling. Although this change in VGlut1 only reaches significance in the visual cortex, all other brain regions showed higher VGlut1 expression in the knockout mice than in the wildtype controls, which indicates that this change may be present to some extent elsewhere in the brain.

MAP2 and spinophilin both represented post-synaptic markers, with MAP2 also a marker of dendrites and spinophilin a marker of dendritic spines, which is where the majority of glutamatergic synapses terminate. The increase in both MAP2 and spinophilin may indicate that there is an increase in the number, structure, or functionality of dendrites and dendritic spines. It should be noted that all these conclusions as to the functional significance of the mRNA changes are subject to the caveat that the mRNA levels may not reflect protein levels or functional activity; equally, there can be changes in protein indices which are not accompanied by mRNA alterations.

The quantity of stathmin was predicted to be higher in the KIS knockout mice compared to the wildtype mice, based on previous findings in VSMCs from KIS knockout mice (Langenickel et al., 2008). Although the quantity of stathmin immunoreactivity was higher in the knockout mice in all three brain regions investigated, these increases were not significant (Table 2.2; Figure 5.12). Quantification of stathmin expression by ISHH also indicated an increase in stathmin in the majority of brain regions investigated, with a significant increase in the dorsolateral striatum, a trend of an increase in the somatosensory cortex, and a significant overall effect of genotype (Figure 5.18 and Table 5.3), consistent with the initial hypothesis. However, the hypothesis of increased stathmin in the knockout mice was based on the reported decrease in stathmin degradation due to reduced phosphorylation of stathmin by KIS (Langenickel et al., 2008). An increase in stathmin mRNA expression does not appear to be consistent with this hypothesis of the mechanism through which KIS knockout would lead to increased stathmin, suggesting that the KIS knockout may have a more general effect on microtubule regulation, independent of its role in phosphorylation of stathmin.

It is noticeable that there was a significant increase in the expression of three of the four genes measured (MAP2, spinophilin, and stathmin) in the dorsolateral striatum, indicating that the absence of KIS had a particularly large impact on this region. This may indicate that the dorsolateral striatum is less able to compensate for the absence of KIS, possibly reflecting the distribution of other kinases which may take on the roles of KIS in other brain regions.

In the stereological measurements there was very little evidence of differences between the KIS knockout and wildtype mice, indicating that KIS is unlikely to have a major

effect on brain development, at least in the parameters investigated here. The only significant change was that the hippocampal formation was smaller as a percentage of the representative measure of total brain volume in the knockout mice, indicating that KIS may have a subtle role in the development or maintenance of the hippocampus. The decrease in relative size of the hippocampus in the KIS knockout mice may be linked to the reduced GAP43 expression, given that the latter is a growth-associated protein and is centrally involved in hippocampal synaptic plasticity (Benowitz et al., 1997).

Some of these findings could, speculatively, be linked to the potential role of KIS in schizophrenia susceptibility. Increased expression of several transcripts in the dorsolateral striatum implies a particularly significant effect of KIS in this region, and the striatum has been implicated to play a role in the pathogenesis of the cognitive and psychotic symptoms of schizophrenia (Epstein et al., 1999; Simpson et al., 2010), related to excessive dopamine release (Abi-Dargham et al., 1998). Also, a smaller hippocampus is a neuropathological feature of schizophrenia (Lawrie and Abukmeil, 1998; Nelson et al., 1998; Wright et al., 2000), albeit in the disease it is smaller in absolute terms rather than just relative to whole brain volume.

A point that is important to the interpretation of the findings reported here is that the wildtype mice are not littermate controls. The KIS knockout mice were produced by cross-breeding KIS knockout mice, so each litter contained only knockout mice. The previous publication which used this strain of knockout mice refers to crossing $KIS^{+/-}$ mice to produce $KIS^{+/+}$ and $KIS^{-/-}$ mice (Langenickel et al., 2008), but at the stage we received the tissue all that was available was from $KIS^{+/+}$ and $KIS^{-/-}$ mice which had been bred independently from the same genetic background. This could potentially add some

variability between the knockout and wildtype mice, which could raise questions as to whether the results obtained from these mice are genuinely as a result of the difference in genotype and not from subtle differences in genetic or epigenetic factors. A recent study has found behavioural differences between substrains of C57BL6 mice, indicating that slight genetic differences can produce a significant effect (Matsuo et al., 2010).

5.5. Summary

The data presented in the second part of this chapter indicate that in the KIS knockout mice there is no change in the total quantity or phosphorylation states of the KIS targets stathmin and $p27^{kip1}$ in adult mice. There is however evidence of alterations in expression of several molecular markers of synaptic function and plasticity in the mice. There was also a relative decrease in the volume of the hippocampal formation in the KIS knockout mice. These data may reflect a role of KIS in the formation and/or maintenance of normal neural connections. However, the results are subject to the caveats about the knockout status of the mice, and the use of non-littermate controls.

Chapter 6: General Discussion

6.1. Summary of the Findings Presented in this Thesis

With reference to the aims stated in Section 1.3, the work presented in this thesis has achieved:

(1) Characterisation of the regional and cellular distribution of KIS mRNA and protein in the adult human brain.

(2) The quantification of KIS expression in the developing rodent brain.

(3) The quantification of KIS with regard to diagnostic group and (4) KIS genotype in the human brain.

(5) The characterisation of several molecular markers and reported KIS phosphorylation targets in a selection of brain regions in KIS knockout mice.

In the human brain, KIS expression was detected through the depth of the cortex and was particularly prominent in the deeper cortical layers. KIS expression was also detected in dentate gyrus, CA1, CA3, and CA4 regions of the hippocampus, and in both Purkinje cells and the granule cell layer of the cerebellum. KIS expression was not detected in the white matter. KIS immunoreactivity was strongest in the nucleus of pyramidal neurons and Purkinje cells, although there was also immunoreactivity in the cytoplasm.

The peak of KIS expression in all brain regions measured in mice was at P7, which is around a period of rapid brain development equivalent to the third trimester of human development. This peak in KIS expression may indicate a role for KIS in neurodevelopment at this point.

No difference in the quantity of KIS expression was found between diagnostic groups or the schizophrenia associated SNP rs7513662 genotype groups in human post mortem samples from the STG, DLPFC, ACC, and cerebellum, or in lymphoblast cell lines. No evidence of KIS splice variants were detected in the brain. The failure to find any significant change in KIS with regard to diagnostic groups weakens the case for KIS as a schizophrenia susceptibility gene, and the absence of any change in KIS expression with regard to SNP genotype means that the mechanism through which this SNP could regulate the KIS gene and confer schizophrenia susceptibility remains unknown.

Characterisation of KIS knockout mice found no change in the quantity or phosphorylation state of the reported KIS targets stathmin and $p27^{kip1}$, which may indicate that these proteins are not phosphorylated by KIS in the adult brain, or at least that KIS is not the only kinase which phosphorylates these proteins in the brain. The volume of the hippocampal formation, in relation to a representative measure of total brain volume, was smaller in the KIS knockout mice than in the wildtype mice. Molecular markers relating to connectivity and glutamatergic signalling, such as MAP2, spinophilin, and VGlut1, were found to have increased expression in the KIS knockout mice. The microtubule regulatory protein stathmin was also found to have increased expression, whereas the expression of GAP43, a marker of neuronal plasticity, was decreased. These findings imply a role for KIS in development and/or maintenance of normal connectivity in the brain.

6.2. Limitation of these Studies

In the quantitative studies of KIS in humans, it should be noted that only a selection of brain regions were studied, only one KIS SNP was investigated, and subjects who were

heterozygous for this SNP genotype were grouped together with the homozygous G allele groups. However the negative findings in several brain regions in these relatively large collections of post mortem samples indicate that it would be unlikely that changes would be found in other brain regions. The KIS SNP investigated had previously shown the strongest association with schizophrenia in genetic association studies (Puri et al., 2007; 2008) and tags a haplotype block which includes all of the other SNPs within the KIS gene which have been associated with schizophrenia. The grouping of SNP genotypes was necessary due to low numbers of subjects which were G allele heterozygotes, and preliminary analysis of the data which did not group the genotypes in this way also showed no indication of an effect of genotype on KIS expression (data not shown).

The failure to confirm the absence of the KIS protein in the KIS knockout mice does present a problem in these studies. As discussed in Section 5.3.2, these results either indicate that the knockout mice are not genuine KIS knockouts, or that the antibodies are detecting something other than the KIS protein. This affects the interpretation of either the results obtained from the KIS knockout mice tissue in Chapter 5, or the results of the KIS distribution experiments in Chapter 3 and KIS quantification in Chapter 4 which used this same KIS antibody.

In the NIH mice there was no indication of the presence of any form of KIS transcript, and in the Wyeth mice there was a partial KIS transcript, and the construct of the knockout would mean that any residual KIS expression would contain a frame shift and produce a truncated protein, if any protein at all. However, a selection of KIS antibodies detected no difference between KIS knockout and wildtype mice in both series. All of

these antibodies detected a band of the expected size in a western blot using recombinant KIS protein, suggesting that the antibodies do detect the KIS protein. The JH1998 antibody tested here has previously been shown to be sensitive to induced changes in KIS expression in cell lines (Francone et al., 2010), providing a further indication that this antibody does detect KIS. Further to this, the distribution of KIS immunoreactivity in the human brain described in Chapter 3 matches the distribution of KIS mRNA expression, with this convergence of results reported to be a suitable method of validating the specificity of immunohistochemistry in the brain (Rhodes and Trimmer, 2006).

These antibody problems in the knockout mice are not unique to KIS. A previous study investigating estrogen receptor (ER) beta found that while a selection of antibodies could detect a purified sample of ER beta, none of these antibodies detected any difference between wildtype and ER beta knockout mice using samples from the brain, despite the absence of the ER beta mRNA transcript as determined by RT-PCR (Snyder et al., 2010). While the ability of an antibody to distinguish between wildtype mice and mice which do not express the target protein can be regarded as a key test of determining antibody specificity (Saper and Sawchenko, 2003), the data obtained using the KIS antibody in humans should be regarded with caution rather than entirely dismissed. As detailed above, there are several examples of tests which indicate that the antibodies do detect KIS. The apparent lack of specificity of the KIS antibody in the knockout mice could be due to compensation for the absence of KIS in the brain by increasing the expression of other proteins which, if they happen to have a similar molecular weight, are likely candidates for cross-reactivity of the antibody in the western blot (Lorincz and Nusser, 2008). KIS knockout at the protein level was claimed in the NIH knockout mice, using one of the antibodies (AP8067a) tested in Chapter 5, but this confirmation was only

made in vascular smooth muscle cells (Langenickel et al., 2008), and could not be replicated in mouse embryonic fibroblasts (personal communication), indicating that any problem with the specificity of the antibody may be specific to particular tissues.

Further tests of the antibodies used could be carried out by knocking down or over expressing KIS in a (preferably human) cell line to determine whether a change in KIS could be detected in these samples using the KIS antibodies, as has been reported for the JH1998 KIS antibody (Francone et al., 2010). Mass spectrometry could also be used to identify the bands detected in the western blots; this was beyond the scope of this thesis.

6.3. Can KIS still be considered to be a Schizophrenia Susceptibility Gene?

Had the results presented in this thesis identified changes in KIS expression associated with diagnostic group or risk genotype then it would have been considered to strengthen the case of KIS as schizophrenia susceptibility gene. Conversely, as no significant changes were identified, these results should be considered to weaken the case. However, these results in no way eliminate the possibility that KIS is a schizophrenia susceptibility gene, but the supporting evidence remains limited to the initial genetic association studies which first identified this possibility (Puri et al., 2007; 2008). KIS remains a biologically plausible susceptibility gene, with its role in neuronal migration (Cambray et al., 2009) and the gene expression findings in KIS knockout mice, described in Chapter 5, reflecting mechanisms through which KIS function could contribute to the pathophysiology of schizophrenia. A modest change in KIS in the adult brain may not be detectable using the parameters investigated here, particularly if it is not present in all cases and, as discussed in Section 4.4, it could be that changes in expression KIS in schizophrenia are more prominent in particular human populations, are limited particular

points during development, or affects isoforms of the gene yet to be identified – as is being reported for an increasing number of other schizophrenia susceptibility genes (Kleinman et al., 2011).

6.4. Further Work

Based on the absence of any identified changes in KIS expression in the human brain with regard to diagnostic or genotype groups in any of the brain regions investigated here, there appears to be little point in further investigating KIS expression in human post mortem samples. Even if KIS expression was investigated in an alternative brain collection, for example one from a British Caucasian background similar to that in which the initial association of KIS with schizophrenia was found, the chances of finding a change in KIS expression would be slim considering the complete absence of a change in several brain regions of the two quite large brain series studied here. In continuing work on KIS in humans, it is critical to see if the association of KIS with schizophrenia could be replicated in further genetic association studies. To date there are only three studies which have investigated the SNPs within the KIS gene, each of which found a degree of association of SNP genotype with schizophrenia (Puri et al., 2007, 2008; Betcheva et al., 2009; see Section 1.2.1), but no evidence has emerged from GWAS. A further point which could be investigated in humans is the possibility of identifying splice variants of KIS, which could be carried out using 3' and 5' RACE as described in Section 4.4, and the functional relevance of any such variants could be investigated in the brain. Further sequencing of the KIS gene may also be of use to attempt to identify coding SNPs or novel rare variants which could affect KIS function or expression.

Before any additional work were conducted on genetically-modified KIS mice, it would be essential to clarify and confirm their true knockout status. If this were achieved, and assuming that littermate controls were also available, it may be worthwhile to investigate the phosphorylation state of other reported KIS targets such as PAM and SF1, which were not investigated in the studies presented here due to problems obtaining antibodies which could be used to accurately quantify these targets. Co-immunoprecipitation experiments could also be utilised to try to determine the proteins with which KIS is associated in neural tissue. In addition, behavioural studies that included a range of tests to demonstrate how 'schizophrenia-like' their phenotype is would be of interest (Arguello and Gogos, 2006; Amann et al., 2010). The results from the behavioural studies could also direct further molecular experiments to particular brain regions or systems. Finally, the potential role of KIS in neurodevelopment may also merit further study. This could be carried out by examining the phosphorylation state of stathmin, $p27^{kip1}$, and other KIS targets in younger knockout mice, for example at P7 where KIS expression was found to be at its highest, to try and elucidate the function of KIS at this stage in neurodevelopment.

6.5. Final Summary

The studies presented here have investigated the putative schizophrenia susceptibility gene KIS, by determining its expression in the brain, quantifying its expression in the disorder and in relation to risk genotype, and by investigating its function in the brain using knockout mice. The results provide new information about the expression and function of the KIS gene in the brain and, although negative, are also relevant to the understanding of the roles which KIS may play in schizophrenia.

Appendix

Results Tables

Stathmin	WT	KO		
Striatum	1.78 ± 0.33	2.15 ± 0.37	$F_{1,9}$=0.570	P=0.469
N	6	5		
Hippocampus	0.94 ± 0.27	1.49 ± 0.27	$F_{1,10}$=2.052	P=0.183
N	6	6		
Cerebellum	0.13 ± 0.04	0.14 ± 0.04	$F_{1,10}$=0.039	P=0.847
N	6	6		

Table A1: Relative abundance of stathmin immunoreactivity in the NIH KIS knockout mice series as measured by western blot.
All data are normalised to GAPDH. Values shown are mean ± standard error of the mean; WT, wildtype; KO, knockout.

Phosphorylated Stathmin	WT	KO		
Striatum	1.28 ± 0.28	1.29 ± 0.28	$F_{1,8}$=0.001	P=0.977
N	5	5		
Hippocampus	0.17 ± 0.04	0.21 ± 0.04	$F_{1,10}$=0.360	P=0.562
N	6	6		

Table A2: Relative abundance of stathmin phosphorylated on the serine 38 residue immunoreactivity in the NIH KIS knockout mice series as measured by western blot.
All data are normalised to GAPDH. Values shown are mean ± standard error of the mean; WT, wildtype; KO, knockout.

$p27^{kip1}$	WT	KO		
Striatum	0.20 ± 0.03	0.16 ± 0.03	$F_{1,9}$=0.855	P=0.379
N	6	5		
Hippocampus	0.15 ± 0.05	0.13 ± 0.05	$F_{1,10}$=0.141	P=0.715
N	6	6		
Cerebellum	0.21 ± 0.04	0.18 ± 0.05	$F_{1,9}$=0.107	P=0.751
N	6	5		

Table A3: Relative abundance of $p27^{kip1}$ immunoreactivity in the NIH KIS knockout mice series as measured by western blot.
All data are normalised to GAPDH. Values shown are mean ± standard error of the mean; WT, wildtype; KO, knockout.

Phosphorylated $p27^{kip1}$	WT	KO		
Striatum	0.33 ± 0.07	0.37 ± 0.07	$F_{1,9}$=0.241	P=0.635
N	6	5		
Hippocampus	0.32 ± 0.06	0.15 ± 0.06	$F_{1,10}$=4.199	P=0.068
N	6	6		
Cerebellum	0.45 ± 0.09	0.64 ± 0.07	$F_{1,8}$=2.990	P=0.122
N	4	6		

Table A4: Relative abundance of $p27^{kip1}$ phosphorylated on the serine 10 residue immunoreactivity in the NIH KIS knockout mice series as measured by western blot.
All data are normalised to GAPDH. Values are mean ± standard error of the mean; WT, wildtype; KO, knockout.

GAP43	WT	KO		
SSCx	78.7 ± 7.9	88.3 ± 7.91	$F_{1,10}$=0.746	P=0.408
N	6	6		
Cingulate Cortex	244 ± 17.2	206 ± 18.8	$F_{1,9}$=2.233	P=0.169
N	6	5		
Dorsolateral Striatum	98.2 ± 8.1	111 ± 8.09	$F_{1,10}$=1.193	P=0.300
N	6	6		
Visual Cortex	110 ± 13.9	93.8 ± 13.9	$F_{1,10}$=0.680	P=0.429
N	6	6		
CA1	130 ± 10.2	91.0 ± 10.2	$F_{1,10}$=7.380	P=0.022*
N	6	6		
CA3	116 ± 15.6	94.7 ± 15.6	$F_{1,10}$=0.968	P=0.348
N	6	6		
Dentate Gyrus	-	-	-	-
N	-	-		
Cerebellum	410 ± 30.1	408 ± 30.1	$F_{1,10}$=0.002	P=0.970
N	6	6		

Table A5: ISHH of GAP43 mRNA expression as measured in NIH KIS knockout mice. mRNA quantities are presented as ^{35}SnCi/g tissue equivalents. Values are mean ± standard error of the mean. SSCx, somatosensory cortex; CA, cornu ammonis; WT, wildtype; KO, knockout. * = $p<0.05$.

VGlut1	WT	KO		
SSCx	1510 ± 80.8	1559 ± 80.8	$F_{1,10}$=0.181	P=0.679
N	6	6		
Cingulate Cortex	1480 ± 70.1	1519 ± 76.8	$F_{1,9}$=0.145	P=0.712
N	6	5		
Dorsolateral Striatum	-	-	-	-
N	-	-		
Visual Cortex	1584 ± 79.6	1872 ± 79.6	$F_{1,10}$=6.554	P=0.028*
N	6	6		
CA1	3271 ± 179	3690 ± 179	$F_{1,10}$=2.739	P=0.129
N	6	6		
CA3	5624 ± 189	6007 ± 189	$F_{1,10}$=2.059	P=0.182
N	6	6		
Dentate Gyrus	3507 ± 205	3717 ± 205	$F_{1,10}$=0.525	P=0.485
N	6	6		
Cerebellum	2173 ± 96.8	2401 ± 106	$F_{1,9}$=2.503	P=0.148
N	6	5		

Table A6: ISHH of VGlut1 mRNA expression as measured in NIH KIS knockout mice. mRNA quantities are presented as ^{35}SnCi/g tissue equivalents. SSCx, somatosensory cortex; CA, cornu ammonis; Values are mean ± standard error of the mean; WT, wildtype; KO, knockout. * = $p<0.05$.

MAP2	WT	KO		
SSCx	582 ± 10.8	634 ± 9.88	$F_{1,9}$=12.880	P=0.006*
N	5	6		
Cingulate Cortex	600 ± 23.8	627 ± 23.8	$F_{1,10}$=0.634	P=0.444
N	6	6		
Dorsolateral Striatum	364 ± 12.5	413 ± 12.5	$F_{1,10}$=7.902	P=0.018*
N	6	6		
Visual Cortex	537 ± 21.0	573 ± 21.0	$F_{1,10}$=1.474	P=0.253
N	6	6		
CA1	839 ± 22.4	820 ± 20.4	$F_{1,9}$=0.431	P=0.528
N	5	6		
CA3	771 ± 26.3	776 ± 24.0	$F_{1,9}$=0.021	P=0.888
N	5	6		
Dentate Gyrus	1164 ± 32.7	1098 ± 29.9	$F_{1,9}$=2.195	P=0.173
N	5	6		
Cerebellum	761 ± 28.9	911 ± 31.7	$F_{1,9}$=12.290	P=0.007*
N	6	5		

Table A7: ISHH of MAP2 mRNA expression as measured in NIH KIS knockout mice. mRNA quantities are presented as ^{35}SnCi/g tissue equivalents. SSCx, somatosensory cortex; CA, cornu ammonis; Values are mean ± standard error of the mean; WT, wildtype; KO, knockout. * = $p<0.05$.

Spinophilin	WT	KO		
SSCx	646 ± 7.3	651 ± 7.96	$F_{1,9}$=0.218	P=0.652
N	6	5		
Cingulate Cortex	677 ± 18.1	713 ± 19.8	$F_{1,9}$=1.892	P=0.202
N	6	5		
Dorsolateral Striatum	591 ± 10.6	672 ± 10.6	$F_{1,10}$=29.392	P<0.001*
N	6	6		
Visual Cortex	734 ± 27.7	733 ± 27.7	$F_{1,10}$=0.000	P=0.987
N	6	6		
CA1	1570 ± 61.0	1576 ± 61.0	$F_{1,10}$=0.006	P=0.941
N	6	6		
CA3	1707 ± 60.3	1710 ± 60.3	$F_{1,10}$=0.002	P=0.968
N	6	6		
Dentate Gyrus	1985 ± 89.9	2044 ± 89.9	$F_{1,10}$=0.218	P=0.651
N	6	6		
Cerebellum	1406 ± 95.6	1607 ± 95.6	$F_{1,10}$=2.230	P=0.166
N	6	6		

Table A8: ISHH of spinophilin mRNA expression as measured in NIH KIS knockout mice.
mRNA quantities are presented as ^{35}SnCi/g tissue equivalents. SSCx, somatosensory cortex; CA, cornu ammonis; Values are mean ± standard error of the mean; WT, wildtype; KO, knockout. * = p<0.05.

Stathmin	WT	KO		
SSCx	999 ± 74.4	1228 ± 74.4	$F_{1,10}$=4.720	P=0.055
N	6	6		
Cingulate Cortex	1332 ± 82.5	1501 ± 82.5	$F_{1,10}$=2.081	P=0.180
N	6	6		
Dorsolateral Striatum	143 ± 26.0	229 ± 26.0	$F_{1,10}$=5.429	P=0.042*
N	6	6		
Visual Cortex	1196 ± 58.9	1281 ± 58.9	$F_{1,10}$=1.036	P=0.333
N	6	6		
CA1	614 ± 35.1	593 ± 35.1	$F_{1,10}$=0.168	P=0.690
N	6	6		
CA3	644 ± 34.0	655 ± 34.0	$F_{1,10}$=0.056	P=0.818
N	6	6		
Dentate Gyrus	1201 ± 51.0	1201 ± 51.0	$F_{1,10}$=0.000	P=0.998
N	6	6		
Cerebellum	686 ± 54.9	769 ± 54.9	$F_{1,10}$=1.139	P=0.311
N	6	6		

Table A9: ISHH of stathmin mRNA expression as measured in NIH KIS knockout mice. mRNA quantities are presented as ^{35}SnCi/g tissue equivalents. SSCx, somatosensory cortex; CA, cornu ammonis; Values are mean ± standard error of the mean; WT, wildtype; KO, knockout. * = $p<0.05$.

Region	WT	KO		
Ventricles	1.80 ± 0.16	1.87 ± 0.16	$F_{1,14}$=0.070	P=0.795
N	8	8		
Striatum	7.07 ± 0.36	7.48 ± 0.42	$F_{1,12}$=0.549	P=0.473
N	8	6		
Hippocampal Formation	14.31 ± 0.63	14.19 ± 0.63	$F_{1,14}$=0.018	P=0.896
N	8	8		
Total Brain	137.7 ± 5.67	145.2 ± 5.67	$F_{1,14}$=0.877	P=0.365
N	8	8		

Table A10: Stereological measurements of brain structure volumes in NIH KIS knockout mice and wildtype controls.
Values are mean (mm^3) ± standard error of the mean; WT, wildtype; KO, knockout.

Region	WT	KO		
Ventricles	1.31 ± 0.07	1.26 ± 0.07	$F_{1,14}$=0.266	P=0.614
N	8	8		
Striatum	5.14 ± 0.17	5.18 ± 0.20	$F_{1,12}$=0.022	P=0.884
N	8	6		
Hippocampal Formation	10.40 ± 0.20	9.78 ± 0.20	$F_{1,14}$=4.615	P=0.050*
N	8	8		

Table A11: Stereological measurements of brain structure volumes as a percentage of total brain volume in NIH KIS knockout mice and wildtype controls.
Values are mean (%) ± standard error of the mean; WT, wildtype; KO, knockout. * = $p \leq 0.05$.

Buffers and Reagents

Hybridisation Buffer:
To make 50ml
Using sterile 50ml falcon tube
5g dextran sulphate –reduces effective volume, improving reaction kinetics
25ml 100% deionised formamide –reduces energy required for hybridistaion
10ml 20x SSC - autoclaved
5ml Denhardts solution (50X concentrate) –blocks non-specific binding to repetitive sequences
1ml salmon sperm –blocks non-specific binding to repetitive sequences
1ml polyadenylic acid (5mg/ml) –blocks non-specific binding to repetitive sequences
50µl Heparin (125mg/ml)
2.5ml 0.5M sodium phosphate buffer pH 7.4
0.5ml 0.1M sodium pyrophosphate –competes with free nucleotides

Mix by vortexing. Wrap tube in foil and leave to dissolve at 4°C overnight.
The following day vortex to mix. Store at –20°C.

4% Paraformaldehyde:
4% paraformaldehyde was prepared on the day (4g for every 100ml DEPC PBS). Heated and stirred for approx 30mins, but must not be heated over 60°C. Conc NaOH may be used to help dissolve PfA, but conc HCl must be used to return pH to around 7.4.

Protein Loading Buffer (5X):
1.6g Tris HCL
2g SDS
10ml Glycerol
1ml ß-mercaptoethanol
0.02g Bromophenol Blue

Add Tris HCL and Bromophenol Blue to glycerol and some dH_2O and mix to dissolve. Add SDS and mix to dissolve. Allow froth to settle. Make up to 19ml with dH_2O then add ß-mercaptoethanol. ß-mercaptoethanol is included as it prevents the formation of disulphide bonds, reducing proteins tertiary and quaternary structure and so keeping the proteins denatured

Protein Suspension Buffer:
0.1M NaCl, 0.01M TrisHCl, 1M EDTA, 1µg/ml aprotinin, 1% SDS

Resolving Gel (Western Blot):
12%
1.6ml dH_2O
2ml 30% acrylamide mix
1.3ml 1.5M Tris pH8.8
50µl 10% SDS
50µl 10% Ammonium persulfate
2µl Tetramethylethylenediamine (TEMED)

15%
1.1ml dH_2O
2.5ml 30% acrylamide mix
1.3ml 1.5M Tris pH8.8
50µl 10% SDS
50µl 10% Ammonium persulfate
2µl TEMED

Approx 5ml needed for each gel

TEMED and Ammonium persulfate make the gel set by catalysing the polymerisation of acrylamide, and so are added last.
A layer of isopropanol is added on top of gel, which forms a flat layer on top of the gel to ensure even setting of the acrylamide.

Running Buffer (Western Blot, 5X):
30.2g Tris base
188g Glycine
100ml 10% SDS
Made to 2 litres with dH_2O

Saline Sodium Citrate (SSC) 20X:
To make 1litre
175.32g Sodium chloride
88.2g Tri-Sodium citrate
pH 7.4
Make to 1 litre with dH_2O

Stacking Gel (Western Blot):
1.4ml dH_2O
0.33ml 30% acrylamide mix
0.25ml 1.0M Tris pH6.8
20µl 10% SDS
20µl 10% Ammonium persulfate
2µl TEMED
Approx 2ml needed for each gel

Tris-Acetic Acid-EDTA (TAE) Running Buffer:
4.84g Tris base
1.14ml Glacial Acetic Acid
2ml 0.5M EDTA
Make to 1 litre with ddH_2O and autoclave

Tris-EDTA (TE) Buffer:
0.16g Tris HCl
0.2ml 0.5 EDTA
Make to 100ml with dH_2O
pH 7.5
Autoclave before use.

Triethanolamine (TEA) Buffer:
18.5g Triethanolamine
9g Sodium Chloride
pH 8.0
Make to 1 litre with dH_2O

References

Abi-Dargham A, Gil R, Krystal J, Baldwin RM, Seibyl JP, Bowers M, van Dyck CH, Charney DS, Innis RB, Laruelle M (1998). Increased striatal dopamine transmission in schizophrenia: confirmation in a second cohort. Am J Psychiatry. 155(6):761-7.

Aigner L, Arber S, Kapfhammer JP, Laux T, Schneider C, Botteri F, Brenner HR, Caroni P (1995). Overexpression of the neural growth-associated protein GAP-43 induces nerve sprouting in the adult nervous system of transgenic mice. Cell. 83(2):269-78.

Alam MR, Caldwell BD, Johnson RC, Darlington DN, Mains RE, Eipper BA (1996). Novel proteins that interact with the COOH-terminal cytosolic routing determinants of an integral membrane peptide-processing enzyme. J Biol Chem. 271(45):28636-40.

Aleman A, Kahn RS, Selten JP (2003). Sex differences in the risk of schizophrenia: evidence from meta-analysis. Arch Gen Psychiatry. 60(6):565-71.

Amann LC, Gandal MJ, Halene TB, Ehrlichman RS, White SL, McCarren HS, Siegel SJ (2010). Mouse behavioral endophenotypes for schizophrenia. Brain Res Bull. 83(3-4):147-61.

Andreasen NC (1995). Symptoms, signs, and diagnosis of schizophrenia. Lancet. 346(8973):477-81.

Andreasen NC, Pierson R (2008). The role of the cerebellum in schizophrenia. Biol Psychiatry. 64(2):81-8.

Andrieux A, Salin PA, Vernet M, Kujala P, Baratier J, Gory-Fauré S, Bosc C, Pointu H, Proietto D, Schweitzer A, Denarier E, Klumperman J, Job D (2002). The suppression of brain cold-stable microtubules in mice induces synaptic defects associated with neuroleptic-sensitive behavioral disorders. Genes Dev. 16(18):2350-64.

Arguello PA, Gogos JA (2006). Modeling madness in mice: one piece at a time. Neuron. 52(1):179-96.

Aronov S, Aranda G, Behar L, Ginzburg I (2002). Visualization of translated tau protein in the axons of neuronal P19 cells and characterization of tau RNP granules. J Cell Sci. 115(Pt 19):3817-27.

Baldassarre G, Belletti B, Nicoloso MS, Schiappacassi M, Vecchione A, Spessotto P, Morrione A, Canzonieri V, Colombatti A (2005). p27(Kip1)-stathmin interaction influences sarcoma cell migration and invasion. Cancer Cell. 7(1):51-63.

Bassett AS, Costain G, Alan Fung WL, Russell KJ, Pierce L, Kapadia R, Carter RF, Chow EW, Forsythe PJ (2010). Clinically detectable copy number variations in a Canadian catchment population of schizophrenia. J Psychiatr Res. 44(15):1005-9.

Bellocchio EE, Hu H, Pohorille A, Chan J, Pickel VM, Edwards RH (1998). The localization of the brain-specific inorganic phosphate transporter suggests a specific presynaptic role in glutamatergic transmission. J Neurosci. 18(21):8648-59.

Bellocchio EE, Reimer RJ, Fremeau RT Jr, Edwards RH (2000). Uptake of glutamate into synaptic vesicles by an inorganic phosphate transporter. Science. 289(5481):957-60.

Belmont LD, Mitchison TJ (1996). Identification of a protein that interacts with tubulin dimers and increases the catastrophe rate of microtubules. Cell. 84(4):623-31.

Benowitz LI, Routtenberg A (1997). GAP-43: an intrinsic determinant of neuronal development and plasticity. Trends Neurosci. 20(2):84-91.

Berglund JA, Abovich N, Rosbash M (1998). A cooperative interaction between U2AF65 and mBBP/SF1 facilitates branchpoint region recognition. Genes Dev. 12(6):858-67.

Betcheva ET, Mushiroda T, Takahashi A, Kubo M, Karachanak SK, Zaharieva IT, Vazharova RV, Dimova II, Milanova VK, Tolev T, Kirov G, Owen MJ, O'Donovan MC, Kamatani N, Nakamura Y, Toncheva DI (2009). Case-control association study of 59 candidate genes reveals the DRD2 SNP rs6277 (C957T) as the only susceptibility factor for schizophrenia in the Bulgarian population. J Hum Genet. 54(2):98-107.

Bièche I, Manceau V, Curmi PA, Laurendeau I, Lachkar S, Leroy K, Vidaud D, Sobel A, Maucuer A (2003). Quantitative RT-PCR reveals a ubiquitous but preferentially neural expression of the KIS gene in rat and human. Brain Res Mol Brain Res. 114(1):55-64.

Boehm M, Yoshimoto T, Crook MF, Nallamshetty S, True A, Nabel GJ, Nabel EG (2002). A growth factor-dependent nuclear kinase phosphorylates p27(Kip1) and regulates cell cycle progression. EMBO J. 21(13):3390-401.

Bräuer AU, Savaskan NE, Plaschke M, Ninnemann O, Nitsch R (2001). Perforant path lesion induces up-regulation of stathmin messenger RNA, but not SCG10 messenger RNA, in the adult rat hippocampus. Neuroscience.102(3):515-26.

Brown AS (2006). Prenatal infection as a risk factor for schizophrenia. Schizophr Bull. Apr;32(2):200-2.

Brown AS, Bottiglieri T, Schaefer CA, Quesenberry CP Jr, Liu L, Bresnahan M, Susser ES (2007). Elevated prenatal homocysteine levels as a risk factor for schizophrenia. Arch Gen Psychiatry. 64(1):31-9.

Brzustowicz LM, Hodgkinson KA, Chow EW, Honer WG, Bassett AS (2000). Location of a major susceptibility locus for familial schizophrenia on chromosome 1q21-q22. Science. 288(5466):678-82.

Brzustowicz LM, Simone J, Mohseni P, Hayter JE, Hodgkinson KA, Chow EW, Bassett AS (2004). Linkage disequilibrium mapping of schizophrenia susceptibility to the CAPON region of chromosome 1q22. Am J Hum Genet. 74(5):1057-63.

Caldwell BD, Darlington DN, Penzes P, Johnson RC, Eipper BA, Mains RE (1999). The novel kinase peptidylglycine alpha-amidating monooxygenase cytosolic interactor protein 2 interacts with the cytosolic routing determinants of the peptide processing enzyme peptidylglycine alpha-amidating monooxygenase. J Biol Chem. 274(49):34646-56.

Cambray S, Pedraza N, Rafel M, Garí E, Aldea M, Gallego C (2009). Protein kinase KIS localizes to RNA granules and enhances local translation. Mol Cell Biol. 29(3):726-35.

Camoletto P, Peretto P, Bonfanti L, Manceau V, Sobel A, Fasolo A (1997). The cytosolic phosphoprotein stathmin is expressed in the olfactory system of the adult rat. Neuroreport. 8(13):2825-9.

Camoletto P, Colesanti A, Ozon S, Sobel A, Fasolo A (2001). Expression of stathmin and SCG10 proteins in the olfactory neurogenesis during development and after lesion in the adulthood. Brain Res Bull. 54(1):19-28.

Campagnoni AT (1988). Molecular biology of myelin proteins from the central nervous system. J Neurochem. 51(1):1-14.

Cannon M, Jones PB, Murray RM (2002). Obstetric complications and schizophrenia: historical and meta-analytic review. Am J Psychiatry. 159(7):1080-92.

Cantor-Graae E, Selten JP (2005). Schizophrenia and migration: a meta-analysis and review. Am J Psychiatry. 162(1):12-24.

Cardno AG, Marshall EJ, Coid B, Macdonald AM, Ribchester TR, Davies NJ, Venturi P, Jones LA, Lewis SW, Sham PC, Gottesman II, Farmer AE, McGuffin P, Reveley AM, Murray RM (1999). Heritability estimates for psychotic disorders: the Maudsley twin psychosis series. Arch Gen Psychiatry. 56(2):162-8.

Carter CS, Mintun M, Nichols T, Cohen JD (1997). Anterior cingulate gyrus dysfunction and selective attention deficits in schizophrenia: [15O]H2O PET study during single-trial Stroop task performance. Am J Psychiatry. 154(12):1670-5.

Caspi A, Moffitt TE, Cannon M, McClay J, Murray R, Harrington H, Taylor A, Arseneault L, Williams B, Braithwaite A, Poulton R, Craig IW (2005). Moderation of the effect of adolescent-onset cannabis use on adult psychosis by a functional polymorphism in the catechol-O-methyltransferase gene: longitudinal evidence of a gene X environment interaction. Biol Psychiatry. 57(10):1117-27.

Chen X, Dunham C, Kendler S, Wang X, O'Neill FA, Walsh D, Kendler KS (2004). Regulator of G-protein signaling 4 (RGS4) gene is associated with schizophrenia in Irish high density families. Am J Med Genet B Neuropsychiatr Genet. 129B(1):23-6

Chin LS, Li L, Ferreira A, Kosik KS, Greengard P (1995). Impairment of axonal development and of synaptogenesis in hippocampal neurons of synapsin I-deficient mice. Proc Natl Acad Sci U S A. 92(20):9230-4.

Chong VZ, Thompson M, Beltaifa S, Webster MJ, Law AJ, Weickert CS (2008). Elevated neuregulin-1 and ErbB4 protein in the prefrontal cortex of schizophrenic patients. Schizophr Res. 100(1-3):270-80.

Chowdari KV, Mirnics K, Semwal P, Wood J, Lawrence E, Bhatia T, Deshpande SN, B K T, Ferrell RE, Middleton FA, Devlin B, Levitt P, Lewis DA, Nimgaonkar VL (2002). Association and linkage analyses of RGS4 polymorphisms in schizophrenia. Hum Mol Genet. 11(12):1373-80.

Chubb JE, Bradshaw NJ, Soares DC, Porteous DJ, Millar JK (2008). The DISC locus in psychiatric illness. Mol Psychiatry. 13(1):36-64.

Clark D, Dedova I, Cordwell S, Matsumoto I (2006). A proteome analysis of the anterior cingulate cortex gray matter in schizophrenia. Mol Psychiatry. 11(5):459-70, 423.

Clarke MC, Harley M, Cannon M (2006). The role of obstetric events in schizophrenia. Schizophr Bull. 32(1):3-8.

Clarke GM, Cardon LR (2010). Aspects of observing and claiming allele flips in association studies. Genet Epidemiol. 34(3):266-74.

Cotter D, Miszkiel K, Al-Sarraj S, Wilkinson ID, Paley M, Harrison MJ, Hall-Craggs MA, Everall IP (1999). The assessment of postmortem brain volume; a comparison of stereological and planimetric methodologies. Neuroradiology. 41(7):493-6.

Coyle JT (2006). Glutamate and schizophrenia: beyond the dopamine hypothesis. Cell Mol Neurobiol. 26(4-6):365-84.

Craddock N, O'Donovan MC, Owen MJ (2006). Genes for schizophrenia and bipolar disorder? Implications for psychiatric nosology. Schizophr Bull. 32(1):9-16.

Crook MF, Olive M, Xue HH, Langenickel TH, Boehm M, Leonard WJ, Nabel EG (2008). GA-binding protein regulates KIS gene expression, cell migration, and cell cycle progression. FASEB J. 22(1):225-35.

Dagerlind A, Friberg K, Bean AJ, Hokfelt T (1992). Sensitive mRNA detection using unfixed tissue: combined radioactive and non-radioactive in situ hybridisation Histochemistry. Histochemistry 98:39-49.

Davies G, Welham J, Chant D, Torrey EF, McGrath J (2003). A systematic review and meta-analysis of Northern Hemisphere season of birth studies in schizophrenia. Schizophr Bull. 29(3):587-93.

Di Paolo G, Lutjens R, Osen-Sand A, Sobel A, Catsicas S, Grenningloh G (1997). Differential distribution of stathmin and SCG10 in developing neurons in culture. J Neurosci Res. 50(6):1000-9.

Driscoll DA, Spinner NB, Budarf ML, McDonald-McGinn DM, Zackai EH, Goldberg RB, Shprintzen RJ, Saal HM, Zonana J, Jones MC (1992). Deletions and microdeletions of 22q11.2 in velo-cardio-facial syndrome. Am J Med Genet. 44(2):261-8.

Eastwood SL, Harrison PJ (1995). Decreased synaptophysin in the medial temporal lobe in schizophrenia demonstrated using immunoautoradiography. Neuroscience. 69(2):339-43.

Eastwood SL, Harrison PJ (1998). Hippocampal and cortical growth-associated protein-43 messenger RNA in schizophrenia. Neuroscience. 86(2):437-48.

Eastwood SL, Burnet PW, Harrison PJ (2000). Expression of complexin I and II mRNAs and their regulation by antipsychotic drugs in the rat forebrain. Synapse. 36(3):167-77.

Eastwood SL, Harrison PJ (2005). Decreased expression of vesicular glutamate transporter 1 and complexin II mRNAs in schizophrenia: further evidence for a synaptic pathology affecting glutamate neurons. Schizophr Res. 73(2-3):159-72.

Eastwood SL, Lyon L, George L, Andrieux A, Job D, Harrison PJ (2007). Altered expression of synaptic protein mRNAs in STOP (MAP6) mutant mice. J Psychopharmacol. 21(6):635-44.

Eastwood SL, Harrison PJ (2008). Decreased mRNA expression of netrin-G1 and netrin-G2 in the temporal lobe in schizophrenia and bipolar disorder. Neuropsychopharmacology. 33(4):933-45

Eipper BA, Milgram SL, Husten EJ, Yun HY, Mains RE (1993). Peptidylglycine alpha-amidating monooxygenase: a multifunctional protein with catalytic, processing, and routing domains. Protein Sci. 2(4):489-97.

Ekelund J, Hovatta I, Parker A, Paunio T, Varilo T, Martin R, Suhonen J, Ellonen P, Chan G, Sinsheimer JS, Sobel E, Juvonen H, Arajärvi R, Partonen T, Suvisaari J, Lönnqvist J, Meyer J, Peltonen L (2001). Chromosome 1 loci in Finnish schizophrenia families. Hum Mol Genet. 10(15):1611-7.

Emamian ES, Hall D, Birnbaum MJ, Karayiorgou M, Gogos JA (2004). Convergent evidence for impaired AKT1-GSK3beta signaling in schizophrenia. Nat Genet. 36(2):131-7.

Epstein J, Stern E, Silbersweig D (1999). Mesolimbic activity associated with psychosis in schizophrenia. Symptom-specific PET studies. Ann N Y Acad Sci. 877:562-74.

Feng J, Yan Z, Ferreira A, Tomizawa K, Liauw JA, Zhuo M, Allen PB, Ouimet CC, Greengard P (2000). Spinophilin regulates the formation and function of dendritic spines. Proc Natl Acad Sci U S A. 97(16):9287-92.

Fero ML, Rivkin M, Tasch M, Porter P, Carow CE, Firpo E, Polyak K, Tsai LH, Broudy V, Perlmutter RM, Kaushansky K, Roberts JM (1996). A syndrome of multiorgan hyperplasia with features of gigantism, tumorigenesis, and female sterility in p27(Kip1)-deficient mice. Cell. 85(5):733-44.

Ferreira A, Rapoport M (2002). The synapsins: beyond the regulation of neurotransmitter release. Cell Mol Life Sci. 59(4):589-95.

Fornito A, Yücel M, Dean B, Wood SJ, Pantelis C (2009). Anatomical abnormalities of the anterior cingulate cortex in schizophrenia: bridging the gap between neuroimaging and neuropathology. Schizophr Bull. 35(5):973-93.

Francone VP, Ifrim MF, Rajagopal C, Leddy CJ, Wang Y, Carson JH, Mains RE, Eipper BA (2010). Signaling from the secretory granule to the nucleus: Uhmk1 and PAM. Mol Endocrinol. 24(8):1543-58.

Frankle WG, Lerma J, Laruelle M (2003). The synaptic hypothesis of schizophrenia. Neuron. 39(2):205-16.

Fuller R, Nopoulos P, Arndt S, O'Leary D, Ho BC, Andreasen NC (2002). Longitudinal assessment of premorbid cognitive functioning in patients with schizophrenia through examination of standardized scholastic test performance. Am J Psychiatry. 159(7):1183-9.

Gabriel SB, Schaffner SF, Nguyen H, Moore JM, Roy J, Blumenstiel B, Higgins J, DeFelice M, Lochner A, Faggart M, Liu-Cordero SN, Rotimi C, Adeyemo A, Cooper R, Ward R, Lander ES, Daly MJ, Altshuler D (2002). The structure of haplotype blocks in the human genome. Science. 296(5576):2225-9.

Geddes JR, Lawrie SM (1995). Obstetric complications and schizophrenia: a meta-analysis. Br J Psychiatry. 167(6):786-93.

Gilmore JH, Kang C, Evans DD, Wolfe HM, Smith JK, Lieberman JA, Lin W, Hamer RM, Styner M, Gerig G (2010). Prenatal and neonatal brain structure and white matter maturation in children at high risk for schizophrenia. Am J Psychiatry. 167(9):1083-91.

Glessner JT, Reilly MP, Kim CE, Takahashi N, Albano A, Hou C, Bradfield JP, Zhang H, Sleiman PM, Flory JH, Imielinski M, Frackelton EC, Chiavacci R, Thomas KA, Garris M, Otieno FG, Davidson M, Weiser M, Reichenberg A, Davis KL, Friedman JI, Cappola TP, Margulies KB, Rader DJ, Grant SF, Buxbaum JD, Gur RE, Hakonarson H (2010). Strong synaptic transmission impact by copy number variations in schizophrenia. Proc Natl Acad Sci U S A. 107(23):10584-9.

Goto T, Mitsuhashi T, Takahashi T (2004). Altered patterns of neuron production in the p27 knockout mouse. Dev Neurosci. 26(2-4):208-17.

Gottesman II (1991). Schizophrenia genesis. New York: WH Freeman

Gozani O, Potashkin J, Reed R (1998). A potential role for U2AF-SAP 155 interactions in recruiting U2 snRNP to the branch site. Mol Cell Biol. 18(8):4752-60.

Gurling HM, Kalsi G, Brynjolfson J, Sigmundsson T, Sherrington R, Mankoo BS, Read T, Murphy P, Blaveri E, McQuillin A, Petursson H, Curtis D (2001). Genomewide genetic linkage analysis confirms the presence of susceptibility loci for schizophrenia, on chromosomes 1q32.2, 5q33.2, and 8p21-22 and provides support for linkage to schizophrenia, on chromosomes 11q23.3-24 and 20q12.1-11.23. Am J Hum Genet. 68(3):661-73.

Hirayasu Y, Shenton ME, Salisbury DF, Dickey CC, Fischer IA, Mazzoni P, Kisler T, Arakaki H, Kwon JS, Anderson JE, Yurgelun-Todd D, Tohen M, McCarley RW (1998). Lower left temporal lobe MRI volumes in patients with first-episode schizophrenia compared with psychotic patients with first-episode affective disorder and normal subjects. Am J Psychiatry. 155(10):1384-91.

Harrison PJ (2005). Neuropathology of schizophrenia. Psychiatry 4(10):18-21.

Harrison PJ, Law AJ (2006). Neuregulin 1 and schizophrenia: genetics, gene expression, and neurobiology. Biol Psychiatry. 60(2):132-40.

Hashimoto R, Straub RE, Weickert CS, Hyde TM, Kleinman JE, Weinberger DR (2004). Expression analysis of neuregulin-1 in the dorsolateral prefrontal cortex in schizophrenia. Mol Psychiatry. 9(3):299-307.

Hilfiker S, Pieribone VA, Czernik AJ, Kao HT, Augustine GJ, Greengard P (1999). Synapsins as regulators of neurotransmitter release. Philos Trans R Soc Lond B Biol Sci. 354(1381):269-79.

Hüttelmaier S, Zenklusen D, Lederer M, Dictenberg J, Lorenz M, Meng X, Bassell GJ, Condeelis J, Singer RH (2005). Spatial regulation of beta-actin translation by Src-dependent phosphorylation of ZBP1. Nature. 438(7067):512-5.

Hwu HG, Liu CM, Fann CS, Ou-Yang WC, Lee SF (2003). Linkage of schizophrenia with chromosome 1q loci in Taiwanese families. Mol Psychiatry. 8(4):445-52.

Javitt DC, Zukin SR (1991). Recent advances in the phencyclidine model of schizophrenia. Am J Psychiatry. 148(10):1301-8.

Jin K, Mao XO, Cottrell B, Schilling B, Xie L, Row RH, Sun Y, Peel A, Childs J, Gendeh G, Gibson BW, Greenberg DA (2004). Proteomic and immunochemical characterization of a role for stathmin in adult neurogenesis. FASEB J. 18(2):287-99.

Jones P, Rodgers B, Murray R, Marmot M (1994). Child development risk factors for adult schizophrenia in the British 1946 birth cohort. Lancet. 344(8934):1398-402.

Jourdain L, Curmi P, Sobel A, Pantaloni D, Carlier MF (1997). Stathmin: a tubulin-sequestering protein which forms a ternary T2S complex with two tubulin molecules. Biochemistry. 36(36):10817-21.

Kerwin RW (1993). Glutamate receptors, microtubule associated proteins and developmental anomaly in schizophrenia: an hypothesis. Psychol Med. 23(3):547-51.

Kielkopf CL, Rodionova NA, Green MR, Burley SK (2001). A novel peptide recognition mode revealed by the X-ray structure of a core U2AF35/U2AF65 heterodimer. Cell. 106(5):595-605.

Kielkopf CL, Lücke S, Green MR (2004). U2AF homology motifs: protein recognition in the RRM world. Genes Dev. 18(13):1513-26.

Kirov G, Grozeva D, Norton N, Ivanov D, Mantripragada KK, Holmans P; International Schizophrenia Consortium; Wellcome Trust Case Control Consortium, Craddock N, Owen MJ, O'Donovan MC (2009). Support for the involvement of large copy number variants in the pathogenesis of schizophrenia. Hum Mol Genet. 18(8):1497-503.

Kleinman JE et al. (2011). Genetic neuropathology of schizophrenia: New approaches to an old question, and new uses for port mortem brains. Biol Psychiatry. 69(2):140-5.

Koppel J, Boutterin MC, Doye V, Peyro-Saint-Paul H, Sobel A (1990). Developmental tissue expression and phylogenetic conservation of stathmin, a phosphoprotein associated with cell regulations. J Biol Chem. 265(7):3703-7.

Kumar V, Becker T, Jansen S, van Barneveld A, Boztug K, Wölfl S, Tümmler B, Stanke F (2008). Expression levels of FAS are regulated through an evolutionary conserved element in intron 2, which modulates cystic fibrosis disease severity. Genes Immun. 9(8):689-96.

Kurtz MM (2005). Neurocognitive impairment across the lifespan in schizophrenia: an update. Schizophr Res. 74(1):15-26.

Langenickel TH, Olive M, Boehm M, San H, Crook MF, Nabel EG (2008). KIS protects against adverse vascular remodeling by opposing stathmin-mediated VSMC migration in mice. J Clin Invest. 118(12):3848-59.

Larsson N, Marklund U, Gradin HM, Brattsand G, Gullberg M (1997). Control of microtubule dynamics by oncoprotein 18: dissection of the regulatory role of multisite phosphorylation during mitosis. Mol Cell Biol. 17(9):5530-9.

Law AJ, Hutchinson LJ, Burnet PW, Harrison PJ (2004a). Antipsychotics increase microtubule-associated protein 2 mRNA but not spinophilin mRNA in rat hippocampus and cortex. J Neurosci Res. 76(3):376-82.

Law AJ, Weickert CS, Hyde TM, Kleinman JE, Harrison PJ (2004b). Reduced spinophilin but not microtubule-associated protein 2 expression in the hippocampal formation in schizophrenia and mood disorders: molecular evidence for a pathology of dendritic spines. Am J Psychiatry. 161(10):1848-55.

Law AJ, Lipska BK, Weickert CS, Hyde TM, Straub RE, Hashimoto R, Harrison PJ, Kleinman JE, Weinberger DR (2006). Neuregulin 1 transcripts are differentially expressed in schizophrenia and regulated by 5' SNPs associated with the disease. Proc Natl Acad Sci U S A. 103(17):6747-52.

Law AJ, Kleinman JE, Weinberger DR, Weickert CS (2007). Disease-associated intronic variants in the ErbB4 gene are related to altered ErbB4 splice-variant expression in the brain in schizophrenia. Hum Mol Genet. 16(2):129-41.

Lawrie SM, Abukmeil SS (1998). Brain abnormality in schizophrenia. A systematic and quantitative review of volumetric magnetic resonance imaging studies. Br J Psychiatry. 172:110-20.

Lee JG, Kay EP (2010). Activation of PI 3-kinase/Rac1 and ERK1/2 regulates FGF-2-mediated cell proliferation through phosphorylation of p27 at Ser10 by KIS and at Thr187 by Cdc25A/Cdk2. Invest Ophthalmol Vis Sci. 52(1):417-26.

Levine SZ, Lurie I, Kohn R, Levav I (2010). Trajectories of the course of schizophrenia: From progressive deterioration to amelioration over three decades. Schizophr Res. 126(1-3):184-91.

Lewis CM, Levinson DF, Wise LH, DeLisi LE, Straub RE, Hovatta I, Williams NM, Schwab SG, Pulver AE, Faraone SV, Brzustowicz LM, Kaufmann CA, Garver DL, Gurling HM, Lindholm E, Coon H, Moises HW, Byerley W, Shaw SH, Mesen A, Sherrington R, O'Neill FA, Walsh D, Kendler KS, Ekelund J, Paunio T, Lönnqvist J, Peltonen L, O'Donovan MC, Owen MJ, Wildenauer DB, Maier W, Nestadt G, Blouin JL, Antonarakis SE, Mowry BJ, Silverman JM, Crowe RR, Cloninger CR, Tsuang MT, Malaspina D, Harkavy-Friedman JM, Svrakic DM, Bassett AS, Holcomb J, Kalsi G, McQuillin A, Brynjolfson J, Sigmundsson T, Petursson H, Jazin E, Zoëga T, Helgason T (2003). Genome scan meta-analysis of schizophrenia and bipolar disorder, part II: Schizophrenia. Am J Hum Genet. 73(1):34-48

Lewis DA (2009). Neuroplasticity of excitatory and inhibitory cortical circuits in schizophrenia. Dialogues Clin Neurosci. 11(3):269-80.

Lieberman JA, Kane JM, Alvir J (1987). Provocative tests with psychostimulant drugs in schizophrenia. Psychopharmacology (Berl). 91(4):415-33.

Lieberman JA (1999). Pathophysiologic mechanisms in the pathogenesis and clinical course of schizophrenia. J Clin Psychiatry.60 Suppl 12:9-12.

Lipska BK, Weinberger DR (2000). To model a psychiatric disorder in animals: schizophrenia as a reality test. Neuropsychopharmacology. 23(3):223-39.

Lipska BK, Deep-Soboslay A, Weickert CS, Hyde TM, Martin CE, Herman MM, Kleinman JE (2006). Critical factors in gene expression in postmortem human brain: Focus on studies in schizophrenia. Biol Psychiatry. 60(6):650-8.

Liu M, Dai B, Kang SH, Ban K, Huang FJ, Lang FF, Aldape KD, Xie TX, Pelloski CE, Xie K, Sawaya R, Huang S (2006). FoxM1B is overexpressed in human glioblastomas and critically regulates the tumorigenicity of glioma cells. Cancer Res. 66(7):3593-602.

Liu YL, Fann CS, Liu CM, Chang CC, Yang WC, Hung SI, Yu SL, Hwang TJ, Hsieh MH, Liu CC, Tsuang MM, Wu JY, Jou YS, Faraone SV, Tsuang MT, Chen WJ, Hwu HG (2007).More evidence supports the association of PPP3CC with schizophrenia. Mol Psychiatry. 12(10):966-74.

Lorincz A, Nusser Z (2008). Specificity of immunoreactions: the importance of testing specificity in each method. J Neurosci. 28(37):9083-6.

Manceau V, Swenson M, Le Caer JP, Sobel A, Kielkopf CL, Maucuer A (2006). Major phosphorylation of SF1 on adjacent Ser-Pro motifs enhances interaction with U2AF65. FEBS J. 273(3):577-87.

Manceau V, Kielkopf CL, Sobel A, Maucuer A (2008). Different requirements of the kinase and UHM domains of KIS for its nuclear localization and binding to splicing factors. J Mol Biol. 381(3):748-62.

Mangalore R, Knapp M (2007). Cost of schizophrenia in England. J Ment Health Policy Econ. 10(1):23-41.

Manna T, Thrower DA, Honnappa S, Steinmetz MO, Wilson L (2009). Regulation of microtubule dynamic instability in vitro by differentially phosphorylated stathmin. J Biol Chem. 284(23):15640-9.

Marklund U, Osterman O, Melander H, Bergh A, Gullberg M (1994). The phenotype of a "Cdc2 kinase target site-deficient" mutant of oncoprotein 18 reveals a role of this protein in cell cycle control. J Biol Chem. 269(48):30626-35.

Matsuo N, Takao K, Nakanishi K, Yamasaki N, Tanda K, Miyakawa T (2010). Behavioral profiles of three C57BL/6 substrains. Front Behav Neurosci. 4:29.

Maucuer A, Camonis JH, Sobel A (1995). Stathmin interaction with a putative kinase and coiled-coil-forming protein domains. Proc Natl Acad Sci U S A. 92(8):3100-4.

Maucuer A, Ozon S, Manceau V, Gavet O, Lawler S, Curmi P, Sobel A (1997). KIS is a protein kinase with an RNA recognition motif. J Biol Chem. 272(37):23151-6.

Maucuer A, Le Caer JP, Manceau V, Sobel A (2000). Specific Ser-Pro phosphorylation by the RNA-recognition motif containing kinase KIS. Eur J Biochem. 267(14):4456-64.

McCarthy SE, Makarov V, Kirov G, Addington AM, McClellan J, Yoon S, Perkins DO, Dickel DE, Kusenda M, Krastoshevsky O, Krause V, Kumar RA, Grozeva D, Malhotra D, Walsh T, Zackai EH, Kaplan P, Ganesh J, Krantz ID, Spinner NB, Roccanova P, Bhandari A, Pavon K, Lakshmi B, Leotta A, Kendall J, Lee YH, Vacic V, Gary S, Iakoucheva LM, Crow TJ, Christian SL, Lieberman JA, Stroup TS, Lehtimäki T, Puura K, Haldeman-Englert C, Pearl J, Goodell M, Willour VL, Derosse P, Steele J, Kassem L, Wolff J, Chitkara N, McMahon FJ, Malhotra AK, Potash JB, Schulze TG, Nöthen MM, Cichon S, Rietschel M, Leibenluft E, Kustanovich V, Lajonchere CM, Sutcliffe JS, Skuse D, Gill M, Gallagher L, Mendell NR; Wellcome Trust Case Control Consortium, Craddock N, Owen MJ, O'Donovan MC, Shaikh TH, Susser E, Delisi LE, Sullivan PF, Deutsch CK, Rapoport J, Levy DL, King MC, Sebat J (2009). Microduplications of 16p11.2 are associated with schizophrenia. Nat Genet. 41(11):1223-7.

Mei L, Xiong WC (2008). Neuregulin 1 in neural development, synaptic plasticity and schizophrenia. Nat Rev Neurosci. 9(6):437-52.

Millar M, Urban J, Dorsa D (1989). Quantification of mRNA in discrete cell groups by in situ hybridization Histochemistry. Methods in Neuroscience, volume 1, Academic Press, San Diego. 164-181.

Millar JK, Wilson-Annan JC, Anderson S, Christie S, Taylor MS, Semple CA, Devon RS, St Clair DM, Muir WJ, Blackwood DH, Porteous DJ (2000). Disruption of two novel genes by a translocation co-segregating with schizophrenia. Hum Mol Genet. 9(9):1415-23.

Mirnics K, Middleton FA, Lewis DA, Levitt P (2001). Analysis of complex brain disorders with gene expression microarrays: schizophrenia as a disease of the synapse. Trends Neurosci. 24(8):479-86.

Morris DW, Rodgers A, McGhee KA, Schwaiger S, Scully P, Quinn J, Meagher D, Waddington JL, Gill M, Corvin AP (2004). Confirming RGS4 as a susceptibility gene for schizophrenia. Am J Med Genet B Neuropsychiatr Genet. 125B(1):50-3.

Murphy KC, Jones LA, Owen MJ (1999). High rates of schizophrenia in adults with velo-cardio-facial syndrome. Arch Gen Psychiatry. 56(10):940-5.

Nacusi LP, Sheaff RJ (2006). Akt1 sequentially phosphorylates $p27^{kip1}$ within a conserved but non-canonical region. Cell Div. 1:11.

Nakamura K, Zhang X, Kuramitsu Y, Fujimoto M, Yuan X, Akada J, Aoshima-Okuda M, Mitani N, Itoh Y, Katoh T, Morita Y, Nagasaka Y, Yamazaki Y, Kuriki T, Sobel A (2006). Analysis on heat stress-induced hyperphosphorylation of stathmin at serine 37 in Jurkat cells by means of two-dimensional gel electrophoresis and tandem mass spectrometry. J Chromatogr A. 1106(1-2):181-9.

Nakamura S, Okinaka K, Hirano I, Ono T, Sugimoto Y, Shigeno K, Fujisawa S, Shinjo K, Ohnishi K (2008). KIS induces proliferation and the cell cycle progression through the phosphorylation of $p27^{Kip1}$ in leukemia cells. Leuk Res. 32(9):1358-65.

Nelson MD, Saykin AJ, Flashman LA, Riordan HJ (1998). Hippocampal volume reduction in schizophrenia as assessed by magnetic resonance imaging: a meta-analytic study. Arch Gen Psychiatry. 55(5):433-40.

Ng MY, Levinson DF, Faraone SV, Suarez BK, DeLisi LE, Arinami T, Riley B, Paunio T, Pulver AE, Irmansyah, Holmans PA, Escamilla M, Wildenauer DB, Williams NM, Laurent C, Mowry BJ, Brzustowicz LM, Maziade M, Sklar P, Garver DL, Abecasis GR, Lerer B, Fallin MD, Gurling HM, Gejman PV, Lindholm E, Moises HW, Byerley W, Wijsman EM, Forabosco P, Tsuang MT, Hwu HG, Okazaki Y, Kendler KS, Wormley B, Fanous A, Walsh D, O'Neill FA, Peltonen L, Nestadt G, Lasseter VK, Liang KY, Papadimitriou GM, Dikeos DG, Schwab SG, Owen MJ, O'Donovan MC, Norton N, Hare E, Raventos H, Nicolini H, Albus M, Maier W, Nimgaonkar VL, Terenius L, Mallet J, Jay M, Godard S, Nertney D, Alexander M, Crowe RR, Silverman JM, Bassett AS, Roy MA, Mérette C, Pato CN, Pato MT, Roos JL, Kohn Y, Amann-Zalcenstein D, Kalsi G, McQuillin A, Curtis D, Brynjolfson J, Sigmundsson T, Petursson H, Sanders AR, Duan J, Jazin E, Myles-Worsley M, Karayiorgou M, Lewis CM (2009). Meta-analysis of 32 genome-wide linkage studies of schizophrenia. Mol Psychiatry. 14(8):774-85.

Nguyen L, Besson A, Heng JI, Schuurmans C, Teboul L, Parras C, Philpott A, Roberts JM, Guillemot F (2006a). $p27^{kip1}$ independently promotes neuronal differentiation and migration in the cerebral cortex. Genes Dev. 20(11):1511-24.

Nguyen L, Besson A, Roberts JM, Guillemot F (2006b). Coupling cell cycle exit, neuronal differentiation and migration in cortical neurogenesis. Cell Cycle. 5(20):2314-8.

Niendam TA, Bearden CE, Rosso IM, Sanchez LE, Hadley T, Nuechterlein KH, Cannon TD (2003). A prospective study of childhood neurocognitive functioning in schizophrenic patients and their siblings. Am J Psychiatry. 160(11):2060-2.

Nishimura M, Koeda A, Suzuki E, Shimizu T, Kawano Y, Nakayama M, Satoh T, Narimatsu S, Naito S (2006). Effects of prototypical drug-metabolizing enzyme inducers on mRNA expression of housekeeping genes in primary cultures of human and rat hepatocytes. Biochem Biophys Res Commun. 346(3):1033-9.

O'Donovan MC, Craddock N, Norton N, Williams H, Peirce T, Moskvina V, Nikolov I, Hamshere M, Carroll L, Georgieva L, Dwyer S, Holmans P, Marchini JL, Spencer CC, Howie B, Leung HT, Hartmann AM, Möller HJ, Morris DW, Shi Y, Feng G, Hoffmann P, Propping P, Vasilescu C, Maier W, Rietschel M, Zammit S, Schumacher J, Quinn EM, Schulze TG, Williams NM, Giegling I, Iwata N, Ikeda M, Darvasi A, Shifman S, He L, Duan J, Sanders AR, Levinson DF, Gejman PV, Cichon S, Nöthen MM, Gill M, Corvin A, Rujescu D, Kirov G, Owen MJ, Buccola NG, Mowry BJ, Freedman R, Amin F, Black DW, Silverman JM, Byerley WF, Cloninger CR (2008). Identification of loci associated with schizophrenia by genome-wide association and follow-up. Molecular Genetics of Schizophrenia Collaboration. Nat Genet. 40(9):1053-5.

Owen MJ, Williams HJ, O'Donovan MC (2009). Schizophrenia genetics: advancing on two fronts. Curr Opin Genet Dev. 19(3):266-70.

Ozon S, Guichet A, Gavet O, Roth S, Sobel A (2002). Drosophila stathmin: a microtubule-destabilizing factor involved in nervous system formation. Mol Biol Cell. 13(2):698-710.

Pal N, Alkana RL (1997). Use of inhalation to study the effect of ethanol and ethanol dependence on neonatal mouse development without maternal separation: a preliminary study. Life Sci. 61(13):1269-81.

Paz RD, Andreasen NC, Daoud SZ, Conley R, Roberts R, Bustillo J, Perrone-Bizzozero NI (2006). Increased expression of activity-dependent genes in cerebellar glutamatergic neurons of patients with schizophrenia. Am J Psychiatry. 163(10):1829-31.

Paulson L, Martin P, Persson A, Nilsson CL, Ljung E, Westman-Brinkmalm A, Eriksson PS, Blennow K, Davidsson P (2003). Comparative genome- and proteome analysis of cerebral cortex from MK-801-treated rats. J Neurosci Res. 71(4):526-33.

Paxinos G, Franklin KBJ (2004). The mouse brain in stereotaxic coordinates, second edition. Elsevier, San Diego.

Pedersen CB, Mortensen PB (2001). Evidence of a dose-response relationship between urbanicity during upbringing and schizophrenia risk. Arch Gen Psychiatry. 58(11):1039-46.

Petrovic V, Costa RH, Lau LF, Raychaudhuri P, Tyner AL (2008). FoxM1 regulates growth factor-induced expression of kinase-interacting stathmin (KIS) to promote cell cycle progression. J Biol Chem. 283(1):453-60.

Pollard H, Khrestchatisky M, Moreau J, Ben-Ari Y, Represa A (1994). Correlation between reactive sprouting and microtubule protein expression in epileptic hippocampus. Neuroscience. 61(4):773-87.

Puri V, McQuillin A, Choudhury K, Datta S, Pimm J, Thirumalai S, Krasucki R, Lawrence J, Quested D, Bass N, Moorey H, Morgan J, Punukollu B, Kandasami G, Curtis D, Gurling H (2007). Fine mapping by genetic association implicates the chromosome 1q23.3 gene UHMK1, encoding a serine/threonine protein kinase, as a novel schizophrenia susceptibility gene. Biol Psychiatry. Apr 1;61(7):873-9.

Puri V, McQuillin A, Thirumalai S, Lawrence J, Krasucki R, Choudhury K, Datta S, Kerwin S, Quested D, Bass N, Pimm J, Lamb G, Moorey H, Kandasami G, Badacsonyi A, Kelly K, Morgan J, Punukollu B, Nadeem H, Curtis D, Gurling HM (2006). Failure to confirm allelic association between markers at the CAPON gene locus and schizophrenia in a British sample. Biol Psychiatry. 15;59(2):195-7.

Puri V, McQuillin A, Datta S, Choudhury K, Pimm J, Thirumalai S, Krasucki R, Lawrence J, Quested D, Bass N, Crombie C, Fraser G, Walker N, Moorey H, Ray MK, Sule A, Curtis D, St Clair D, Gurling H (2008). Confirmation of the genetic association between the U2AF homology motif (UHM) kinase 1 (UHMK1) gene and schizophrenia on chromosome 1q23.3. Eur J Hum Genet. 16(10):1275-82.

Quintana J, Wong T, Ortiz-Portillo E, Marder SR, Mazziotta JC (2004). Anterior cingulate dysfunction during choice anticipation in schizophrenia. Psychiatry Res. 132(2):117-30.

Rajarethinam RP, DeQuardo JR, Nalepa R, Tandon R (2000). Superior temporal gyrus in schizophrenia: a volumetric magnetic resonance imaging study. Schizophr Res. 41(2):303-12.

Rapoport JL, Addington AM, Frangou S, Psych MR (2005). The neurodevelopmental model of schizophrenia: update 2005. Mol Psychiatry. 10(5):434-49.

Rhodes KJ, Trimmer JS (2006). Antibodies as valuable neuroscience research tools versus reagents of mass distraction. J Neurosci. 26(31):8017-20.

Rizig MA, McQuillin A, Puri V, Choudhury K, Datta S, Thirumalai S, Lawrence J, Quested D, Pimm J, Bass N, Lamb G, Moorey H, Badacsonyi A, Kelly K, Morgan J, Punukollu B, Kandasami G, Curtis D, Gurling H (2006). Failure to confirm genetic association between schizophrenia and markers on chromosome 1q23.3 in the region of the gene encoding the regulator of G-protein signaling 4 protein (RGS4). Am J Med Genet B Neuropsychiatr Genet. 141B(3):296-300.

Rodriguez S, Gaunt TR, Day IN (2009). Hardy-Weinberg equilibrium testing of biological ascertainment for Mendelian randomization studies. Am J Epidemiol. 169(4):505-14.

Rollins B, Martin MV, Morgan L, Vawter MP (2010). Analysis of whole genome biomarker expression in blood and brain. Am J Med Genet B Neuropsychiatr Genet. 153B(4):919-36.

Rosoklija G, Keilp JG, Toomayan G, Mancevski B, Haroutunian V, Liu D, Malespina D, Hays AP, Sadiq S, Latov N, Dwork AJ (2005). Altered subicular MAP2 immunoreactivity in schizophrenia. Prilozi. 26(2):13-34.

Ross CA, Margolis RL, Reading SA, Pletnikov M, Coyle JT (2006). Neurobiology of schizophrenia. Neuron. 52(1):139-53.

Rubin CI, Atweh GF (2004). The role of stathmin in the regulation of the cell cycle. J Cell Biochem. 93(2):242-50.

Rund BR (1998). A review of longitudinal studies of cognitive functions in schizophrenia patients. Schizophr Bull. 24(3):425-35

Saha S, Chant D, Welham J, McGrath J (2005). A systematic review of the prevalence of schizophrenia. PLoS Med. 2(5):e141.

Saha S, Chant D, McGrath J (2007). A systematic review of mortality in schizophrenia: is the differential mortality gap worsening over time? Arch Gen Psychiatry. 64(10):1123-31

Saper CB, Sawchenko PE (2003). Magic peptides, magic antibodies: guidelines for appropriate controls for immunohistochemistry. J Comp Neurol. 465(2):161-3.

Schmahmann JD, Sherman JC (1998). The cerebellar cognitive affective syndrome. Brain. 121(4):561-79.

Schwab SG, Wildenauer DB (2009). Update on key previously proposed candidate genes for schizophrenia. Curr Opin Psychiatry. 22(2):147-53.

Sei Y, Ren-Patterson R, Li Z, Tunbridge EM, Egan MF, Kolachana BS, Weinberger DR (2007). Neuregulin1-induced cell migration is impaired in schizophrenia: association with neuregulin1 and catechol-o-methyltransferase gene polymorphisms. Mol Psychiatry. 12(10):946-57.

Seeman P, Chau-Wong M, Tedesco J, Wong K (1975). Brain receptors for antipsychotic drugs and dopamine: direct binding assays. Proc Natl Acad Sci U S A. 72(11):4376-80.

Semple DM, McIntosh AM, Lawrie SM (2005). Cannabis as a risk factor for psychosis: systematic review. J Psychopharmacol. 19(2):187-94.

Selenko P, Gregorovic G, Sprangers R, Stier G, Rhani Z, Krämer A, Sattler M (2003). Structural basis for the molecular recognition between human splicing factors U2AF65 and SF1/mBBP. Mol Cell. 11(4):965-76.

Sherr CJ, Roberts JM (1999). CDK inhibitors: positive and negative regulators of G1-phase progression. Genes Dev. 13(12):1501-12.

Simpson EH, Kellendonk C, Kandel E (2010). A possible role for the striatum in the pathogenesis of the cognitive symptoms of schizophrenia. Neuron. 65(5):585-96.

Slonimsky A, Levy I, Kohn Y, Rigbi A, Ben-Asher E, Lancet D, Agam G, Lerer B (2010). Lymphoblast and brain expression of AHI1 and the novel primate-specific gene, C6orf217, in schizophrenia and bipolar disorder. Schizophr Res. 120(1-3):159-66.

Snyder MA, Smejkalova T, Forlano PM, Woolley CS (2010). Multiple ERbeta antisera label in ERbeta knockout and null mouse tissues. J Neurosci Methods. 188(2):226-34.

Sørensen HJ, Mortensen EL, Reinisch JM, Mednick SA (2003). Do hypertension and diuretic treatment in pregnancy increase the risk of schizophrenia in offspring? Am J Psychiatry. 160(3):464-8.

St Clair D, Xu M, Wang P, Yu Y, Fang Y, Zhang F, Zheng X, Gu N, Feng G, Sham P, He L (2005). Rates of adult schizophrenia following prenatal exposure to the Chinese famine of 1959-1961. JAMA. 294(5):557-62.

Stefansson H, Sigurdsson E, Steinthorsdottir V, Bjornsdottir S, Sigmundsson T, Ghosh S, Brynjolfsson J, Gunnarsdottir S, Ivarsson O, Chou TT, Hjaltason O, Birgisdottir B, Jonsson H, Gudnadottir VG, Gudmundsdottir E, Bjornsson A, Ingvarsson B, Ingason A, Sigfusson S, Hardardottir H, Harvey RP, Lai D, Zhou M, Brunner D, Mutel V, Gonzalo A, Lemke G, Sainz J, Johannesson G, Andresson T, Gudbjartsson D, Manolescu A, Frigge ML, Gurney ME, Kong A, Gulcher JR, Petursson H, Stefansson K (2002). Neuregulin 1 and susceptibility to schizophrenia. Am J Hum Genet. 71(4):877-92.

Stefansson H, Rujescu D, Cichon S, Pietiläinen OP, Ingason A, Steinberg S, Fossdal R, Sigurdsson E, Sigmundsson T, Buizer-Voskamp JE, Hansen T, Jakobsen KD, Muglia P, Francks C, Matthews PM, Gylfason A, Halldorsson BV, Gudbjartsson D, Thorgeirsson TE, Sigurdsson A, Jonasdottir A, Jonasdottir A, Bjornsson A, Mattiasdottir S, Blondal T, Haraldsson M, Magnusdottir BB, Giegling I, Möller HJ, Hartmann A, Shianna KV, Ge D, Need AC, Crombie C, Fraser G, Walker N, Lonnqvist J, Suvisaari J, Tuulio-Henriksson A, Paunio T, Toulopoulou T, Bramon E, Di Forti M, Murray R, Ruggeri M, Vassos E, Tosato S, Walshe M, Li T, Vasilescu C, Mühleisen TW, Wang AG, Ullum H, Djurovic S, Melle I, Olesen J, Kiemeney LA, Franke B; GROUP, Sabatti C, Freimer NB, Gulcher JR, Thorsteinsdottir U, Kong A, Andreassen OA, Ophoff RA, Georgi A, Rietschel M, Werge T, Petursson H, Goldstein DB, Nöthen MM, Peltonen L, Collier DA, St Clair D, Stefansson K (2008). Large recurrent microdeletions associated with schizophrenia. Nature. 455(7210):232-6.

Steveson TC, Zhao GC, Keutmann HT, Mains RE, Eipper BA (2001). Access of a membrane protein to secretory granules is facilitated by phosphorylation. J Biol Chem. 276(43):40326-37.

Straub RE, Jiang Y, MacLean CJ, Ma Y, Webb BT, Myakishev MV, Harris-Kerr C, Wormley B, Sadek H, Kadambi B, Cesare AJ, Gibberman A, Wang X, O'Neill FA, Walsh D, Kendler KS (2002). Genetic variation in the 6p22.3 gene DTNBP1, the human ortholog of the mouse dysbindin gene, is associated with schizophrenia. Am J Hum Genet. 71(2):337-48.

Susser E, Neugebauer R, Hoek HW, Brown AS, Lin S, Labovitz D, Gorman JM (1996). Schizophrenia after prenatal famine. Further evidence. Arch Gen Psychiatry. 53(1):25-31.

Tarui T, Takahashi T, Nowakowski RS, Hayes NL, Bhide PG, Caviness VS (2005). Overexpression of p27 Kip 1, probability of cell cycle exit, and laminar destination of neocortical neurons. Cereb Cortex. 15(9):1343-55.

Tienari P, Wynne LC, Sorri A, Lahti I, Läksy K, Moring J, Naarala M, Nieminen P, Wahlberg KE (2004). Genotype-environment interaction in schizophrenia-spectrum disorder. Long-term follow-up study of Finnish adoptees. Br J Psychiatry. 184:216-22.

Tunbridge EM, Eastwood SL, Harrison PJ (2010). Changed Relative to What? Housekeeping Genes and Normalization Strategies in Human Brain Gene Expression Studies. Biol Psychiatry. 69(2):173-9.

Vandesompele J, De Preter K, Pattyn F, Poppe B, Van Roy N, De Paepe A, Speleman F (2002). Accurate normalization of real-time quantitative RT-PCR data by geometric averaging of multiple internal control genes. Genome Biol. Jun 18;3(7)

Vita A, De Peri L, Silenzi C, Dieci M (2006). Brain morphology in first-episode schizophrenia: a meta-analysis of quantitative magnetic resonance imaging studies. Schizophr Res. 82(1):75-88.

Walsh T, McClellan JM, McCarthy SE, Addington AM, Pierce SB, Cooper GM, Nord AS, Kusenda M, Malhotra D, Bhandari A, Stray SM, Rippey CF, Roccanova P, Makarov V, Lakshmi B, Findling RL, Sikich L, Stromberg T, Merriman B, Gogtay N, Butler P, Eckstrand K, Noory L, Gochman P, Long R, Chen Z, Davis S, Baker C, Eichler EE, Meltzer PS, Nelson SF, Singleton AB, Lee MK, Rapoport JL, King MC, Sebat J (2008). Rare structural variants disrupt multiple genes in neurodevelopmental pathways in schizophrenia. Science. 320(5875):539-43.

Weinberger DR (1987). Implications of normal brain development for the pathogenesis of schizophrenia. Arch Gen Psychiatry. 44(7):660-9.

Weinberger DR, McClure RK (2002). Neurotoxicity, neuroplasticity, and magnetic resonance imaging morphometry: what is happening in the schizophrenic brain? Arch Gen Psychiatry. 59(6):553-8.

Wilson NR, Kang J, Hueske EV, Leung T, Varoqui H, Murnick JG, Erickson JD, Liu G (2005). Presynaptic regulation of quantal size by the vesicular glutamate transporter VGLUT1. J Neurosci. 25(26):6221-34.

Wojcik SM, Rhee JS, Herzog E, Sigler A, Jahn R, Takamori S, Brose N, Rosenmund C (2004). An essential role for vesicular glutamate transporter 1 (VGLUT1) in postnatal development and control of quantal size. Proc Natl Acad Sci U S A. 101(18):7158-63.

Wright IC, Rabe-Hesketh S, Woodruff PW, David AS, Murray RM, Bullmore ET (2000). Meta-analysis of regional brain volumes in schizophrenia. Am J Psychiatry. 157(1):16-25.

Yamada K, Matsuzaki S, Hattori T, Kuwahara R, Taniguchi M, Hashimoto H, Shintani N, Baba A, Kumamoto N, Yamada K, Yoshikawa T, Katayama T, Tohyama M (2010). Increased stathmin1 expression in the dentate gyrus of mice causes abnormal axonal arborizations. PLoS One. 5(1):e8596.

Yamaguchi M, Yamauchi A, Nishimura M, Ueda N, Naito S (2005). Soybean oil fat emulsion prevents cytochrome P450 mRNA down-regulation induced by fat-free overdose total parenteral nutrition in infant rats. Biol Pharm Bull. 28(1):143-7.

Yoshikawa M, Oka T, Kawaguchi M, Hashimoto A (2004). MK-801 upregulates the expression of d-amino acid oxidase mRNA in rat brain. Brain Res Mol Brain Res. 131(1-2):141-4.

Zheng Y, Li H, Qin W, Chen W, Duan Y, Xiao Y, Li C, Zhang J, Li X, Feng G, He L (2005). Association of the carboxyl-terminal PDZ ligand of neuronal nitric oxide synthase gene with schizophrenia in the Chinese Han population. Biochem Biophys Res Commun. 328(4):809-15.